UNIVERSITY OF ALBERTA

The Role of K^+ Channels in Macrophage Activation During *Leishmania major* Infection

by

Kristine Dawn Scott ©

A thesis submitted to the Faculty of Graduate Studies and Research in partial fulfillment of the requirements for the degree of Master of Science

in

Physiology and Cell Biology

DEPARTMENT OF BIOLOGICAL SCIENCES

EDMONTON, ALBERTA

Fall 2003

National Library
of Canada

Acquisitions and
Bibliographic Services

395 Wellington Street
Ottawa ON K1A 0N4
Canada

Bibliothèque nationale
du Canada

Acquisisitons et
services bibliographiques

395, rue Wellington
Ottawa ON K1A 0N4
Canada

Your file Votre référence
ISBN: 0-612-87877-5
Our file Notre référence
ISBN: 0-612-87877-5

The author has granted a non-exclusive licence allowing the National Library of Canada to reproduce, loan, distribute or sell copies of this thesis in microform, paper or electronic formats.

The author retains ownership of the copyright in this thesis. Neither the thesis nor substantial extracts from it may be printed or otherwise reproduced without the author's permission.

L'auteur a accordé une licence non exclusive permettant à la Bibliothèque nationale du Canada de reproduire, prêter, distribuer ou vendre des copies de cette thèse sous la forme de microfiche/film, de reproduction sur papier ou sur format électronique.

L'auteur conserve la propriété du droit d'auteur qui protège cette thèse. Ni la thèse ni des extraits substantiels de celle-ci ne doivent être imprimés ou aturement reproduits sans son autorisation.

Canada

University of Alberta

Library Release Form

Name of Author: Kristine Dawn Scott

Title of Thesis: The Role of K^+ Channels in Macrophage Activation During *Leishmania major* Infection

Degree: Master of Science

Year this Degree Granted: 2003

Permission is hereby granted to the University of Alberta Library to reproduce single copies of this thesis and to lend or sell such copies for private, scholarly, or scientific research purposes only.

The author reserves all other publication and other rights in association with the copyright in the thesis, and except as hereinbefore provided, neither the thesis nor any substantial portion thereof may be printed or otherwise reproduced in any material form whatever without the author's prior written permission.

June 24/03

UNIVERSITY OF ALBERTA

FACULTY OF GRADUATE STUDIES AND RESEARCH

The undersigned certify that they have read, and recommend to the Faculty of Graduate Studies and Research for acceptance, a thesis entitled "The Role of K^+ Channels in Macrophage Activation During *Leishmania major* Infection" submitted by Kristine Dawn Scott in partial fulfillment of the requirements for the degree of Master of Science in Physiology and Cell Biology.

Dr. Larry Guilbert
Committee member

June 17/03

Abstract

The role of K^+ channels in antimicrobial responses was examined at the interface between mammalian macrophages and an obligate intracellular protozoan parasite, *Leishmania major*. P388D.1 macrophage-like cells infected with *L. major* promastigotes or treated with the K^+ channel blocker 4-aminopyridine (4-AP) displayed reduced nitric oxide (NO) production and respiratory burst which correlated with depolarization of the macrophage membrane and increased influx of radiolabeled rubidium, a tracer for K^+ ions, comparable to that induced by 4-AP at 24 hours. Similar 4-AP-induced inhibition of NO and respiratory burst were seen in bone marrow-derived macrophages (BMDM) although 4-AP affected the activation of P388D.1 cells more dramatically than BMDM, perhaps as a result of unique K^+ channel profiles. Infection with *L. major* promastigotes did not suppress NO production by BMDM unless in the presence of 4-AP. *L. major* suppression of macrophage immune responses through modulation of K^+ channel-dependent activation pathways may be essential for parasite survival.

Acknowledgements

I am grateful to the following for providing financial support throughout my program of studies: Natural Sciences and Engineering Research Council (PGS A), Faculty of Science (Entrance Scholarship), and the Department of Biological Sciences (Walter H. Johns Fellowship and Graduate Teaching Assistantship).

I sincerely thank my supervisor Dr. M. Belosevic for his support and guidance and for teaching me how to think in an independent, expansive, and critical way. I thank my co-supervisor Dr. G. Goss for his direction, support, and encouragement. I would also like to thank Dr. J. Goldberg and Dr. L. Guilbert for helpful advice and suggestions throughout the project.

I would like to thank Dr. Fernando Galvez and James Stafford for the data from the rubidium influx experiments. I also wish to acknowledge several technicians, past and present, who were very helpful to me during my program: Cezary Kucharski (particularly for his help with *Leishmania major* infections and isolation of parasites from BALB/c mice), Sarah Delorenzo (for help in isolation of bone marrow cells) and Dawn Kieller (for introducing me to the techniques of SDS-PAGE and immunoblotting).

I would like to thank the graduate students of the Belosevic lab: James Stafford, Daniel Barreda, Patrick Hanington, and especially Debbie Plouffe for always being so willing to lend a hand or some advice, and for making the lab a fun place to work.

Special thanks to Mike and the rest of my family! I would never have been able to complete this work without your love, support, and words of encouragement.

Table of Contents

Chapter 1:....1
- 1.1 Introduction....1
- 1.2 Thesis outline....3

Chapter 2: Literature Review....5
- 2.1 Macrophages....5
  - 2.1.1 Origin of macrophages....5
  - 2.1.2 Constituitive effector functions of macrophages....7
    - 2.1.2.1 Phagocytosis and lysosomal enzymes....7
    - 2.1.2.2 Antigen presentation....8
  - 2.1.3 Inducible effector functions of macrophages....8
    - 2.1.3.1 The two-stage model of macrophage activation....9
    - 2.1.3.2 Production of reactive oxygen intermediates (ROI)....9
    - 2.1.3.3 Production of reactive nitrogen intermediates (RNI)....10
  - 2.1.4 Macrophage-pathogen interactions....12
    - 2.1.4.1 Recognition and uptake: how ingesting pathogens leads to macrophage activation....12
    - 2.1.4.2 Intracellular signaling in macrophages....13

- 2.2 *Leishmania*: An Intracellular Parasite of Macrophages....15
  - 2.2.1 The leishmaniases....15
  - 2.2.2 Life history of *Leishmania major*....18
  - 2.2.3 *Leishmania*-macrophage interactions: evasion of host immune response....20
    - 2.2.3.1 Life in the bloodstream: evasion of serum complement proteins and antibodies....20
    - 2.2.3.2 Parasite recognition and uptake into macrophages....20
    - 2.2.3.3 Encountering the macrophage cytotoxic molecules....21
    - 2.2.3.4 Propagation of infection....22
  - 2.2.4 Survival of *Leishmania major* in macrophages: alteration of ion channel function?....22
- 2.3 Ion Channels....23
  - 2.3.1 General structure and function of ion channels....23
  - 2.3.2 Potassium (K^+) channels....24
    - 2.3.2.1 Major classes of K^+ channels....24
    - 2.3.2.2 Structure of K^+ channels....25
    - 2.3.2.3 Pharmacological blocking of K^+ channels....27
  - 2.3.3 Functions of K^+ channels....28
    - 2.3.3.1 Evidence for the role of K^+ channels in macrophage physiology....28
    - 2.3.3.2 Evidence for the role of K^+ channels in macrophage immune responses....28

- 2.4 Objectives of Thesis....30

Chapter 3: General Materials and Methods... 34
3.1 Media and Reagents... 34
3.2 Cell Culture... 35
3.2.1 Culture of P388D.1 macrophage-like cells... 35
3.2.2 Culture of bone marrow-derived macrophages... 36
3.2.3 *Leishmania major* parasites... 37
3.2.3.1 Maintenance of *L. major* in mice... 37
3.2.3.2 Isolation of amastigotes... 38
3.2.3.3 Promastigote culture... 38
3.2.3.4 Viability stain for promastigotes and amastigotes... 39

3.3 Experimental Procedures: Macrophage Immune Responses... 39
3.3.1 Dihydrorhodamine (DHR) assay for measurement of respiratory burst... 39

3.3.2 Griess reaction for measurement of nitric oxide production... 40
3.3.3 Analysis of iNOS mRNA... 41
3.3.3.1 RNA Isolation... 41
3.3.3.2 Reverse-transcriptase based PCR... 43
3.3.3.3 Primers... 43
3.3.3.4 Polymerase chain reaction (PCR)... 44
3.3.3.5 Gel electrophoresis and staining for visualization of bands... 44
3.3.4 Analysis of iNOS protein... 45
3.3.4.1 Protein isolation... 45
3.3.4.2 Protein quantification... 45
3.3.4.3 Separation of proteins by SDS-PAGE... 46
3.3.4.4 Transfer and immunoblotting... 46
3.3.4.5 Colorimetric and fluorescent detection of protein... 47
3.3.4.6 Staining of SDS-PAGE gels... 47
3.4 Experimental Procedures: Macrophage Physiology... 47
3.4.1 Bis-oxonol assay for analysis of changes in membrane potential (V_m)... 47
3.4.2 Rubidium influx experiments to measure K^+ flux... 48
3.4.3 Analysis... 50

Chapter 4: Effect of K^+ Channel Blockers on Macrophage Effector Functions During *Leishmania major* Infection... 51
4.1 Introduction... 51
4.1.1 Respiratory burst response... 52
4.1.2 Nitric oxide production... 53

4.2 Determination of Macrophage Respiratory Burst Activity... 55
4.2.1 Experimental design and objectives... 55
4.2.1.1 Effect of K^+ channel blockers on respiratory burst activity of macrophages... 55

4.2.1.2 Effect of K^+ channel blockers and *L. major* infection on respiratory burst of macrophages.................. 55
4.2.1.3 Effect of latex bead phagocytosis on respiratory burst of macrophages.................. 56
4.2.2 Analysis.................. 56
4.2.3 Results.................. 56
4.3 Determination of Macrophage Nitric Oxide Production.................. 63
4.3.1 Experimental design and objectives.................. 63
4.3.1.1 Constructing the standard curve for the Griess reaction for NO production.................. 63
4.3.1.2 Effect of increasing extracellular K^+ on NO production by P388D.1 macrophages.................. 63
4.3.1.3 Effect of K^+ channel blockers on NO production by macrophages.................. 63
4.3.1.4 Effect of *L. major* on NO production by activated macrophages.................. 64
4.3.1.5 Effect of LPG on NO production by activated macrophages.................. 64
4.3.1.6 Effect of combined treatments with *L. major* and K^+ channel blockers on NO production by activated macrophages.................. 65
4.3.1.7 Expression of iNOS mRNA in P388D.1 cells.................. 65
4.3.1.8 Quantification of iNOS enzyme in P388D.1 cells.................. 66
4.3.2 Analysis.................. 66
4.3.3 Results.................. 67
4.4 Discussion.................. 89

Chapter 5: Effect of K^+ Channel Blockers on Macrophage Membrane Physiology During *Leishmania major* Infection.................. 96

5.1 Introduction.................. 96
5.2 Determination of Changes in Macrophage Membrane Potential.................. 98
5.2.1 Experimental design and objectives.................. 98
5.2.1.1 Estimating and calibrating macrophage V_m.................. 98
5.2.1.2 Effect of K^+ channel blockers on V_m.................. 100
5.2.1.3 Reversibility of altered V_m by removal of K^+ channel blockers.................. 100
5.2.1.4 Effect of *L. major* infection on V_m.................. 101
5.2.2 Analysis.................. 101
5.2.3 Results.................. 102

5.3 Determination of Changes in Macrophage K^+ Flux.................. 112
5.3.1 Experimental design and objectives.................. 112
5.3.2 Analysis.................. 112
5.3.3 Results.................. 112

5.4 Discussion..116

Chapter 6: General Discussion..121
6.1 Discussion..121
6.2 Future Directions..129

Literature Cited..132

Appendix 1: Reagent recipes..148

Curriculum vitae...153

List of Tables

Table 2-1. The major surface molecules expressed by *Leishmania* parasites……… 32

List of Figures

Figure # Page

Figure 2-1. Life cycle of *Leishmania major*.. 31

Figure 2-2. General structure of potassium channels...................................... 33

Figure 4-1. Effect of *Leishmania major* promastigotes or latex beads on the respiratory burst of P388D.1 macrophage-like cells.. 59

Figure 4-2. Effect of the potassium channel blocker 4-AP and *Leishmania major* promastigotes on the respiratory burst of P388D.1 macrophage-like cells.. 60

Figure 4-3. Effect of the potassium channel blocker 4-AP and *Leishmania major* promastigotes on the respiratory burst of bone marrow-derived macrophages... 61

Figure 4-4. Effect of the potassium channel blocker 4-AP and *Leishmania major* amastigotes on the respiratory burst of P388D.1 macrophage-like cells. 62

Figure 4-5. Calibration of the nitric oxide assay (Griess reaction) using sodium nitrite.. 73

Figure 4-6. Effect of increased extracellular K^+ on NO production by P388D.1 macrophage-like cells... 74

Figure 4-7. Effect of various K^+ channel blockers on NO production by P388D.1 macrophage-like cells... 75

Figure 4-8. Effect of increasing doses of 4-AP on NO production by P388D.1 macrophage-like cells... 76

Figure 4-9. Effect of 4-AP washout on NO production by P388D.1 macrophage-like cells.. 77

Figure 4-10. Effect of increasing doses of 4-AP on NO production by bone marrow-derived macrophages... 78

Figure 4-11. Effect of TEA on NO production by bone marrow-derived macrophages.. 79

Figure 4-12. Effect of quinine on NO production by bone marrow-derived macrophages....80

Figure 4-13. Effect of simultaneous activation and infection versus 3-hour pretreatment with *Leishmania major* promastigotes or 4-AP on NO production by P388D.1 macrophage-like cells....81

Figure 4-14. Effect of *Leishmania major* promastigote-to-macrophage ratio on NO production by P388D.1 macrophage-like cells....82

Figure 4-15. Effect of *Leishmania* lipophosphoglycan (LPG) on NO production by P388D.1 macrophage-like cells....83

Figure 4-16. Effect of *Leishmania major* amastigote-to-macrophage ratio on NO production by P388D.1 macrophage-like cells....84

Figure 4-17. Effect of *Leishmania major* promastigotes and 4-AP on NO production by P388D.1 macrophage-like cells....85

Figure 4-18. Effect of *Leishmania major* promastigotes, alone or in combination with 4-AP, on NO production by bone marrow-derived macrophages....86

Figure 4-19. Effect of *Leishmania major* or 4-AP on iNOS mRNA expression in P388D.1 macrophage-like cells....87

Figure 4-20. Effect of *Leishmania major* or K^+ channel blockers on iNOS enzyme availability in P388D.1 macrophage-like cells....88

Figure 5-1. Effect of increased extracellular K^+ and gramicidin on membrane potential of P388D.1 macrophage-like cells....105

Figure 5-2. Calibration of membrane potential as changes in bis-oxonol fluorescence of P388D.1 macrophage-like cells....106

Figure 5-3. Effect of increasing doses of 4-AP on membrane potential of P388D.1 macrophage-like cells....107

Figure 5-4. Effect of 4-AP on membrane potential of P388D.1 macrophage-like cells....108

Figure 5-5. Effect of 4-AP and *Leishmania major* promastigotes on membrane potential of P388D.1 macrophage-like cells....109

Figure 5-6. Effect of *Leishmania major* promastigotes, alone or in combination with 4-AP, on membrane potential of bone marrow-derived macrophages....110

Figure 5-7. Flow cytometric profile of macrophages and *Leishmania major*......... 111

Figure 5-8. Time course of radiolabeled rubidium uptake into P388D.1 macrophage-like cells.. 114

Figure 5-9. Effect of *Leishmania major* promastigotes and 4-AP on the unidirectional flux of radiolabeled rubidium in P388D.1 macrophage-like cells........ 115

List of Abbreviations

4-AP: 4-aminopyridine

ATCC: American Type Culture Collection

APC: Antigen-Presenting Cell

BMDM: Bone Marrow-Derived Macrophage(s)

bp: Base Pairs

BSA: Bovine Serum Albumin

cDNA: Complementary Deoxyribonucleic Acid

DEPC: Diethyl Pyrocarbonate

DHR: Dihydrorhodamine

DMEM: Dulbecco's Modified Eagles Medium

DMSO: Dimethyl Sulfoxide

FBS: Fetal Bovine Serum

FDA: Fluorescein Diacetate

GIPL: Glycoinositolphospholipid

GM-CSF: Granulocyte-Macrophage Colony Stimulating Factor

IFNγ: Interferon Gamma

IL: Interleukin

iNOS: Inducible Nitric Oxide Synthase

L-CCM: L-929 Cell-Conditioned Medium

kDa: Kilodalton

$[K^+]_e$: Concentration of Extracellular Potassium

LPG: Lipophosphoglycan

LPS: Lipopolysaccharide

M-CSF: Macrophage Colony-Stimulating Factor

MHC: Major Histocompatibility Complex

mRNA: Messenger Ribonucleic Acid

mV: Millivolts

NO: Nitric Oxide

PAMPs: Pathogen-Associated Molecular Patterns

PBS: Phosphate-Buffered Saline

PCR: Polymerase Chain Reaction
PKC: Protein Kinase C
PMA: Phorbol Myristate Acetate
PMSF: Phenylmethylsulfonylfluoride
PRR: Pattern Recognition Receptor
RFU: Relative Fluorescent Units
RNA: Ribonucleic Acid
RNI: Reactive Nitrogen Intermediates
ROI: Reactive Oxygen Intermediates
SDS-PAGE: Sodium Dodecyl Sulfate Polyacrylamide Gel Electrophoresis
s.e.m.: Standard Error of the Mean
SPF: Specific Pathogen-Free
TAE: TrisHCl-Acetic Acid-EDTA
TE: TrisHCl-EDTA
TEA: Tetraethylammonium
TLR: Toll-Like Receptor

Chapter 1

1.1 Introduction

Macrophages are white blood cells that play a major role in innate host defense, as they are found in nearly all tissues of the body and are capable of engulfing and destroying many types of invading pathogens. All metazoan organisms have cells functionally reminiscent of macrophages. Macrophages act as sentinel cells by constantly surveying and sampling their tissue environment for potential pathogens, and then ingesting foreign material, degrading it, and presenting the peptide antigens of the pathogens to T-helper cells. Therefore, macrophages are involved in the initiation and coordination of both the innate and acquired "arms" of the immune response in mammals, making them crucial mediators of host defense against infectious diseases.

During the innate immune response, macrophages ingest foreign material by phagocytosis and attempt to destroy it by fusing the vacuole formed around the ingested particle with cellular organelles rich in degradative enzymes. Such antimicrobial mechanisms are constituitive as any particle taken into the macrophage will be exposed to the enzymes of the phagocytic process. Inducible mechanisms of macrophage cytotoxicity on the other hand involve an activation cascade consisting of two stages, the priming with an endogenous (self) molecule such as a cytokine and the triggering with an exogenous (non-self) molecule such as a pathogen or pathogen products. Activated macrophages produce a variety of potent cytotoxic molecules, notably the reactive oxygen and nitrogen intermediates (ROI and RNI, respectively) which are important for the destruction of intracellular pathogens.

Paradoxically, pathogens of macrophages have evolved evasion strategies to ensure their survival and replication within the digestive vacuoles of the very cells attempting to destroy them. Studying the interactions between macrophages and the protozoan parasite *Leishmania* provides an excellent model system to study macrophage dysfunction, as *Leishmania* is known to subvert many, if not most, of the cytotoxic responses of macrophages. In order to sustain an infection, intracellular pathogens must avoid the effects of macrophage-derived cytotoxic molecules; accordingly, *Leishmania* has the ability to inhibit macrophage activation by modulating intracellular signaling pathways (1, 2) preventing the production of antimicrobial molecules and pro-inflammatory cytokines (1, 3-5). There is evidence to suggest that pathogen uptake by macrophages alters ion channel function, in particular potassium (K^+) channels, whose main function within macrophages is believed to be the maintenance of resting membrane potential (V_m). In the few studies that have been carried out on the alteration of plasma membrane physiology in pathogen-infected cells, the effector functions of those cells were not examined. Little is known regarding ion homeostasis during various stages of activation of macrophages, and even less clear are the type(s) of ion alterations that occur during infection with intracellular pathogens.

Our laboratory has previously demonstrated that the potassium (K^+) channel inhibitors 4-AP (4-aminopyridine), TEA (tetraethylammonium), and quinine significantly downregulated nitric oxide (NO) production by activated P388D.1 murine macrophage-like cells (6). In the present study, the role of K^+ channels was examined at the interface of the unique relationship that exists between macrophages (either P388D.1 cells or bone marrow-derived macrophages, BMDM) and the obligate intracellular protozoan parasite

Leishmania major. I investigated the potential of *L. major* to evade the immune response by modulation of the host cell's membrane physiology (and hence the potassium channel activity) ultimately resulting in suppression of several key effector functions of macrophages: nitric oxide production and respiratory burst. This thesis attempts to integrate immunological and physiological studies, by examining changes in the NO production and respiratory burst responses of macrophages, as well as changes in macrophage plasma membrane potential (V_m) and K^+ fluxes. It examines how and why those functions of activated macrophages are affected by K^+ channel blockage, and compares this to the changes that occur during infection with *L. major*.

This generalized suppression of activation may be a prerequisite for the survival of *L. major* in macrophages. However, this may not be a universal property of the *Leishmania*-macrophage relationship, as the two types of macrophages examined in this study (P388D.1 and bone marrow-derived macrophages (BMDM)) may differ slightly in terms of the sensitivity, expression, numbers, types, and/or distribution of K^+ channels in their membranes. While the specific K^+ channel repertoire of each macrophage type is unknown, it is apparent that the unique profile of each cell type does influence their basic physiology and effector functions, particularly as examined here under the conditions of *L. major* infection.

1.2 Thesis outline

The first chapter of this thesis gives general background information and will provide a summary and outline of the thesis. Chapter 2 is a literature review of the developmental, morphological, and functional characteristics of macrophages, an overview of macrophage-pathogen interactions, a description of the *Leishmania major* life history and biology, an investigation of how *Leishmania* spp. evade the macrophage cytotoxic responses, and finally, a description of potassium (K^+) channels and their role in macrophage activation. Chapter 3 is a general materials and methods chapter. In Chapter 4 the experimental designs and results of experiments are reported, focusing on the inducible effector functions of macrophages during both K^+ channel blockage and *L. major* infection. In Chapter 5 the experimental designs and results of experiments are reported, focusing on the role of K^+ channels in macrophage physiology during both K^+ channel blockage and *L. major* infection. Chapter 6 is a synthesis of the results from the previous chapters. A mechanism is proposed by which ion channels may be involved in macrophage activation, comparing murine macrophage-like cells and bone marrow derived macrophages. The results are discussed as they pertain to the downregulation of macrophage cytotoxic responses during *L. major* infection.

Chapter 2: Literature Review

Cells of the macrophage lineage are host to fungal pathogens (*Cryptococcus neoformans*), numerous bacterial pathogens (*Mycobacterium tuberculosis*, *Salmonella* spp., *Legionella* spp., *Listeria monocytogenes, Brucella suis*) and protozoan pathogens (*Toxoplasma gondii*, *Trypanosoma cruzi*, *Leishmania* spp.) (7-9). This Chapter examines the primary functions of macrophages, linking the mechanisms of pathogen recognition and uptake (via phagocytosis) to the induction of specific effector functions. *Leishmania major* was used as an example of a well-studied model of macrophage infection resulting in impaired activation, and in this Chapter attention is given to the biology of the parasite and the clinical aspects of the disease. The evasion strategies of *Leishmania* spp. that allow survival within macrophages are discussed, with particular emphasis on the role of potassium channel modulation in macrophage activation, and how that modulation might be exploited by *L. major* to allow its survival.

2.1 Macrophages

2.1.1 Origin of macrophages

Very early in the formation of blood cells in mammals, a bone marrow stem cell differentiates along one of two pathways, becoming either a lymphoid progenitor cell or a myeloid stem cell (10). These cells are capable of forming a multitude of blood cell types depending on the types of stimuli present in the immediate stromal environment, namely cytokines and growth factors such as interleukins (IL) and colony stimulating factors

(10). In the presence of interleukins-3 and -6 and GM-CSF (granulocyte-macrophage colony stimulating factor), myeloid stem cells differentiate to form the granulocyte-monocyte family of cells (10) which are committed to giving rise to monocytes, neutrophils, dendritic cells, or macrophages, depending on the amounts and types of growth factors and cytokines available. Granulocyte-monocyte progenitors do not have a capacity for self-renewal. They differentiate into promonocytes, which leave the bone marrow and enter the bloodstream to circulate as monocytes (10). After about 8 hours monocytes leave the blood, enter the tissues, and differentiate into macrophages mainly under the influence of M-CSF (macrophage colony stimulating factor). M-CSF is the most important cytokine leading to macrophage maturation. It is synthesized by endothelial cells, fibroblasts, bone marrow stromal cells, osteoblasts, keratinocytes, astrocytes, and other cell types (11).

The straightforward developmental pathway belies the complexity of macrophages; they are actually a very heterogeneous group of cells (12). Macrophages are larger and much more complex than blood monocytes; they have greater phagocytic ability and are much richer in lysosomes (10). Unlike the transient and non-proliferating monocyte-derived macrophages, tissue (resident) macrophages have the capacity to proliferate and maintain their population by self- renewal (13). It is the resident tissue macrophages that form the mainstay of the non-specific immune response. Quiescent macrophages are responsible for surveillance of the immediate tissue environment and are the first line of defense against foreign material, including pathogens and the body's own transformed cells or tumours. While their main role is in non-specific host defense, macrophages are also essential in wound repair, tissue remodeling, and iron metabolism (12).

2.1.2 Constituitive effector functions of macrophages

2.1.2.1 *Phagocytosis and lysosomal enzymes*

Because they are a major functional cell type during the innate immune response, the primary function of macrophages is the non-specific uptake of foreign material (including pathogens) by phagocytosis, a process considered to be the primordial defense mechanism of all metazoan organisms (9).

Phagocytosis has a number of defined stages. First there is attachment of foreign material to extended membrane extensions called pseudopodia (10). The uptake of foreign material is mediated by two main surface receptors on macrophages, the FcR and CR3, depending on whether the material is coated in antibody or complement, respectively ((14) and references therein). This initial receptor-ligand interaction is followed by the ingestion of the particle through invagination of the plasma membrane to form a “phagocytic cup”. Recent studies indicate that the endoplasmic reticulum of macrophages contributes greatly to the supply of membrane needed for the uptake of large particles; such “ER-mediated phagocytosis” appears to be a widely used mechanism of entry into macrophages (15). The phagocytic cup seals off to form a large, complex vesicle called a phagosome containing over 250 different proteins (15, 16).

The phagosome eventually moves toward and fuses with a lysosome, a cellular organelle rich in degradative enzymes such as lysozyme, acid phosphatases, peroxidases, hydrolases, nucleases, neutral proteases, lipases, and esterases (17). A highly unique type of membrane-bound vesicle called a phagolysosome is formed from the fusion of the phagosome and lysosome. The "internal milieu" of the phagolysosome is a lethal environment to most microbes but some bacterial and protozoan pathogens, remarkably, do survive and replicate within the phagolysosomes. Normally, the release of lysosomal enzymes into the phagolysosome initiates the digestion (degradation) of ingested material (10). Digested products are eventually released from the cell, or presented to helper T-cells as described below.

2.1.2.2 *Antigen presentation*

Macrophages are called professional antigen-presenting cells (APCs) because they have the ability to present antigens (peptides) from digested pathogens on their surface via the MHC II (major histocompatibility complex type 2) receptor. The display of peptides in the context of MHC II alerts and recruits helper T-cells which begin a precisely choreographed cell-mediated attack against the foreign intruder. In this manner, macrophages are an important link between the innate and specific immune responses.

2.1.3 Inducible effector functions of macrophages

Resident tissue macrophages are quiescent while in the tissues. In order to initiate and engage their cytotoxic machinery for microbicidal activities, macrophages must become activated. The majority of the work in this thesis focuses on the inducible effector functions of macrophages.

2.1.3.1 *The two-stage model of macrophage activation*

The activation cascade of macrophages has two components. In the "priming" stage macrophages interact with an endogenous (host-derived) molecule such as a cytokine and subsequently enter a state of heightened metabolic activity. During this time, macrophage cytotoxic functions and the machinery associated with those functions may be upregulated or modified, causing the macrophage to become receptive for a specific trigger signal (12). During the priming stage, the cytotoxic machinery is made and readied but no response is executed. The priming signal for the murine macrophages used in this study is IFNγ, normally secreted *in vivo* by helper T-cells.

In the "triggering" stage of activation macrophages execute an appropriate cytotoxic effector response in response to an exogenous (foreign) molecule such as a pathogen or pathogen products. Triggering causes the release of cytotoxic molecules such as reactive oxygen and nitrogen intermediates (ROI and RNI, respectively), which are important for the destruction of intracellular pathogens. The triggering signal for the murine macrophages used in this study is *Salmonella typhimurium* lipopolysaccharide (LPS). Activated macrophages upregulate expression of heat shock proteins, proinflammatory cytokines (such as TNFα, IL-1β, IL-6, IL-12), and cytokine receptors ((9, 12) and references therein) and they dramatically increase their output of cytotoxic molecules.

2.1.3.2 *Production of reactive oxygen intermediates (ROI)*

Certain immune cells undergo a dramatic increase in oxygen consumption upon challenge with phagocytosable particles, or with cell membrane perturbing agents such as chemotactic factors, detergents, lectins, and other cellular ligands. This response, described as a respiratory "burst", is a well-studied antimicrobial mechanism of phagocytic cells such as macrophages, eosinophils, neutrophils, and B-lymphocytes (12). The respiratory burst response in phagocytes can be triggered by a variety of stimuli, including phorbol myristate acetate (PMA), unsaturated fatty acids, leukotrienes, chemoattractants, and receptor-mediated phagocytosis (12).

Reactive oxygen intermediates (ROI) are generally produced early in the cytotoxic response of macrophages and are catabolized by the NADPH oxidase enzyme complex on the plasma membrane. This enzyme transfers protons from NADPH to molecular oxygen, forming potent, highly reactive oxygen products at the site of particle engulfment including superoxide (O_2^-) and breakdown products of superoxide, namely hypochlorous acid (OCl^-), hydroxyl radical ($OH\bullet$), hydrogen peroxide (H_20_2), and peroxynitrite ($ONOO^-$) (9). In macrophages given the appropriate stimuli, the various components of the NADPH oxidase complex are recruited from the cytoplasm and from within the membrane to assemble at the inner surface of the plasma membrane in a process involving protein phosphorylation (18). As a consequence of the enzyme's location in the membrane, ROI can be directed towards either the extracellular environment or towards any pathogens residing in the phagolysosome.

2.1.3.3 *Production of reactive nitrogen intermediates (RNI)*

The reactive nitrogen intermediates include molecules such as nitric oxide, a highly reactive, potent, and freely diffusible gas. Nitric oxide is produced from the catalytic oxidation of the guanidino group of L-arginine by cytoplasmic nitric oxide synthase (NOS) (19). Constituitive, endothelial, neuronal, and inducible isoforms of NOS (cNOS, eNOS, nNOS, and iNOS respectively) have been identified; in activated murine macrophages, high levels of NO are produced following up-regulation of iNOS (20). Inducible NOS is not expressed in resting cells but is induced by three categories of stimuli (21):

1) exogenous or "foreign" products, e.g. bacterial lipopolysaccharide (LPS), lipoarabinomannan from *Mycobacterium*, phorbol ester.
2) endogenous or "self" products, e.g. picolinic acid, tumour necrosis factor alpha (TNFα), interleukin (IL)-1β, and interferon gamma (IFNγ).
3) stressful conditions, e.g. hypoxia (22).

The nitric oxide catalyzed by the iNOS enzyme functions as a both a tumouricidal and an antimicrobial molecule. Nitric oxide also mediates the effects of macrophages on other leukocytes during inflammatory and immune responses (23). It is therefore a molecule of major importance for the cytotoxic ability of macrophages, although other cell types which play a role in the immune response can also be stimulated to produce NO, including fibroblasts, endothelial cells, eosinophils, and neutrophils (12), from various isoforms of NOS.

Since the production of NO must be tightly regulated by the macrophage in order to avoid damage to self or to other cells in the tissue microenvironment, elevated NO acts as a feedback mechanism to control its own production by suppressing iNOS activity (24).

2.1.4 Macrophage-pathogen interactions

The inducible cytotoxic mechanisms discussed above are very effective in eliminating most of the pathogens that choose to reside inside macrophages but there are some parasites that have adapted extremely well to the environment of the macrophage.

2.1.4.1 *Recognition and uptake: how ingesting pathogens leads to macrophage activation*

Receptors on macrophages recognize and bind to pathogen-associated molecular patterns (PAMPs), distinctive configurations of macromolecules found on those species of bacteria, viruses, and protozoans with which macrophages have evolutionarily ancient relationships. These PAMPs are unique enough that they allow macrophages to discriminate between self and non-self (pathogen) molecules. They include ligands such as LPS (Gram negative bacteria), lipoteichoic acids (Gram positive bacteria), lipoarbinomannan (mycobacteria), mannans (yeast), and double-stranded RNA (viruses) (9).

The macrophage receptors that recognize such pathogen molecules are grouped together and classified as pattern recognition receptors (PRRs), which may be soluble or membrane-bound (9). They participate in an array of functions including activation of complement proteins in the serum, opsonization leading to phagocytosis of pathogens, and intracellular signaling leading to cellular activation (9). The opsonin-dependent group of pattern recognition receptors includes the aforementioned CR3 and FcR receptors, which recognize pathogens opsonized by complement component C3 and antibody, respectively, enhancing receptor-mediated phagocytosis of microorganisms.

The opsonin-independent group of PRRs includes such molecules as mannose receptors, which bind pathogen carbohydrates; mannose binding proteins, which recognize molecules with a high percentage of mannose and/or N-acetylglucosamine (e.g. HIV, *Candida albicans, E. coli*); and scavenger receptors (9).

The Toll-like receptors (TLRs) are a special family of pattern recognition receptors that are known to bind to a variety of types and combinations of PAMPs, including bacterial and yeast glycoproteins, double stranded RNA, bacterial flagellin, and CpG DNA (distinct methylated regions of bacterial DNA) which are bound by TLRs 1 or 2, 3, 5, and 9, respectively. Another TLR plays a major role in macrophage activation when lipopolysaccharide (LPS) and the LPS-binding protein (LBP), along with membrane-intercalated CD14, bind to a toll-like receptor called TLR4 which initiates activation through the intracellular signaling domain or "tail" of TLR4. Together, the TLR4, CD14, and several accessory proteins (including MyD88 and MD-2) form the LPS activation cascade or LACK. This is a signaling complex of central importance in macrophage activation (25) through the NF-κB and MAPK cascades (9), ultimately resulting in production of cytokines, chemokines, and cytotoxic intermediates (ROI and RNI).

2.1.4.2 *Intracellular signaling in macrophages*

The various steps involved in pathogen internalization lead to complex signaling cascades, culminating in activation of macrophages for a killing response. "Priming" and "triggering" stimuli cause macrophages to initiate a cascade of signaling events that culminates in altered gene expression. There are three main pathways of intracellular signaling (reviewed in (26)): those involving activation of mitogen-activated protein (MAP) kinases; those involving protein kinases and phospholipases leading to production of the second messengers diacylglycerol (DAG) and IP_3 (inositol (1,4,5)-triphosphate); and those involving the association of small Ras-like guanosine triphosphate binding proteins (G-proteins) with cytokine receptors, also resulting in production of DAG and IP_3. The second messengers DAG and IP_3 directly activate protein kinase C (PKC) enzymes and release intracellular calcium, respectively, to further activate PKC and other signaling intermediates.

Protein kinase C is an 80 kDa enzyme that is recruited from the cytoplasm to the plasma membrane by DAG and, in many cases, by calcium. The enzyme is activated by DAG and phospholipid and undergoes a conformational change upon binding to the membrane. PKC modifies target proteins at tyrosine, serine, or threonine residues. The end result is phosphorylation of a variety of proteins involved in controlling growth and cellular differentiation. The activation of macrophages under the conditions described in this thesis ("priming" and "triggering" with IFNγ and LPS) involves mainly the protein kinase C pathway. Protein kinase activity is important for phagosome-lysosome fusion, respiratory burst, and production of inflammatory mediators (9). Nuclear transcription factors induced by the PKC enzymes and involved in upregulation of inflammatory gene expression include c-fos and NFκB. The regulatory factor NFκB translocates to the nucleus where it binds to enhancer or promoter regions on a number of LPS-inducible genes, including TNFα, various interleukins, GM-CSF and M-CSF, and iNOS. Phagocytosis alone is known to modulate numerous signaling intermediates, including lipid kinases (e.g. phosphatidylinositol 3-kinases or PI3Ks), protein kinases (e.g. Syk), phospholipases (e.g. phospholipase C), and GTPases (e.g. Rac) (14).

2.2 *Leishmania*: An Intracellular Parasite of Macrophages

Perhaps the most studied of the macrophage-pathogen relationships is the one that exists with protozoans of the genus *Leishmania*. This relationship is exquisitely complex and is quite interesting from an immunological perspective. *Leishmania* has parasitized the very cell type whose primary function is to ingest and destroy pathogens. *Leishmania* spp. persist in the intact phagolysosome where they depend on their immune evasion mechanisms to survive. To sustain an infection within the harsh environment of macrophages, *Leishmania* has evolved strategies to inhibit the macrophage activation cascade and prevent the formation and release of cytotoxic products (e.g. ROI and RNI) and pro-inflammatory cytokines (1, 27, 28). The parasite's biology and its ability to evade most of the immune responses of the macrophage will be discussed in detail in the following sections.

2.2.1 The leishmaniases

Leishmaniasis is a parasitic disease of humans and other mammals. It is endemic in 88 countries on 5 continents (29). The causative agents, *Leishmania* spp., are obligate protozoan parasites (order Kinetoplastida, family Trypanosomatidae) of macrophages which are directly transmitted from infected host to naïve host by an insect vector. Humans and animals (wild and domesticated) can act as a reservoir of infection (29).

Members of the *Leishmania* genus are unique among the group of pathogens that parasitize cells of the macrophage lineage in that the development and completion of the life cycle within the definitive host is restricted to macrophages (9).

The clinical manifestation of this parasitic disease depends not only on the particular species of *Leishmania*, but also on the type of tissue hosting the parasite, the immune status of the host, the genetic predisposition of the host, and the type of immune response elicited by the host (9, 30). The uncontrolled spread of the parasite from macrophage to macrophage in the tissues results in the disease called leishmaniasis. The infection manifests clinically as one of three main types of leishmaniasis: a relatively mild and localized dermal or cutaneous form; a severe, disfiguring mucocutaneous form characterized by destruction of the mucous membranes of the nose and mouth; and a systemic, debilitating, and often fatal visceral form in which splenic and hepatic macrophages become infected.

Infections with *Leishmania braziliensis* (subgenus Vianna) and *L. donovani* cause mucocutaneous and visceral leishmaniasis, respectively. The mucocutaneous disease (Central and South America), is sometimes called *espundia* and is characterized by infection of macrophages in the mucous membranes of the nose, lips, throat, and hard and soft palate. The visceral type of leishmaniasis is often called "New World Leishmaniasis", but is also known as kala-azar and dum-dum fever. It is characterized by parasitic infection of liver and spleen macrophages, with enlargement of these organs leading to a condition known as hepatosplenomegaly. More than 90% of visceral leishmaniasis cases occur in Bangladesh, Brazil, India and Sudan (29). A more aggressive and disfiguring form of the disease, called post kala-azar dermal leishmaniasis

(PKDL), is increasingly recognized in Sudan as a complication of visceral leishmaniasis, appearing in about half of patients after or during treatment (31). This manifests as a diffuse sort of cutaneous leishmaniasis producing disseminated and chronic skin lesions resembling those of leprotamous leprosy (29).

The parasite I used in this study (*Leishmania major*) causes the cutaneous type of leishmaniasis. This type is often called "Old World Leishmaniasis" but is variously known as Oriental sore, Baghdad ulcer, Jericho boil, Allepo boil, or Delhi boil. More than 90% of cutaneous leishmaniasis cases occur in Iran, Afghanistan, Syria, Saudi Arabia, Brazil and Peru (29). Depending on geography the cutaneous form of leishmaniasis may be caused by parasites of the "Tropica complex" including *L. tropica* (Ethiopia, Kenya, North Africa, the Middle East, India, the European Mediterranean) and *L. mexicana* (South America) or the "Major complex" including *L. major* (North Africa, the Middle East, West India, Sudan) (32). Cutaneous leishmaniasis presents as a localized sore, ulcer, or lesion at the site of a sandfly bite, where resident tissue macrophages have become infected. In immunocompetent hosts and in the absence of any secondary bacterial infections the lesion heals spontaneously within several months and provides the host with life-long immunity to re-infection. Even though the infection is usually a self-limiting one, the lesion often leaves a depressed, unpigmented scar (33). Of the 1.5 to 2 million new cases of leishmaniasis estimated to occur annually, the cutaneous type makes up 50 to 75% of cases (34).

Some species of the parasite may be clinically associated with more than one type of leishmaniasis. For example *L. infantum* and *L. chagasi* may be associated with either cutaneous or visceral leishmaniasis, and *L. aethiopica* and *L. braziliensis* (subgenus Vianna) may be associated with either cutaneous or mucocutaneous leishmaniasis (35).

2.2.2 Life history of *Leishmania major*

The *L. major* life cycle involves two developmental stages (Fig. 2-1). During the first stage the extracellular infective form (promastigote) is transmitted in the saliva of an insect vector, the sandfly (Family Psychodidae, subfamily Phlebotominae), during a blood meal on a suitable mammalian host. The species of sandflies capable of transmitting *Leishmania* spp. include *Phlebotomus* spp. (in the "old world") and *Lutzomyia* spp. (in the "new world"). In the case of *L. major* infection, *Phlebotomus papatasi* is the most frequent vector. The specificity of the vector-parasite relationship is partly limited by the geographic distribution of the sandfly, and partly limited by the sandfly's capacity to support the internal development of only select species of *Leishmania* (34). Sandflies are naturally refractory to *Leishmania* infection and, as such, only those parasites that have evolved to survive the proteolytic conditions within the blood-fed gut of certain species of sandfly are the parasites that will develop in that vector (36). Differences in vector competence might also be due to differences in parasite attachment to sandfly mid-gut epithelial cells (36) mediated by the parasite's main surface molecule, lipophosphoglycan (LPG).

Female blood-feeding sandflies carrying the parasite regurgitate a bolus of the flagellated promastigotes during a blood meal on a suitable host. The promastigotes that are injected into the host have a single anterior flagellum and are 10 to 15 μm in length and 1 to 2 µm in diameter. Certain molecules in the sandfly saliva enhance the initial uptake of the parasite. For example, the saliva of *Lutzomyia longipalpis* contains maxadilan, a potent vasodilatory and immunomodulatory protein (37). Co-injections of sandfly maxadilan and *L. major* have been shown to enhance the virulence of the parasite in mice (37).

During the second stage of the *L. major* life cycle, the injected parasite targets host macrophages, where it utilizes both the innate function of the macrophages, phagocytosis, and the specific macrophage receptor-*Leishmania* ligand interactions to facilitate its uptake (9, 38). Inside its host cell, the parasite transforms into the spheroid replicating form called an amastigote, which is 2 to 5 µm in diameter and aflagellate (non-motile).

When a sandfly takes a blood meal from an infected host, circulating host macrophages containing amastigotes are taken up and lysed by digestive enzymes, and the parasite goes through a number of developmental and morphological stages in the vector. Most of the (asexual) replication of promastigotes takes place in the sandfly midgut. Eventually there is blockage of the gut (35) resulting in the movement of parasites forward into the pharynx and buccal cavity of the sandfly. Feeding inoculates parasites into a new mammalian host, continuing the life cycle.

2.2.3 *Leishmania*-macrophage interactions: evasion of host immune response

2.2.3.1 *Life in the bloodstream: evasion of serum complement proteins and antibodies*

Many of the very early innate immune responses (e.g. complement-mediated lysis) are ineffective against *Leishmania*. In fact, *Leishmania* promastigotes profit from the fixation of serum complement protein C3 onto their surface coat because it increases their uptake into macrophages through the CR3 receptor (9).

Because *Leishmania* is ultimately an intracellular parasite, exposure to the host's humoural-mediated response is significantly reduced, and any antibodies produced against the parasite will be ineffective. Furthermore, helper T cells of the Th1 subset generally associated with a cell-mediated immune response lead to protection against leishmaniasis, while Th2 expansion associated with the humoural (antibody-mediated) response leads to exacerbation of the disease (39).

The ability of pathogens to prevent respiratory burst initiation has been studied in detail in the *Leishmania*-macrophage model system. To enter the macrophage, *Leishmania* uses complement receptors which do not induce respiratory burst activity (38). The ability of *Leishmania* to evade the respiratory burst of macrophages is examined in more detail in Chapter 4.

2.2.3.2 *Parasite recognition and uptake into macrophages*

Because they face different environments, *Leishmania* spp. promastigote and amastigote surfaces are quite different (Table 2-1, adapted from (33, 40, 41). The macrophage receptors involved in binding and internalization of *Leishmania* spp. include receptors capable of recognizing self or non-self molecules, receptors such as mannose-fucose receptor (MFR), complement receptors (CR1, CR3, and CR4), advanced glycolysation endproduct receptor (AGE-R), fibronectin receptor (FnR), and Fc receptor (FcR) (33). These receptors are utilized as an entry point for the parasite. Once bound, promastigotes are rapidly ingested via phagocytosis.

Most intracellular pathogens of macrophages must devise a strategy to withstand the maturation of their vacuole into a phagolysosome. They may do this by "redirecting traffic" (42) in one of several key ways. Some pathogens inhibit lysosomal fusion with the phagosome (*Toxoplasma gondii*), others prevent phagocytic digestion by lysing the vacuole and escaping to the cytoplasm (*Trypanosoma cruzi*), and some actively modify the vacuole (pH, etc.) to suit their lifestyle (*Salmonella typhimurium*, *Brucella suis*) (43). A very few pathogens, like *Leishmania* spp., do none of the above and rely solely on their ability to subvert the host's inducible cytotoxic responses.

2.2.3.3 *Encountering the macrophage cytotoxic molecules*

In order for *Leishmania* to survive and reproduce, the macrophage cytotoxic mechanisms set in motion by the phagocytosis and internalization of the parasite must be subverted or prevented. *Leishmania* parasites possess molecules such as LPG (lipophosphoglycan) and GIPLs (glycoinositolphospholipids) that suppress NO production. LPG is an especially potent immunomodulatory protein. It down-regulates macrophage TNFα receptors (44) and inhibits PKC activity (45). LPG can also inhibit IL-12 synthesis, indirectly blocking the induction of iNOS (46) because IL-12 causes the maturation and differentiation of helper T-cells, which in turn produce IFNγ to prime macrophages. The proportion of LPG to GIPLs changes with the development of the parasite, with LPG being primarily expressed in the promastigote stage of the life cycle.

2.2.3.4 *Propagation of infection*

Certain surface molecules on *Leishmania* spp. promastigotes (e.g. LPG) help delay the apoptotic death of the macrophage (47), but only long enough to allow sufficient replication. The parasites do eventually destroy the macrophage and it is during necrotic cell death that the amastigotes are released to infect surrounding macrophages, propagating the infection. Furthermore, at this stage in the infection process there is significant inflammation at the lesion site, and as such, many of the cells recruited to the site are macrophages obviously offering a significant advantage to the parasite. In cutaneous leishmaniasis, parasite-laden macrophages are found in the dermis where the inflammatory response recruits lymphocytes, plasma cells, other macrophages, and various antigen-presenting cells (APCs) (30), with Langerhans cells being the main APC in cutaneous leishmaniasis (30). In studies using a murine air pouch system to simulate an inoculation site during a sandfly bite, mice injected with *L. major* quickly and transiently recruited a mixed population of leukocytes to the site, an infiltration of over 30 times more leukocytes than in control mice injected with endotoxin-free PBS (48).

2.2.4 Survival of *L. major* in macrophages: alteration of ion channel activity?

It is well established that *Leishmania* spp. parasites have evolved evasion strategies to ensure survival and replication within the phagolysosomes of macrophages.

Leishmania spp. surface molecules are known to perturb the macrophage membrane, presumably resulting in impaired signal transduction (49).

Potassium channel blockage also results in a dampened cytotoxic response by macrophages (6). Like many *Leishmania* surface molecules, potassium channel blockers are lipid-soluble, membrane-permeant, and alter the intracellular signaling pathways involved in macrophage activation.

It is therefore probable that one of the ways in which the parasite impairs macrophage activation is by altering the function of macrophage potassium channels. A description of potassium channels and their identified roles in macrophage physiology and immunology follows.

2.3 Ion Channels

2.3.1 General structure and function of ion channels

Ion channels are protein molecules embedded in the lipid bilayer of cells, forming pores or channels (50) that allow certain inorganic ions to flow in or out depending on the channel's selectivity, the ion concentration gradient, or the charge across the membrane (51). Ion channels open and close in response to a number of stimuli, including pH changes, ligand binding, and plasma membrane depolarization (52). The resting state of most ion channels is closed. Potassium (K^+) and chloride (Cl^-) are the most concentrated and most permeant ions in tissues, and the concentration of K^+ is ten- to twenty-fold higher in the cell interior than in the extracellular environment (51). The flow of ions through ion-selective channels constitutes an electric current (51).

2.3.2 Potassium (K^+) channels

2.3.2.1 *Major classes of K^+ channels*

The four major functional classes of K^+ channels in cells are ((53) and references therein):

i. voltage dependent K^+ channels (KV) activated by depolarization of the membrane
ii. large (MaxiK) Ca^{2+} activated K^+ channels
iii. small (SK) Ca^{2+}-activated K^+ channels
iv. sodium activated K^+ channels

In human and mouse monocytes and macrophages, there are MaxiK, KV, SK, inwardly rectifying K^+ (KIR) channels (54), outwardly rectifying K^+ (KOR) channels, and delayed rectifier channels, in addition to conductances for other ions such as chloride, protons, and non-specific cations ((26) and references therein). The expression and activity of K^+ channels varies depending on cell origin and culture conditions such as serum availability, time in culture, and adherence (23, 55-57). Furthermore, macrophages may change their K^+ channel expression in response to stimuli such as LPS, PMA, M-CSF, GM-CSF, and infection with certain intracellular parasites (*L. amazonensis*) (53, 58, 59). Over the short term, K^+ channel function may be altered by PAF (platelet activating factor), hsp70, G protein activators, inositol, or zymosan ((53) and references therein).

2.3.2.2 *Structure of K^+ channels*

All potassium channels have transmembrane helices, a selectivity filter, a gate, and an ion pathway or pore. The crystallographic structure of the K^+ channel from *Streptomyces lividans* (KcsA) was elucidated in 1998 (60). This paper was extremely influential, as it contained the first detailed description of the structure of a K^+ channel, and has since been used as a modeling template for studies of a wide array of K^+ channel types (52). Although the physiological properties of K^+ channels might differ (i.e. permeation, gating, and modulation), the KcsA channel is structurally very similar to eukaryotic K^+ channels (61) and therefore provides an excellent model for general K^+ channel structure. The findings of Doyle *et al.* (60) are described below.

The KcsA K^+ channel is a tetramer with four identical subunits, two of which span the membrane (60). The "inverted teepee" or "cone" portion has the selectivity filter at its wide end facing the extracellular environment. The central cavity is filled with water. The selectivity filter is lined with carbonyl oxygen atoms, forming a "cationic core" the diameter of which allows K^+ ions, but not the slightly smaller Na^+ ions, to be transported snugly through the pore two at a time (60). This finding highlights an important feature of a cell's lipid bilayer: it can distinguish ions of approximately the same size and shape. In other words, Na^+ and K^+ are almost the same size yet the resting membrane is much more permeable to K^+ (51). Potassium channels are sometimes called "long pore channels", giving the idea that many ions can line up inside a long, narrow channel in a single line as was shown in the study by Doyle *et al.* (60).

The gate of the KcsA K^+ channel is formed by the inner helix bundle (60). This structure favours K^+ transport by exploiting electrostatic forces which work to repel K^+

ions from the selectivity filter. Potassium channels use many different gating mechanisms but they all exhibit very similar ion permeability characteristics (62).

A recent paper by this same group showed that the prokaryotic channel KcsA channel is functionally and structurally similar to eukaryotic KV (voltage-gated potassium) channels (63) found in neurons. KV channels are thought to contain six membrane-spanning helices per subunit (S1–S6). Of these six, S1 to S4 comprise the selectivity filter, whereas S5 and S6 comprise the K^+-selective pore. Opening of the channel is driven by the movement of arginine residues on S4 (64). Four identical subunits encircle a central ion pathway. A glycine residue in S6 serves as the "hinge", allowing the pore to open (63). This description forms the basis for the figure depicting general potassium channel structure (Figure 2-2).

The structure of another type of potassium channel, the inwardly rectifying potassium (KIR) channel, is discussed here because it is particularly relevant to the work presented in this thesis. KIR channels are used in setting the membrane potential in most cells (50). These channels preferentially conduct potassium into a cell, and appear to have a unique structure. Eukaryotic KIR channels are tetramers of two similar membrane helices spanning the lipid bilayer (akin to the bacterial KcsA channel subunits) and surrounding a central ion conduction pathway ((65) and references therein) but this pore is nearly double the length of the pores of other K^+ channels (65). Furthermore, polar residues like glutamate and asparagine supply an environment that has an overall negative electrostatic potential meaning that potassium ions will tend to concentrate there, leading to increased conductance (65). The ion pore of KIR channels conducts K^+ at negative membrane potentials but not at positive potentials (65).

2.3.2.3 *Pharmacological blocking of K^+ channels*

The three potassium channel blockers used in the experiments throughout this thesis are tetraethylammonium (TEA), 4-aminopyridine (4-AP), and quinine. These are classical K^+ channel blockers whose pharmacology is described below.

TEA is a non-selective potassium channel blocker. The TEA^+ cation binds at the outer mouth of the selectivity filter of KcsA K^+ channels, stabilized by electrostatic and hydrophobic interactions with the four Tyr82 side chains (66). The K^+ channel blocker 4-AP (4-aminopyridine; 4-pyridinamine; fampridine) is a non-selective K^+ channel blocker. It is lipid-soluble and therefore crosses the plasma membrane and exerts its action intracellularly. 4-AP blocks voltage-dependent K^+ channels at two putative receptor sites on the channel's alpha (α) subunit on the cytosolic side of the membrane (67). In macrophages, 4-AP has been shown to block the pore of delayed rectifer type K^+ channels (reviewed in (26)). Quinine blocks potassium channels in a manner similar to 4-AP, as it is also membrane-permeant. It blocks a wide variety of macrophage K^+ channel types, including delayed rectifier, calcium-sensitive, and ATP-sensitive channels (reviewed in (26)).

For each of these drugs, the exact inhibitor concentration for half-maximal inhibition (IC_{50}) of any particular K^+ channel varies from one type of K^+ channel to another ((26) and references therein). Published IC_{50} values for TEA, 4-AP, and quinine are 0.6 mM, 1.2 mM, and 50 μM respectively, for nitric oxide production in goldfish macrophages (68).

2.3.3 Functions of K$^+$ Channels

2.3.3.1 *Evidence for the role of K$^+$ channels in macrophage physiology*

Macrophages mainly use their K$^+$ channels to set the plasma membrane potential. Because resting cell membranes are most permeable to K$^+$ and Cl$^-$, the resting potential of most cells is typically close to the equilibrium potentials of those two ions, generally between -40 and -100 mV where the inside of the cell is negative with respect to outside (51). In macrophages, K$^+$ channels set the membrane potential at a value between -30 and -56 mV (54). Blocking K$^+$ channels results in the membrane potential drifting to a more depolarized state (such that the charge difference between the intracellular and extracellular environments is closer to the resting potential "0"). Consequences of changes in intracellular [K$^+$] may include alterations in [Ca^{2+}], impaired activation of enzymatic reactions, and alteration of gene expression.

2.3.3.2 *Evidence for the role of K$^+$ channels in macrophage immune responses*

It has been established that macrophages and other immune cells possess a number of ion channel types that are important for their cytotoxic functions. There is a growing body of evidence to suggest that K$^+$ channels in particular are important for the effector functions of immune cells. While this thesis will focus on the role of K$^+$ channels in macrophage activation, it is worth noting that other immune cells also demonstrate a requirement for functional K$^+$ channels to become fully activated. For example, neutrophil depolarization after exposure to K$^+$ channel inhibitors results in reduced production of ROI (69, 70). Potassium channels are also known to play a role in mast cell degranulation, as blockage of K$^+$ channels with such agents as quinine, 4-AP, and sparteine induces the release of histamine (71, 72). Natural killer cells are unable to kill target cells when treated with K$^+$ channel blockers (73).

Functional potassium channels are likely involved in the ability of macrophages and macrophage-like cells to carry out an effective cytotoxic response. Quinine, TEA, and barium chloride, inhibited TNFα production by IFNγ-primed, LPS-activated macrophages (74, 75). Quinine also prevents the release of TNFα from the murine macrophage-like cell line RAW 269 (74). Stimulated macrophages exposed to K$^+$ channel blockers demonstrate reduced NO, suggesting a role for K$^+$ channels in macrophage activation and NO production (6). It has also been shown that addition of bacterial lipopolysaccharide (LPS) to J774 macrophage-like cells changes the density of inwardly-rectifying potassium (KIR) channels (76). Production of TNFα and IL-8 by human culture-derived macrophages is regulated by an outwardly rectifying K$^+$ (KOR) channel (53).

As discussed, the secretion of reactive oxygen and nitrogen intermediates by macrophages is regulated by a variety of stimuli including cytokines and endotoxins (LPS). The direct intercalation and lateral diffusion of LPS in the plasma membranes of monocytes and macrophages was in fact proposed to initiate signaling and induce activation by exerting steric stress on a "putative signaling protein" (77), later proposed to be a potassium channel (78).

This review of the recent literature illustrates that there is a growing body of evidence indicating that K$^+$ channels are absolutely required for proper and complete macrophage activation leading to their cytotoxic ability.

2.4 Objectives of Thesis

Ion channels are at the interface between the immediate environment and the cellular processes and signals. The fact that ion channels are distributed throughout the plasma membrane of a cell means that any alteration in the function of the channels could potentially result in immediate, "global" effects on cellular physiology. Host cell ion channels are potential targets for pathogens during the initial stages of infection, i.e. during parasite uptake by phagocytosis. The objective of this thesis was to determine whether perturbation of K^+ channels affects the antimicrobial functions of murine macrophages. The specific aims of this thesis were to:

1) examine whether K^+ channel blockers affect the inducible effector functions (respiratory burst response and nitric oxide production) of macrophages.
2) examine whether K^+ channel blockers affect the physiological functions (membrane potential and potassium flux) of macrophages.
3) determine whether the effects of K^+ channel blockers in macrophages are similar to those seen during parasite-induced activation.
4) compare the effects of K^+ channel blockers and parasite infection on the activation of murine macrophage-like cells (the cell line P388D.1) and bone-marrow-derived macrophages.

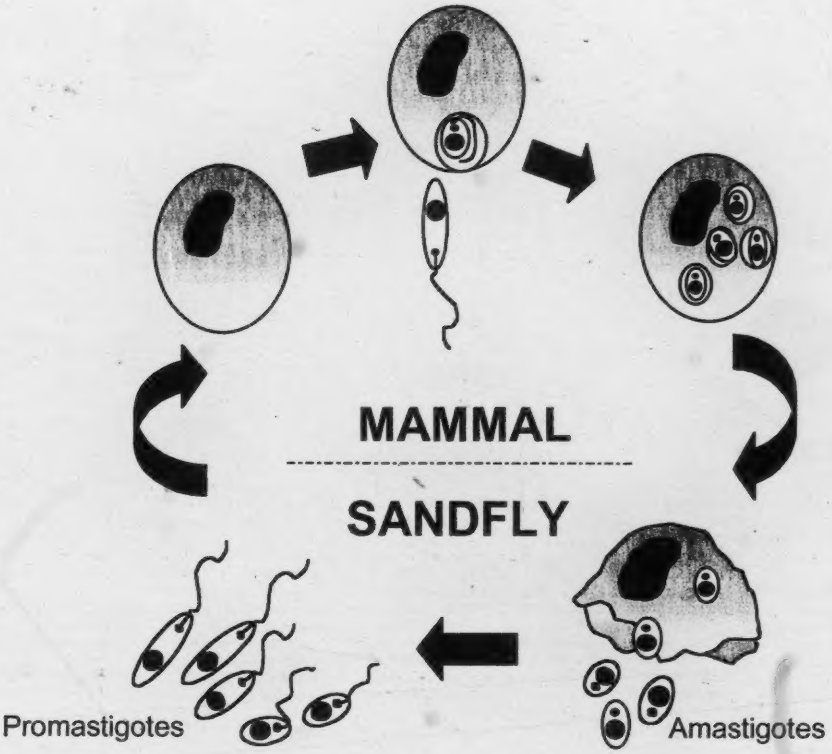

Figure 2-1. Life cycle of *Leishmania*. [Modified from K.P. Chang in Modern Parasite Biology, ed. by D.J. Wyler.]

SURFACE MOLECULE	PROMASTIGOTES	AMASTIGOTES	FUNCTIONS
Glycoprotein 63 (gp63) (also known as leishmanolysin/PSP)	Yes	Yes (<<<)	Binds macrophage receptors for entry; Proteolytic cleavage of CD4 of T-cells; Inhibits neutrophil chemotaxis in vitro; sheds off the membrane attack complex (MAC)
Fucose Mannose Ligand	Yes	No?	Role in entry into macrophages (binds the MFR)
Acid Phosphatases	Yes	Yes	Blocks superoxide anion production by human neutrophils in vitro
gp46 (also known as PSA or Promastigote Surface Antigen)	Yes	No?	Unknown
Kinetoplastid Membrane Protein-11	Yes	Yes	Unknown; Induces strong T-cell response in mice and humans
ICAM-L (*Leishmania* ICAM-like molecule)	Yes	?	Intercellular adhesion molecule
Lipophosphoglycan (LPG)	Yes	Yes, some species (<<<)	Inhibits macrophage chemotaxis, respiratory burst activity, and intracellular signaling through PKC; Attachment to sandfly midgut epithelium; sheds off the membrane attack complex (MAC); binds to the LPS binding site of CR3
Glycoinositol-phospholipids (GIPL)	Yes	Yes	Highly antigenic in humans; inhibits macrophage NO synthesis in response to IFNγ

Table 2-1. The major surface molecules expressed by *Leishmania* parasites. This is not a complete list, and the specifics of the molecules may vary between *Leishmania* species.

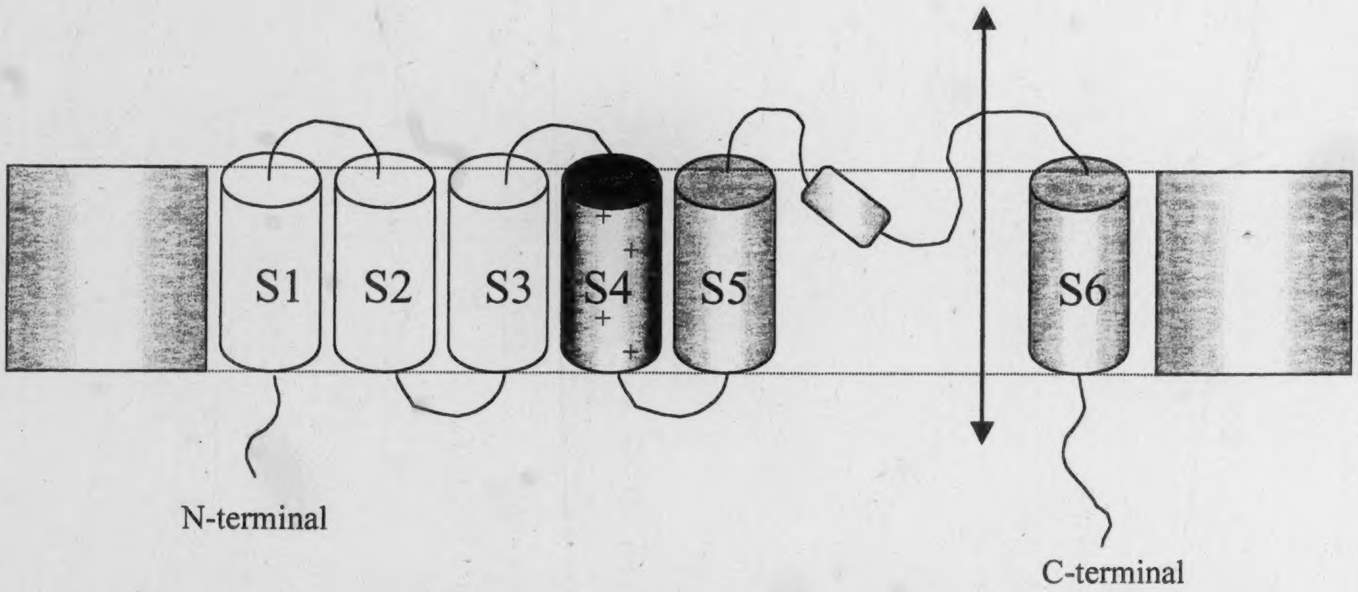

Figure 2-2. The six transmembrane domains of a single subunit of a typical K^+ channel. S1 to S4 comprise the selectivity filter. S4 is the voltage sensor and channel opening is driven by the movement of arginine residues on the S4 segment. S5 and S6 comprise the K^+-selective pore (the double-headed arrow represents the channel pore). These subunits are assembled in tetrameric structures. [Modified from Giorgetti and Carloni, 2003.]

Chapter 3: General Materials and Methods

3.1 Media and Reagents

Dulbecco's Modified Eagle Medium (DMEM), RPMI 1640, and gentamicin were obtained from Gibco BRL (Grand Island, NY) and fetal bovine serum was obtained from either HyClone Laboratories Inc. (Logan, UT) or Atlanta Biologicals (Norcross, GA). Murine recombinant IFNγ was purchased from Genzyme (Boston, MA) and LPS from *Salmonella typhimurium* was obtained from Difco Labs (Detroit, MI). Quinine, 4-aminopyridine (4-AP), tetraethlyammonium (TEA), sulfanilamide, naphthylene diamine dihydrochloride, DNA loading gel, fluorescein diacetate, and ethidium bromide were obtained from Sigma Chemical Company (St. Louis, MO).

The proSTAR First Strand RT-PCR Kit and additional StrataScript Reverse Transcriptase (50,000 U/ml) were purchased from Stratagene (La Jolla, CA). Primers were ordered from R&D Systems (Minneapolis, MN) or Invitrogen (Burlington, ON). The PCR Core Kit was obtained from Roche (Laval, Quebec). Diethylpyrocarbonate (DEPC) was obtained from ICN Biomedicals Inc. (Aurora, OH). For protein quantification, the Micro BCA Protein Quantification Reagent kit was obtained from Pierce (Rockford, IL). Primary antibodies against mouse β-actin and iNOS were obtained from Santa Cruz Biotech (Santa Cruz, CA). For colorimetric detection of protein, BioRad's alkaline phosphatase (AP)-conjugated secondary antibody was used in conjunction with the AP detection kit (BCIP/NBT) from BioRad (Mississauga, ON). For fluorescent scanning of Western blots, the ODYSSEY scanning system from Li-Cor, Inc.

(Lincoln, NE) was used and the IRDye™ 800 conjugated secondary antibody was obtained from Rockland Immunochemicals (Gilbertsville, PA).

Bis-oxonol (DiSBAC$_2$(3); bis-(1,3-diethylthiobarbituric acid) trimethine oxonol) and dihydrorhodamine (DHR) were obtained from Molecular Probes (Eugene, OR). Rubidium-86 ($^{86}Rb^+$) was obtained from NEN Life Sciences Products (Boston, MA) at a concentration of 640 mBq/ml (specific activity=64 MBq/mg) in water. Scintillation fluor was from Amersham (Oakville, ON).

3.2 Cell Culture

Culture flasks (25 cm^2 and 75 cm^2) for macrophages were from Becton-Dickinson Labware (Franklin Lakes, NJ) and Corning Inc. (Corning, NY) respectively. Culture flasks for *L. major* (25 cm^2) and all 15 ml and 50 ml tubes were from Sarstedt (Newton, NC). Polypropylene and polystyrene tubes (5 ml) were obtained from Falcon (Becton Dickinson Labware, Franklin Lakes, NJ). Cell scrapers were from CoStar (Corning, NY).

3.2.1 Culture of P388D.1 macrophage-like cells

The murine macrophage-like cell line P388D.1 was obtained from the American Type Culture Collection (ATCC, Rockville, MD). These cells were formed through a methylcholanthrene-induced tumour in the DBA/2 strain of mice and displayed a mature state of macrophage differentiation (79). Cells were grown and passaged in DMEM containing 50 μg/ml gentamicin and 10% heat-inactivated fetal bovine serum (complete DMEM) and incubated at 37°C in a humid atmosphere of 5% CO$_2$. Cells were passaged every 4 to 5 days by dislodging the cells with a cell scraper and transferring 10% of the culture into fresh complete DMEM. For use in experiments, cells were scraped, decanted, and washed twice by centrifugation in incomplete medium at 1000 rpm for 10 minutes. Cell viability was determined using the trypan blue dye exclusion assay in which a dilution of cells was incubated with 0.4% trypan blue for 2 minutes. Live unstained cells were enumerated using a hemacytometer. Dead cells were unable to exclude the dye and were stained with trypan blue.

3.2.2 Culture of bone marrow-derived macrophages

The methods used to isolate macrophages from bone marrow were as previously described (80, 81).

The L-929 cell line used as a source of M-CSF was purchased from the American Type Culture Collection. This is a fibroblast cell line derived from normal subcutaneous areolar and adipose tissue of a C3H/An mouse (82). These cells were grown to confluency in DMEM containing 50 µg/ml gentamicin and 10% heat-inactivated fetal bovine serum (complete DMEM) and either passaged (as described above for P388D.1 cells) or scraped and centrifuged at 1000 rpm for 10 minutes to collect supernatants (L-929 cell-conditioned medium; L-CCM). Cells were passaged every 5 to 6 days by dislodging the cells with a cell scraper and transferring 10% of the culture into fresh complete DMEM.

Six to ten week old SPF (specific pathogen-free) female C57/BL6 mice were purchased from Charles River (St. Constant, Quebec). Animals were kept at the Biological Sciences Animal Facility, University of Alberta, Edmonton, Canada. Mice were housed in a P-2 barrier facility, given food and water *ad libitum*, and routinely screened for antibodies to a standard panel of murine pathogens. For isolation of bone marrow material, femurs were removed from C57/BL6 mice and washed in alcohol followed by three changes of incomplete DMEM in sterile 16 x 15 mm petri dishes. Under sterile conditions, ends were cut from the femurs and the contents were flushed through with DMEM using a 26-gauge needle attached to a 3 ml syringe. The contents of the femur were homogenized gently by aspiration, decanted into a 50 ml tube, and centrifuged and washed twice in medium. The pellet was resuspended in 1 ml of complete DMEM (per pair of femurs), and placed in 23 ml of DMEM and 6 ml of L-CCM (final concentration of 20%) using one 50 ml tube per pair of femurs. Cells were incubated at 37°C in a humid atmosphere of 5% CO_2 and each tube was supplemented with 3 ml of L-CCM every 4 days until cells were collected for use between days 9 and 11 post-isolation. For use in experiments, cells were dislodged by gently flicking the tube, placing on ice, and washing twice by centrifugation in incomplete DMEM at 1000 rpm for 10 minutes. Cell viability was determined using the trypan blue dye exclusion assay as described above. Cells were enumerated using a hemacytometer.

3.2.3 *Leishmania major* parasites

3.2.3.1 *Maintenance of L. major in mice*

Six to ten week old SPF male BALB/c mice (Charles River, St. Constant, Quebec) were used to maintain *L. major*. Animals were kept at the Biological Sciences Animal Facility, University of Alberta, Edmonton, Canada. Mice were housed in 0.2 µm filter top cages in a P-2 barrier facility, given food and water *ad libitum*, and routinely screened for antibodies to a standard panel of murine pathogens. The NIH/173 (WHOM/Ir/-/173) strain of *L. major* was used in all experiments.

3.2.3.2 *Isolation of amastigotes*

Parasites were maintained by serial passage as amastigotes in BALB/c mice. Mice were anaesthetized with METOFANE (Methoxyflurane) (Pitman-Moore Inc., Missisauga, ON). For five mice, 1 ml of anaesthetic was added to a 5 L beaker containing a wire mesh false bottom overlying some surgical gauze. Mice were inoculated with 2 x 10^6 parasites (in a 50 μl volume) subcutaneously into each hind footpad. Following the development of footpad swelling four to six weeks after infection, the amastigotes were isolated as previously described by disruption of footpad tissue, passage through #50 stainless steel mesh screens, and homogenization (38). The isolated amastigotes were used to infect mice or to establish promastigote cultures as described below.

3.2.3.3 *Promastigote culture*

L. major promastigotes were cultured at room temperature in Cunningham's medium (Appendix 1) containing 50 μg/ml gentamicin and 20% heat-inactivated FBS (complete Cunningham's). Promastigotes were harvested when they were in the stationary phase, at a concentration of 4-7 x 10^7/ml after 5 to 6 days of culture (83). To determine viability, an aliquot of parasites was stained with fluorescein diacetate (FDA) and ethidium bromide as described below and counted with a hemocytometer prior to use in experiments.

3.2.3.4 *Viability stain for promastigotes and amastigotes of L. major*

Ethidium bromide is excluded from live cells and stains the nucleic acid of dead parasites. FDA penetrates live cells; cellular esterases break the dye down into fluorescein. Twenty-five µl of 5 mg/ml FDA in PBS was added to 25 µl of 2µg/ml ethidium bromide. Fifty µl of an appropriate dilution of parasites was added and incubated for 2 minutes at room temperature. The reaction was quenched by adding 50 µl of PBS to 50 µl of the stained parasites. Ten µl aliquots of the parasites were added to a hemocytometer. Parasites were counted using low bright field light and ultraviolet light.

3.3 Experimental Procedures: Macrophage Immune Responses

3.3.1 Dihydrorhodamine (DHR) assay for measurement of respiratory burst

Dihydrorhodamine (DHR) passively diffuses across most cell membranes. According to the manufacturer's description, DHR does not directly detect superoxide but reacts with its breakdown products (hydrogen peroxide, peroxynitrite, and hypochlorous acid). The dye was dissolved in DMSO at a concentration of 29 mM (stock solution) and stored in 30 µl aliquots at -80°C. P388D.1 macrophage-like cells or 9-to-11 day old BMDM were isolated as described above, washed twice by centrifugation at 1000 rpm for 10 minutes, counted, resuspended in complete DMEM, and seeded into 5 ml polypropylene tubes (2.5 x 10^5 cells per tube in 250 µl). Cells were treated and incubated for 3 hours prior to stimulation with 250 µl of LPS (and 250 µl of medium) or 250 µl LPS and 250 µl of IFNγ. Control cells for each treatment were given 500 µl of medium, remaining unstimulated. Respiratory burst activity was assessed in the cells for every treatment group after a 24-hour incubation at 37°C and 5% CO_2. Cells were then incubated with DHR (3.4 μl of stock solution to 1 ml incomplete DMEM, adding 10 μl to each tube for a final concentration of 10 μM) for 10 minutes at 37°C (in the dark). The respiratory burst response was triggered by adding phorbol myristate acetate (PMA), an activator of protein kinase C. A 10 mg/ml stock was diluted to 10 ng/μl, adding 10 μl to each tube for a final concentration of 100 ng PMA per tube. Cells activated with LPS or LPS and IFNγ were included but incubated without PMA as a control for basal respiratory burst. Cells were incubated for 30 minutes at 37°C and 5% CO_2 before reading fluorescence (FL-1) on a flow cytometer (FACSCalibur flow cytometer; Becton Dickinson) using the following settings: forward side scatter-photodiode set to E-00, AmpGain set to 1.00; side scatter-photomultiplier voltage set to 433 V, AmpGain set to 1.00; 10,000 cells collected during analysis. Details of the experimental designs are given in Chapter 4.

3.3.2 Griess reaction for measurement of nitric oxide production

P388D.1 macrophage-like cells or 9-to-11 day old BMDM were isolated as described above, washed twice by centrifugation at 1000 rpm for 10 minutes, counted, resuspended in complete DMEM, and added to a 96-well plate (5×10^4 cells per well in a 50 μl volume) and allowed to attach at 37°C and 5% CO_2 for 1 hour. Control cells were treated with complete DMEM. Triplicate wells containing macrophages were treated and subsequently activated with LPS and IFNγ. Cells were treated with medium or *L. major* promastigotes and the macrophages were simultaneously activated by the addition of LPS and IFNγ. After a 24-hour incubation at 37°C and 5% CO_2, a Griess reaction was performed on the culture supernatants. Supernatants (75 μl) were transferred into a replicate plate. One hundred μl of 1% sulfanilamide in 2.5% phosphoric acid and 100 μl of 0.1% N-napthylethylenediamine in 2.5% phosphoric acid were added to each well. The plate was allowed to sit for 2 minutes before the absorbance at 540 nm was determined using an automated spectrophotometer (Biotek; Winooski, VT). The approximate concentration of nitrite in the samples was determined from a standard curve using known concentrations of sodium nitrite; the limit of sensitivity was determined to be approximately 3 μM. The Griess reaction measures nitrite as an index of NO activity. While nitrite is only one of the intermediates produced through the reaction catalyzed by iNOS, a direct correlation is made between NO and nitrite. To analyze NO production in BMDM and P388D.1 macrophage-like cells, treatments were prepared as described in detail in Chapter 4.

3.3.3 Analysis of iNOS mRNA

3.3.3.1 *RNA Isolation*

Treatments were prepared as described in detail in Chapter 4 using 2 x 10^6 P388D.1 cells per tube. Cells were pre-treated for 3 hours then stimulated with LPS and IFNγ. After treatment, 3 ml of incomplete DMEM (supplemented with K^+ blocker as needed) was added to dilute serum. Cells were pelleted by centrifugation and the supernatant was removed. Cells were homogenized in 500 μl of cold TRIZOL reagent by pipetting rapidly. Samples were transferred to RNAse-free (autoclaved) microfuge tubes. The homogenized samples were incubated for 5 minutes at room temperature to permit the complete dissociation of nucleoprotein complexes. One hundred µl of chloroform was added per tube. Sample tubes were capped securely, shaken vigorously by hand for 15 seconds, and incubated for 2 to 3 minutes at room temperature. Samples were centrifuged at 11,300 rpm for 15 minutes at room temperature. Following centrifugation, the mixture separated into a red phenol-chloroform phase (lower), an interphase, and a colorless aqueous phase (upper). RNA remained exclusively in the aqueous phase. The aqueous phase was transferred to a fresh tube and the RNA was precipitated by mixing with 250 µl of ice-cold isopropyl alcohol. Samples were incubated at room temperature for 10 minutes, and then centrifuged at 11,300 rpm for 10 minutes at room temperature. The RNA precipitate formed a small gel-like pellet on the side and bottom of the tube. The supernatant was removed and the RNA pellet was washed once with 500 µl of ice cold 75% ethanol. Samples were then stored at -20°C or were mixed by vortexing and centrifuged at 8,900 rpm for 5 minutes at room temperature.

To redissolve the RNA at the end of the procedure, the ethanol was poured off and the RNA pellet was air-dried for 10 to 15 minutes with the caps of the tubes open. It was essential to not let the RNA pellet dry completely as this greatly decreases its solubility. The RNA was dissolved in 25 µl of RNAse-free water (DEPC water; Appendix 1) by passing the solution a few times through a pipette tip. To quantify the RNA, a dilution of the sample in DEPC water or TE buffer was read on a spectrophotometer (absorbance at 260/280 nm). Only RNA with a 260/280 ratio greater than 1.8 was used for analysis.

3.3.3.2 *Reverse-transcriptase based polymerase chain reaction (RT- PCR)*

After spectrophotometric quantification of RNA, 5 μg of total RNA was adjusted to 19 μl with DEPC water and 1.5 μl of oligo dT primer was added to each tube. Samples were incubated at 65°C for 5 minutes, followed by incubation at room temperature for 10 minutes. ProSTAR RT-PCR kit reagents were added as follows (in order): 2.5 μl of 10X buffer, 0.5 μl of RNAse block, 1 μl of dNTP mix, and 0.5 μl of reverse transcriptase per reaction. Samples were incubated at 37°C for 1 hour, followed by incubation at 90°C for 5 minutes. Samples were stored on ice.

3.3.3.3 *Primers*

The mouse/rat β-actin primer pair was either bought (R&D Systems, Inc., Minneapolis, MN) in which case a 320 base pair (bp) product was expected, or designed using Gene Tool software based on a known sequence of *Mus musculus* cytoplasmic β-actin mRNA. Gene specific iNOS F and R (forward and reverse) primers were designed using Gene Tool software based on a known sequence of *Mus musculus* iNOS mRNA. These custom primers were ordered from Invitrogen. The sequences for these primers (5′ to 3′) was as follows:

Mouse β-actin mRNA (1470 bp product):

Forward: GCG ACG ATG CTC CCC GGG CTG TA

Reverse: CGG GGT GGA CTC AGG GCA TGG AC

Mouse iNOS mRNA (807 bp product):

Forward: GCC GCA CCA CCC TCC TCG TTC AG

Reverse: GCC GGC ACC CAA ACA CCA AGC TC

3.3.3.4 *Polymerase Chain Reaction (PCR)*

A PCR master mix (containing iNOS forward and reverse primers) was made as follows for a 25 µl reaction: 19.25 µl of DEPC water, 2.5 µl of Taq buffer, 0.5 µl of dNTPs, 0.25 µl of Taq polymerase, 1 µl of iNOS F (of a 1/1000 dilution of stock forward primer), 1 µl of iNOS R (of a 1/1000 dilution of stock reverse primer). The same was done for custom β-actin primers. Each tube had 70 pmol (picomoles) of each primer. Note that for β-actin commercial primers, 1 µl of the primer pair (undiluted) and 1 µl of DEPC water were added in place of the iNOS primers. For a 25 µl reaction, 24.5 µl of master mix and 0.5 µl cDNA were added per tube. PCR conditions were as follows: thermocycler lid temperature 105°C; 2 minutes at 94°C; 30 cycles of: 94°C for 30 seconds, 60°C for 30 seconds, 72°C for 1 minute and 30 seconds; 72°C for ten minutes; hold at 4°C until storage.

3.3.3.5 *Gel electrophoresis and staining for visualization of bands*

Samples were run through either 0.8 or 1.6% agarose gels in TAE buffer (Appendix 1). In the lane containing the DNA size ladder, 4 µl of the marker (=1 µg DNA) was added. DNA samples and loading gel containing sucrose and bromophenol blue were mixed (8 µl and 2 µl respectively) and added to each well. Gel electrophoresis was carried out for 45 minutes to 1.5 hours at 80 to 100 V. The agarose gel was stained with 10 μg/ml ethidium bromide for 10 to 20 minutes and destained for 10 to 20 minutes in water.

3.3.4 Analysis of iNOS protein

3.3.4.1 *Protein isolation*

Treatments were prepared as described in Chapter 4 using 2 x 10^6 P388D.1 cells per tube. After treatment, P388D.1 macrophages were washed one time in ice-cold Dulbecco's phosphate-buffered saline and pelleted by centrifugation at 1000 rpm for 10 minutes. After pouring off the supernatant, cells were homogenized in 500 μl of lysis buffer (Appendix 1) by pipetting rapidly. Samples were transferred to 1.5 ml tubes and centrifuged at 14,000 rpm (approximately 18,000 x g) at 4°C for 10 minutes in a microcentrifuge to pellet the protein. Samples were frozen at -80°C for long term storage.

3.3.4.2 *Protein quantification*

Protein was quantified using the Micro BCA Protein Quantification Reagent kit according to manufacturer's instructions (Pierce). In order to construct a standard curve, serial dilutions of kit BSA (2 mg/ml) and samples of interest were made in water, aliquoted to 5 ml polystyrene tubes, vortexed, and incubated with kit reagents. After 1 hour in a 60°C water bath, 200 μl of each sample was transferred to a 96-well plate and the absorbance at 570 nm was read on a spectrophotometer (Biotek; Winooski, VT). Dilutions of samples of interest were prepared and read in the same manner, and the absorbance values were converted to the quantity of protein present in μg/ml.

3.3.4.3 *Separation of proteins by sodium dodecyl sulfate-polyacrylamide gel electrophoresis (SDS-PAGE)*

Five µg of total protein in Laemilli's reagent containing 10% beta-mercaptoethanol was heat denatured at 95°C for 5 minutes and electrophoresed through either 4% or 10% stacking gel (60 V for approximately 30 minutes) and a 10% separating SDS-polyacrylamide gel (180 V for approximately 50 minutes, or until the bromophenol blue dye front ran off the bottom of the gel). Electrophoresis was carried out in 1X SDS running buffer (25 mM Tris, 192 mM glycine, 0.1% (w/v) SDS, pH 8.3; Appendix 1).

3.3.4.4 *Transfer and immunoblotting*

Transfer of proteins to 0.2 µm nitrocellulose membranes (BioRad) was either by semi-dry blotting method (16 V, 23 minutes) or wet transfer (100 V, 1 hour). In either case, the transfer buffer consisted of 25 mM Tris-HCl, 192 mM glycine, 20% (v/v) methanol, pH 8.3) (Appendix 1). After protein transfer, the nitrocellulose was reversibly stained with Ponceau S (Sigma, St. Louis, MO) for visualization of the SDS-PAGE molecular weight standards (BioRad, Mississauga, ON).

The nitrocellulose membrane was exposed overnight at 4°C to rabbit polyclonal anti-mouse iNOS IgG (Santa Cruz) at a concentration of 1:1000 in blocking buffer containing BSA. For fluorescence detection (described below), the nitrocellulose membrane was exposed overnight at room temperature to ovalbumin blocking buffer (Appendix 1) containing 1:1000 anti-mouse iNOS antibody. Incubation in primary antibody was followed by 3 five-minute washes in Tween-Tris-buffered saline (TTBS) and 2 five-minute washes in Tris-buffered saline (TBS) (Appendix 1).

3.3.4.5 *Colorimetric and fluorescent detection of protein*

For colorimetric detection, an AP (alkaline phosphatase)-conjugated secondary antibody (1:3000) was used and developed using the alkaline phosphatase reaction kit (BCIP/NBT) from BioRad (Mississauga, ON), according to manufacturer's instructions. For fluorescent detection, a goat anti-rabbit IR-800 fluorescent secondary antibody was used in which case the ovalbumin blocking buffer was used throughout the entire procedure. The antibody was detected using the Li-Cor Odyssey System (Lincoln, NE).

3.3.4.6 *Staining of SDS-PAGE gels*

Protein bands were visualized by staining gels with a silver stain kit (BioRad) or by staining for 30 minutes with 0.1% Coomassie Brilliant Blue (BioRad) dissolved in 40% methanol/10% acetic acid (Appendix 1). Staining and destaining were carried out at room temperature on a rotator (LabLine).

3.4 Experimental Procedures: Macrophage Physiology

3.4.1 Bis-oxonol assay for analysis of changes in membrane potential

Changes in membrane potential were measured by fluorescence-activated cell-sorting (FACS) using the membrane dye bis-oxonol. This negatively-charged dye is excluded by the mitochondria and prevents complications of signals derived from mitochondrial origin (84). The dye enters depolarized cells and binds to intracellular proteins or membranes where it exhibits enhanced fluorescence and red spectral shifts (85). Since the quantum yield of the dye increases significantly upon binding, the fluorescence of cells incubated in medium containing bis-oxonol increases upon depolarization and decreases with hyperpolarization. Cells were seeded into 5 ml polypropylene tubes (2.5×10^5 cells per tube in 250 µl). Cells were treated and incubated for 3 hours prior to stimulation with 250 µl LPS (and 250 µl medium) or 250 µl LPS and 250 µl IFNγ. Control cells for each treatment were given 500 µl of medium, remaining unstimulated. The final volume in all tubes was 500 µl with a final concentration of 2% FBS. See Chapter 5 for details of the experimental design.

After the desired incubation time, cells were loaded with 5 µM bis-oxonol and incubated for a further 15 minutes at 37°C. The stock bis-oxonol was diluted 1 in 50 in DMSO, followed by a 1 in 500 dilution in medium. Cells were then washed once (to remove residual bis-oxonol) in 3 ml of medium supplemented with K^+ channel blockers as required and resuspended in the same to a volume of 250 µl. Fluorescence (FL-2) was determined using flow cytometry (FACSCalibur flow cytometer; Becton Dickinson). All flow cytometry was performed by collecting 10,000 cells during analysis with the following settings: forward side scatter-photodiode set to E-00, AmpGain set to 1.00; side scatter-photomultiplier voltage set to 433 V, AmpGain set to 1.00.

3.4.2 Rubidium influx experiments to measure K^+ flux

The details of the experimental design used to determine the effect of K^+ channel blocker and/or *L. major* promastigotes on potassium influx in P388D.1 cells are as described in Chapter 5. Macrophages (10 x 10^6) were seeded into 25 cm^2 flasks, treated, and incubated at 37°C and 5% CO_2 for 24 hours prior to the determination of unidirectional $^{86}Rb^+$ influx. Based on preliminary studies, an influx time of 120 minutes was chosen as the optimal loading time for $^{86}Rb^+$ influx experiments. After 24 hours, macrophages were scraped from the culture flasks, transferred to 50 ml centrifuge tubes and centrifuged at 1000 rpm for 10 minutes. Macrophages were resuspended in RPMI medium (pH 7.4; bicarbonate-free) supplemented with K^+ channel blocker and/or promastigotes (10:1) according to the conditions used during the 24-hour pre-incubation period. Cells were aliquoted to individual 1.5 ml centrifuge tubes (Eppendorf) at concentrations ranging from 0.5 x 10^6 to 2.0 x 10^6 cells/tube and were kept for one hour in a 37°C incubator under an air atmosphere.

Prior to the start of $^{86}Rb^+$ influx measurements, ouabain (100 μM) and bumetanide (20 μM) were added to the cells to inhibit the Na^+/K^+-ATPase and $Na^+/K^+/2Cl^-$ transporters, respectively. At time 0 minutes, 10 μCi $^{86}Rb^+$ was added to each centrifuge tube, gently mixed throughout the cell suspension, and the cells were kept at 37°C with continuous mixing. After 120 minutes macrophages were given 3 rapid washes in ice-cold wash buffer (PBS buffer at 330 mOsm with 1 mM barium, 20 μM bumetanide) to remove extracellular $^{86}Rb^+$. Cells were lysed in scintillation fluor and aliquots of flux solution were counted for determination of extracellular specific activity. Washed cells were resuspended in 1 ml of PBS, and 500 μl of the cell suspension was counted for analysis of intracellular $^{86}Rb^+$ activity on a beta-counter (Beckman LS, 6500) using a wide-open channel. $^{86}Rb^+$ counts were normalized to total cell counts as measured using the trypan blue dye exclusion method of counting.

3.4.3 Analysis

Data were analyzed using the Super-ANOVA software for the Power Macintosh. Differences between groups were measured using one and two-factor analysis of variance and a least-squares means test. Probability level of $P<0.05$ was considered significant. All experiments were performed two or more times.

Chapter 4: Effect of K^+ Channel Blockers on Macrophage Effector Functions During *Leishmania major* Infection

4.1 Introduction

Macrophages possess a number of ion channels that may be important for their cytotoxic functions (54, 55, 57, 62). We previously reported that the treatment of macrophages with K^+ channel blockers significantly alters their ability to respond to the activating factors LPS and IFNγ (6). In that study, murine macrophages treated with a variety of K^+ channel blockers (4-AP, quinine, and TEA) exhibited a dose-dependent decrease in the production of nitric oxide (NO). The alteration of NO production was hypothesized to result from a direct effect on K^+ channels leading to an impairment of intracellular signaling steps (6).

Infection with certain intracellular pathogens, for example, *Leishmania* spp. is also known to downregulate the cytotoxic response of macrophages. The invasion mechanism employed by *Leishmania* parasites, regardless of the morphological stage, dictates the type of immune response used to prevent multiplication and dissemination of the parasite. That is, promastigotes encountering primed macrophages are more susceptible to the reactive oxygen products of the respiratory burst response (ROI) which are mainly directed extracellularly. Once an infection with amastigotes is established, resident tissue macrophages can be activated to kill parasites through mechanisms such as upregulation of iNOS gene expression resulting in production of nitric oxide (9). Since amastigotes thrive and replicate intracellularly, intracellular killing mechanisms such as NO production are most often employed and are most effective for controlling infections with *Leishmania* spp.

4.1.1 Respiratory burst response

Priming macrophages with IFNγ or other cytokines does not directly activate the respiratory burst enzyme NADPH oxidase, but it does upregulate certain components of the enzyme complex, such that cytokine-primed macrophages will generate more ROI than non-stimulated cells upon ingestion of a pathogen (12). The production and release of ROI, particularly superoxide anion, is crucial during the initial stages of infection, when *Leishmania* spp. promastigotes are being taken up by macrophages. Results of a recent study by Kumar *et al.* (86) suggest that low NADH-oxidase, NADPH-oxidase and myeloperoxidase activities may account for persistence of *L. donovani* parasites.

During the receptor-mediated phagocytic uptake of *Leishmania* spp. promastigotes, macrophages elicit a respiratory burst response in which the NADPH oxidase complex assembles and reactive oxygen intermediates (ROI) are formed (e.g. superoxide, H_2O_2, and hydroxyl radicals) which are important for killing of intracellular parasites. *Leishmania* spp. employ a number of mechanisms to deal with the respiratory burst products of macrophages including: 1) enzymes which detoxify the free oxygen radicals (e.g. superoxide dismutase, trypanothione peroxidase) (9); 2) the lipophosphoglycan (LPG) surface coat which interferes with the PKC signaling involved in triggering the respiratory burst (87); and 3) amastigote binding to CR3 receptors which circumvents the induction of the respiratory burst response (33). In addition, respiratory burst products will kill both stages of the parasite but the response elicited by amastigotes has been shown to be significantly lower than the respiratory burst induced by phagocytosis of promastigotes, most likely a result of the macrophages' mannose fucose receptor not being used for uptake of amastigotes therefore offering no trigger for respiratory burst (9).

There is evidence to suggest that K^+ channels are involved in the respiratory burst of various cell types. In a study of human eosinophils the NADPH oxidase complex was shown to be insensitive to wide fluctuations in membrane potential, a feature which ensures that the enzyme functions optimally unless faced with drastic depolarization of the membrane (88). Depolarization of the cell membrane inhibits the respiratory burst of neutrophils (70).

4.1.2 Nitric oxide production

Nitric oxide (NO) is a highly reactive molecule central to the anti-microbial activity of macrophages. NO production by activated macrophages has been shown to be instrumental in the resolution of leishmaniasis and infections with other intracellular pathogens. For example, pharmacological inhibition of iNOS results in higher parasite loads, larger skin lesions, and reduced killing ability in *L. major*-infected mice (89). In addition, iNOS knock-out mice are unable to control *L. donovani* infection (90). As mentioned previously, LPG is one of the main leishmanial surface glycoconjugates that suppresses nitric oxide production (46), allowing survival of the parasite. The virulence of promastigotes depends on the developmental stage, and correlates with the types and amounts of parasite surface molecules; metacyclic promastigotes are considered the most infectious and have the most LPG on their surface. The importance of NO lies not only in its leishmanicidal function but in its ability to modulate the immune functions, e.g. promoting IL-12 and IFNα and IFNβ-mediated activation of natural killer (NK) cells, thereby promoting NK cell release of IFNγ which further activates macrophages to become potent killer cells.

In murine macrophages the kinetics of NO production following stimulation involves an initial 6 to 12 hour lag phase; by 24 hours cells reach their maximal NO production (20). Murine macrophages stimulated with LPS secrete measurable quantities of nitrate and nitrite into culture supernatants (20). Nitrite is the compound that is usually measured by the Griess reaction.

There is evidence to suggest that K^+ channels are involved in nitric oxide production in various cell types. In a study of murine P388D.1 macrophage-like cells, K^+ channel blockers inhibited the NO response of LPS or LPS and IFNγ-stimulated cells (6). Glibenclamide, an inhibitor of ATP-sensitive potassium channels, downregulated NO production by LPS-stimulated J774 macrophage-like cells and inhibited the induction, but not the activity, of iNOS (91). Blockage of K^+ channels was also shown to downregulate NO production by non-mammalian macrophages (68).

The experiments outlined in this Chapter aimed to examine the role of K^+ channels in the effector functions of macrophages, particularly in the context of *Leishmania major* infection.

4.2 Determination of Respiratory Burst Activity

4.2.1 Experimental design and objectives

4.2.1.1 *Effect of K^+ channel blockers on respiratory burst activity of macrophages*

The objective of these experiments was to determine whether there was a suppression of respiratory burst when activated macrophages were treated with potassium channel blockers. P388D.1 cells or BMDM (2.5×10^5) were treated with 125 μl of 4 mM 4-AP (final concentration of 1 mM 4-AP) and 375 μl of medium for a final volume of 500 μl. Macrophages were incubated for 24 hours before measuring the respiratory burst response using the dihydrorhodamine (DHR) assay as described in Materials and Methods.

4.2.1.2 *Effect of K^+ channel blockers and L. major infection on respiratory burst of macrophages*

To assess the effect that *L. major* has on the respiratory burst, 2.5×10^5 P388D.1 macrophage-like cells and bone marrow-derived macrophages (BMDM) in 125 μl were treated with 125 μl of 4 mM 4-AP (final concentration of 1 mM 4-AP), 125 μl stationary phase *L. major* promastigotes (final promastigote-to-macrophage ratio of 25:1), or both K^+ channel blockers and *L. major* promastigotes (250 μl total), and made up to a final volume of 500 μl with medium. Macrophages were incubated for 24 hours before measuring the respiratory burst response as described in Materials and Methods.

4.2.1.3 *Effect of latex bead phagocytosis on respiratory burst activity of macrophages*

The objective of this experiment was to assess the effect that phagocytosis alone has on the respiratory burst of P388D.1 macrophage-like cells. Cells were seeded into tubes (2.5 x 10^5) and were treated with 125 µl of 3 µm latex beads (final bead-to-macrophage ratio of 25:1) or with 125 µl of 4 mM 4-AP and 125 µl beads together. Medium was added to a final volume of 500 µl. Macrophages were incubated for 24 hours before measuring the respiratory burst response as described in Materials and Methods.

4.2.2 Analysis

Data are shown as mean FL-1 fluorescence values corrected for background fluorescence (fluorescence from unstained cells) and basal respiratory burst fluorescence (respiratory burst as measured from cells stimulated with PMA only). All experiments were repeated two or more times. Representative graphs are shown. Data were not analyzed statistically.

4.2.3 Results

In all experiments, cells stimulated with LPS or LPS and IFNγ exhibited a limited respiratory burst response in the absence of PMA. The respiratory burst of control LPS-stimulated cells was enhanced after treatment with IFNγ.

After 24 hours of infection, *L. major* promastigotes inhibited the respiratory burst of LPS- or LPS and IFNγ- stimulated P388D.1 cells. Cells exposed to latex beads and stimulated with LPS showed a respiratory burst response similar to the LPS-stimulated controls; this effect was enhanced in the presence of IFNγ such that there was a higher respiratory burst in cells exposed to beads and stimulated with LPS and IFNγ. Latex beads or parasites elicited a small respiratory burst in non-stimulated cells, which was likely due to the process of phagocytosis (Fig. 4-1). The data are a representative of two experiments that were performed.

L. major promastigotes alone or in combination with the potassium channel blocker 4-AP suppressed the respiratory burst of LPS or LPS and IFNγ-stimulated P388D.1 cells (Fig. 4-2). 4-AP alone also suppressed the respiratory burst compared to the respective stimulated controls. The blocker 4-AP and *L. major* both elicited a small respiratory burst in non-stimulated P388D.1 cells. Data shown are from two experiments that were performed.

L. major promastigotes alone or in combination with the potassium channel blocker 4-AP also suppressed the respiratory burst of LPS or LPS and IFNγ-stimulated bone marrow-derived macrophages (Fig. 4-3). 4-AP alone also suppressed the respiratory burst compared to the respective stimulated controls. 4-AP elicited a small respiratory burst in non-stimulated BMDM. Data shown are from two experiments that were performed.

L. major amastigotes alone or in combination with the potassium channel blocker 4-AP appeared to enhance the respiratory burst of LPS or LPS and IFNγ-stimulated P388D.1 cells (Fig. 4-4). 4-AP alone suppressed the respiratory burst compared to the respective stimulated controls. *L. major* amastigotes, or a combined treatment of 4-AP and amastigotes, elicited a small respiratory burst in non-stimulated P388D.1 cells. The data are a representative of two experiments that were performed.

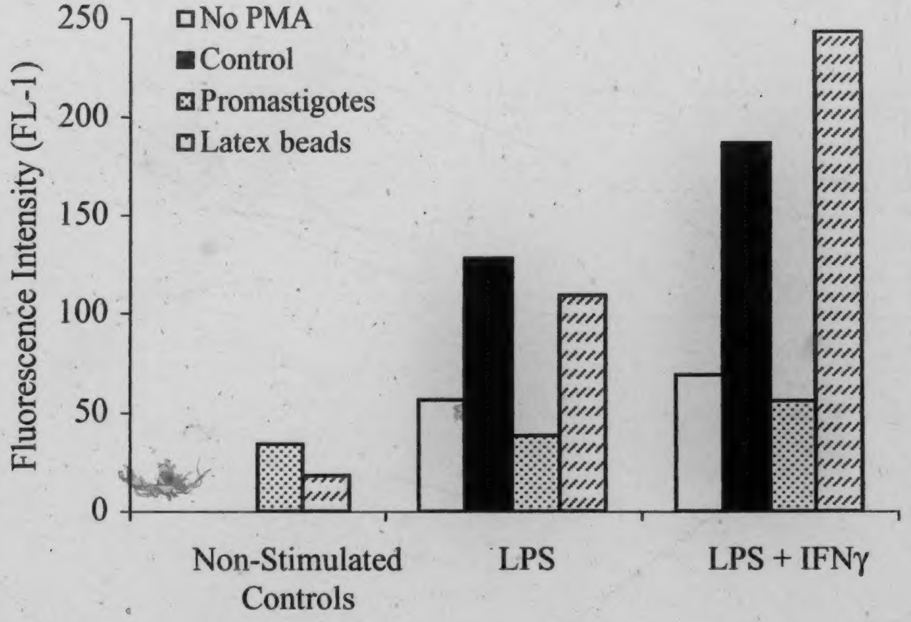

Figure 4-1. Effect of *Leishmania major* promastigotes or latex beads on the respiratory burst of P388D.1 macrophage-like cells. After 24 hours, phagocytosis of *L. major* (25:1), but not 3 μm beads (25:1), suppressed the PMA-induced respiratory burst response compared to respective stimulated controls. Data shown are a representative of two experiments that were performed.

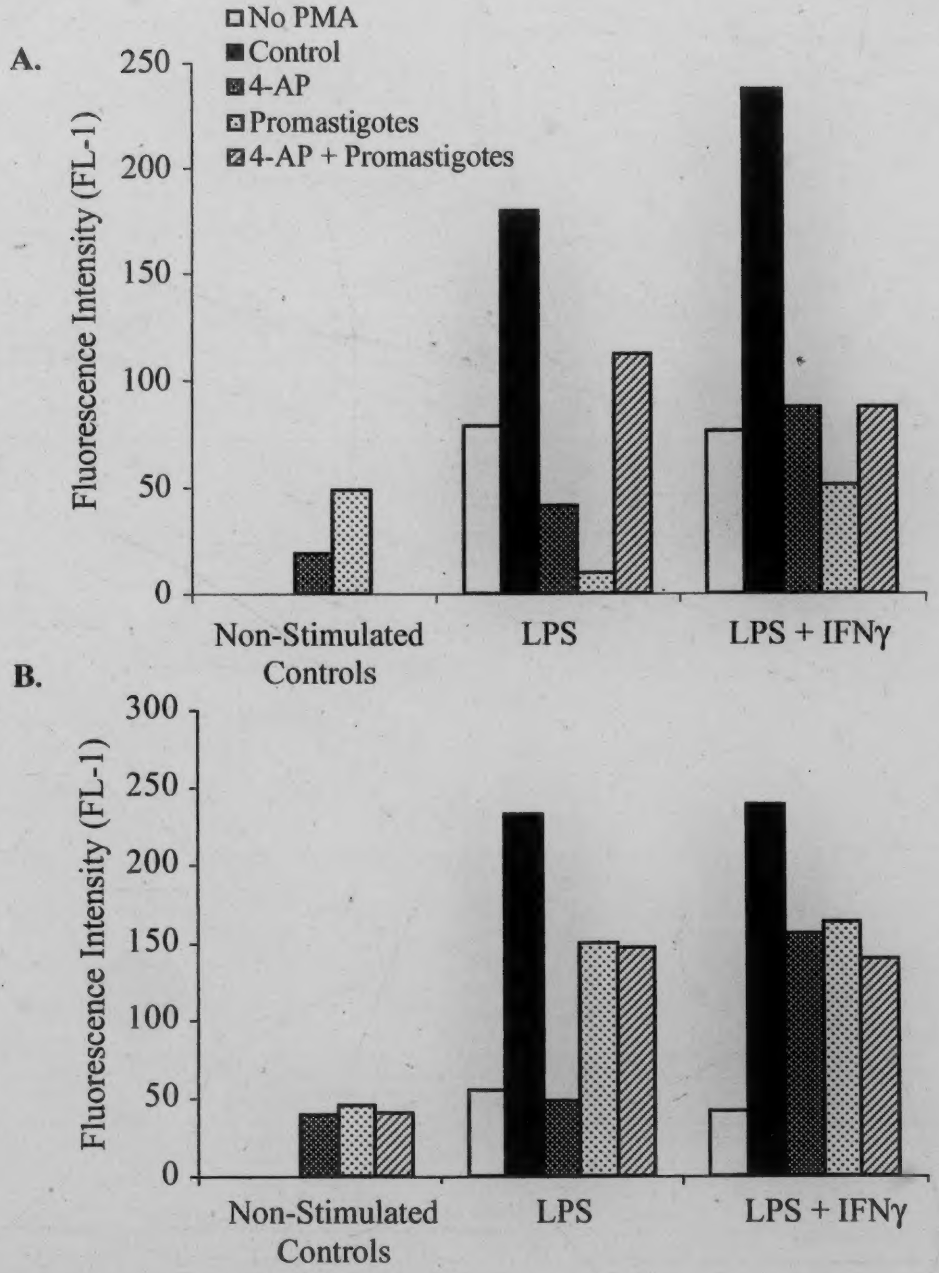

Figure 4-2. Effect of the potassium channel blocker 4-AP and *Leishmania major* promastigotes on the respiratory burst of P388D.1 macrophage-like cells. After 24 hours, both 4-AP (1 mM) and *L. major* (25:1) suppressed the PMA-induced respiratory burst compared to respective stimulated controls. Data shown in A and B are from two independent experiments.

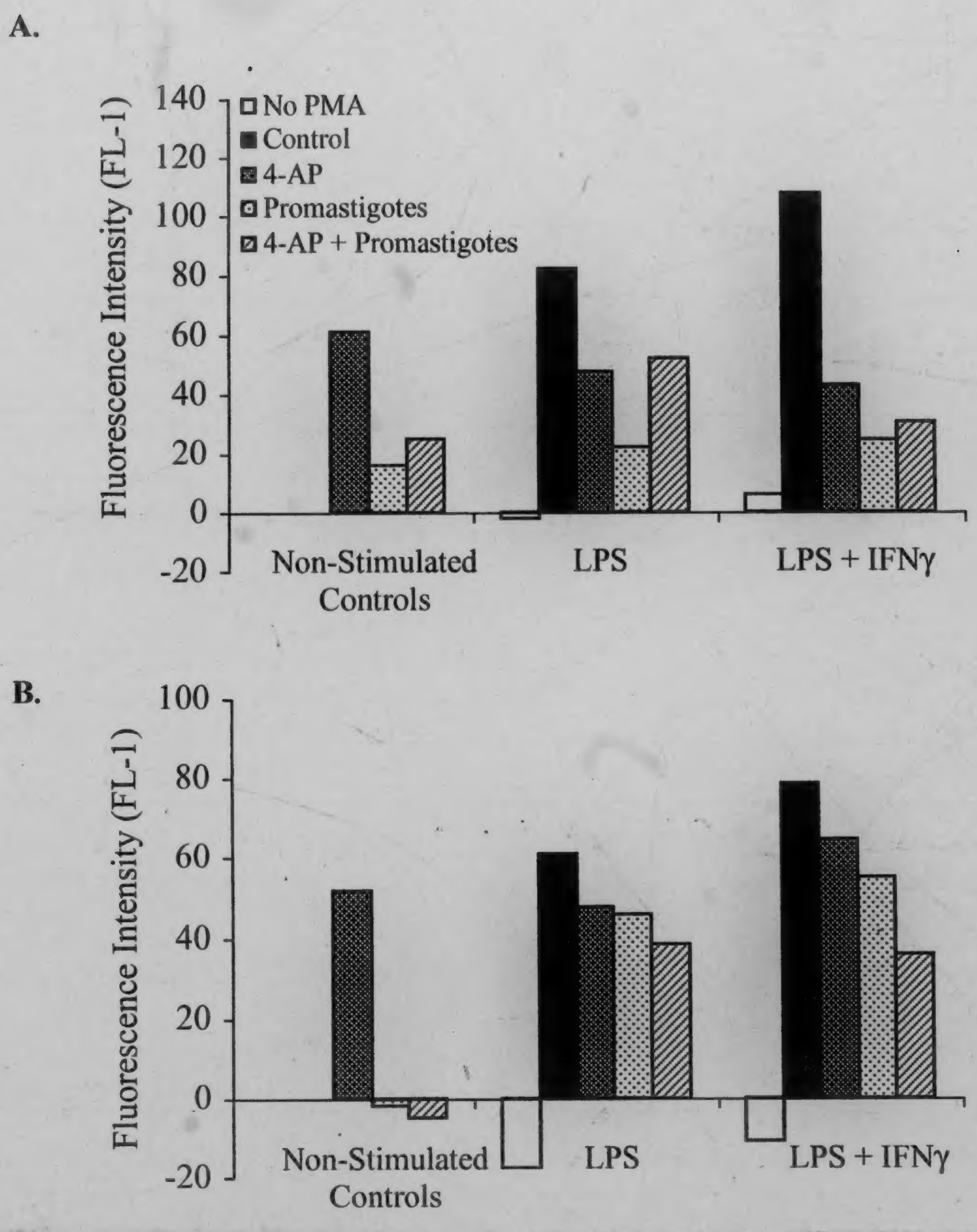

Figure 4-3. The effect of the potassium channel blocker 4-AP and *Leishmania major* promastigotes on the respiratory burst of LPS- or LPS and IFNγ-stimulated bone marrow-derived macrophages. After 24 hours, both 4-AP (1 mM) and *L. major* (25:1) suppressed the PMA-induced respiratory burst compared to respective stimulated controls. Data shown in A and B are from two independent experiments.

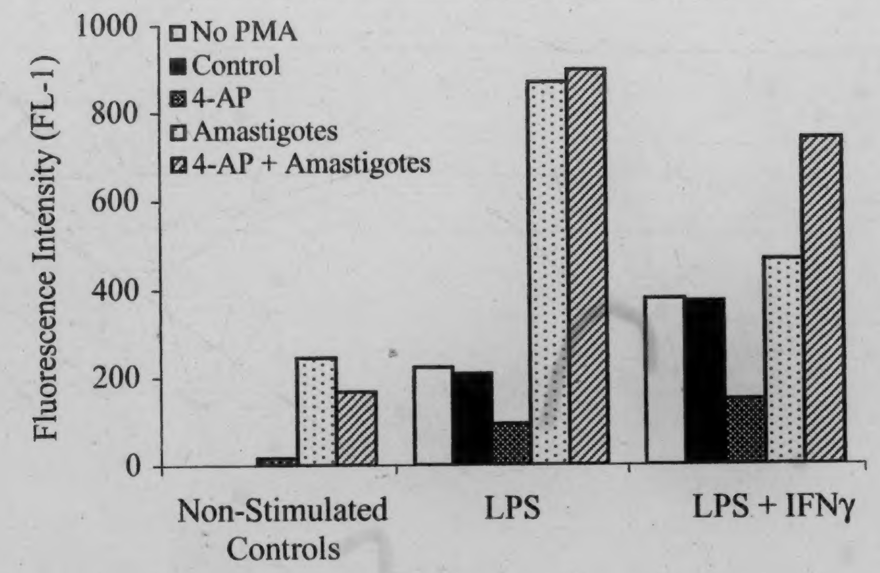

Figure 4-4. Effect of the potassium channel blocker 4-AP and *Leishmania major* amastigotes on the respiratory burst of P388D.1 macrophage-like cells. Amastigotes (25:1) enhanced the PMA-induced respiratory burst response of P388D.1 cells. Data shown are a representative of two experiments that were performed.

4.3 Determination of Macrophage Nitric Oxide Production

4.3.1 Experimental design and objectives

4.3.1.1 *Constructing the standard curve for the Griess reaction for NO production*

Known concentrations of sodium nitrite (75 µl) were combined with 100 µl of 1% sulfanilamide and 0.1% N-napthylethylenediamine, respectively, and the absorbance at 540 nm was determined (see Materials and Methods for details on the Griess assay).

4.3.1.2 *Effect of increasing extracellular K^+ on NO production by P388D.1 macrophages*

The objective of these experiments was to determine whether there was a suppression of nitric oxide (NO) production when activated macrophages were treated with various concentrations of potassium. P388D.1 cells ($1x10^5$ per well) were resuspended in isoosmotic, filter-sterilized KCl solutions (pH 7.4) containing 1.3, 4, 10, 20, 40, and 80 K^+ (mM) balanced to 144 mM total Na^+/K^+. Solutions were pre-adjusted to the normal osmolarity of DMEM by the addition of 1 M NaCl. KCl solutions contained 2% FBS and 1/4 the glucose and amino acids of normal DMEM. Macrophages were activated by the addition of 1 U/ml IFNγ and 10 ng/ml LPS. After 24 hours, nitrite accumulation in the culture supernatants was measured using the Griess reaction.

4.3.1.3 *Effect of K^+ channel blockers on NO production by macrophages*

The objective of this series of experiments was to determine whether there was a suppression of nitric oxide production when activated macrophages were treated with potassium channel blockers known to depolarize V_m in other cell types. Cells ($1x10^5$ per well) were treated in triplicate with the K^+ channel blocker 4-aminopyridine in PBS (4-AP; final concentrations of 0.25 to 2 mM), TEA (final concentrations of 2.5 and 10 mM), or quinine (final concentrations of 10 to 250 μM). Control cells were treated with complete DMEM. Macrophages were treated with blockers for 3 hours, then activated with 1 U/ml IFNγ and 10 ng/ml LPS. The nitric oxide response was determined using the Griess reaction. Wash-out experiments were carried out in the same way, except the potassium channel blocker was washed out of cells after 3 hours and cells were stimulated with LPS or LPS and IFNγ. After 24 hours, the nitric oxide response of the cells was determined using the Griess reaction.

4.3.1.4 *Effect of L. major on NO production by activated macrophages*

To determine the effect that *L. major* had on the nitric oxide response of P388D.1 macrophages and BMDM, cells were infected with *L. major* stationary phase promastigotes or amastigotes (parasite to macrophage ratios ranging from 1:1 to 60:1) and infected for 3 hours prior to activation by the addition of 10 ng/ml LPS or 1 U/ml IFNγ or both. Control cells were treated with complete DMEM only and then activated with IFNγ and LPS. Following a 24-hour incubation, the NO response by activated cells was determined using the Griess reaction.

4.3.1.5 *Effect of LPG on NO production by activated macrophages*

To determine the effect that isolated *L. donovani* LPG had on the nitric oxide response of P388D.1 macrophages, cells were treated with soluble LPG (ranging from

0.625 to 5 μM) and simultaneously activated by the addition of 10 ng/ml LPS or 1 U/ml IFNγ and 10 ng/ml LPS. Control cells were treated with complete DMEM only and stimulated in the same way. Following a 24-hour incubation, the NO response by activated cells was determined using the Griess reaction.

4.3.1.6 *Effect of combined treatments with L. major and K^+ channel blockers on NO production by activated macrophages*

To determine the effects of combined treatments with *L. major* and K^+ channel inhibitors, P388D.1 cells and BMDM were exposed for 3 hours to *L. major* promastigotes (10:1) and 1 mM 4-AP and then activated with LPS (10, 100, or 1000 ng/ml) or LPS and IFNγ (1 U/ml). Control cells were treated with complete DMEM prior to activation. After 24 hours, the NO response by macrophages was determined using the Griess reaction.

4.3.1.7 *Expression of iNOS mRNA in P388D.1 cells*

To determine whether the inhibition of NO production was due to changes in iNOS at the transcriptional level, P388D.1 cells were infected with *L. major* promastigotes (10:1) for 3 hours in the presence of medium with or without 1 mM 4-AP and then activated for 3 hours by the addition of 1 U/ml IFNγ and 10 ng/ml LPS. To assess iNOS mRNA in maximally stimulated cells, the positive control group received only complete DMEM prior to activation. After 3 hours of stimulation, total RNA was extracted and mRNA expression was analyzed by RT-PCR as described in detail in Materials and Methods. To assess iNOS mRNA in non-stimulated cells and to show that the iNOS gene expression was induced by stimuli, the negative control group received only DMEM for 6 hours. Band intensity was analyzed using Scion Image 1.62c software.

4.3.1.8 *Quantification of iNOS enzyme in P388D.1 cells*

To determine whether the inhibition of NO production was due to changes in iNOS at the level of protein translation, P388D.1 cells were exposed to *L. major* promastigotes (10:1) for 3 hours in the presence of medium alone, or medium containing 1 mM 4-AP, 100 μM quinine, or 10 mM TEA. Cells were then activated for 6 hours by the addition of 1 U/ml IFNγ and 10 ng/ml LPS. To assess iNOS enzyme availability in maximally stimulated cells, the positive control group received only complete DMEM prior to activation. After 6 hours of stimulation, protein was extracted and analyzed by SDS-PAGE and immunblotting as described in detail in Materials and Methods. To assess iNOS enzyme availability in non-stimulated cells and to show that the iNOS enzyme was induced by stimuli, the negative control group received only DMEM for 6 hours.

4.3.2 Analysis

Data were analyzed using the Super-ANOVA software for the Power Macintosh. Differences between groups were measured using one and two-factor analysis of variance and a least-squares means test. Probability level of $P<0.05$ was considered significant. All experiments were performed at least two or more times.

4.3.3 Results

A standard curve of absorbance at 540 nm of various concentrations of sodium nitrite combined with the reagents of the Griess assay (N-napthylenediamine and sulfanilamide) was constructed to allow conversion of absorbance values to nitrite (μM) in the experiments examining nitric oxide production (Fig. 4-5). Values of nitrite less than 3 μM were determined to be below the limit of sensitivity for this assay. Treatment with increasing concentrations of extracellular K^+ (Fig. 4-6) significantly inhibited NO production by LPS-stimulated P388D.1 cells, compared to cells in low (1.3 mM) K^+ (P=0.0001). Normal DMEM contained 5.3 mM K^+. In the presence of IFNγ the suppression was lessened, indicating that priming with IFNγ allows full activation of macrophages treated with K^+ channel blocker. Only at concentrations of 40 and 80 mM K^+ was NO production by LPS and IFNγ-stimulated cells significantly inhibited (P=0.038 and P=0.0001 respectively). Non-stimulated cells did not produce NO at any of the K^+ concentrations tested (R_2=0.012, P=0.633). Stimulation with LPS or LPS and IFNγ enhanced NO production compared to unstimulated cells (P=0.0001 for all K^+ concentrations, except P=0.6684 for LPS-stimulated cells in 96 mM K^+). LPS and IFNγ-stimulated cells had significantly higher NO production than cells stimulated with LPS only (P=0.0001 for all K^+ concentrations).

LPS-stimulated P388D.1 cells treated with 1 mM 4-AP, 10 mM TEA, or 100 μM quinine (Fig. 4-7) demonstrated 50%, 52%, and 82% reductions in nitric oxide production compared to LPS-stimulated controls (P=0.0001 for each of 4-AP, TEA, and quinine). Treatment with increasing concentrations of the K^+ channel blocker 4-AP caused a dose-dependent decrease in the production of NO by LPS or LPS and IFNγ-stimulated P388D.1 cells (Fig. 4-8), in agreement with our earlier observations (6). The highest concentration of 4-AP tested (2 mM) caused maximal inhibition of NO production with no effect on cell viability (6). LPS-stimulated P388D.1 cells treated with 0.25, 0.5, 1, and 2 mM 4-AP showed 30%, 41%, 57%, and 81% inhibition of NO production compared to DMEM-treated cells. Non-stimulated cells produced no nitric oxide. Stimulation with LPS or LPS and IFNγ significantly enhanced NO production compared to unstimulated cells ($P=0.0001$) and LPS and IFNγ-stimulated cells had significantly higher NO production than LPS-stimulated cells ($P=0.0001$ for all 4-AP concentrations).

The effects of 4-AP on the inhibition of NO production ($P=0.008$) were specific and reversible in P388D.1 cells stimulated with LPS and IFNγ (Fig. 4-9 A). Cells stimulated with LPS and IFNγ after wash-out of the K^+ channel blocker showed partial recovery of NO production ($P=0.046$ compared to control) which was significantly different from cells exposed to 4-AP ($P=0.012$). 4-AP significantly inhibited NO production by LPS-stimulated cells ($P=0.003$). Cells stimulated with LPS after wash-out of the K^+ channel blocker showed poor recovery of NO-producing ability compared to controls ($P=0.0014$) which was not significantly different from cells exposed to 4-AP ($P=0.125$), indicating a requirement for IFNγ in recovery of NO-producing ability after K^+ channel blockage (Fig. 4-9 B).

Bone marrow-derived macrophages (BMDM) stimulated with LPS alone produced relatively little NO compared to P388D.1 cells. Non-stimulated cells showed no nitric oxide production ($R_2=0.051$, $P=0.367$). Stimulation with LPS or LPS and IFNγ significantly enhanced NO production compared to unstimulated macrophages

(P=0.0001) and LPS and IFNγ-stimulated cells had significantly higher NO production than cells stimulated with LPS only (P=0.0001 for all 4-AP concentrations). Exposure to increasing concentrations of the K^+ channel blocker 4-AP did not have the same dramatic effect as in P388D.1 cells. Compared to LPS-stimulated cells without 4-AP, LPS-stimulated cells in 0.25, 0.5, 1, and 2 mM 4-AP displayed significant inhibition of NO production (P=0.044, 0.013, 0.0014, and 0.033 respectively) (Fig. 4-10) which correspond to 21%, 26%, 35%, and 22% inhibition of NO production. Compared to LPS and IFNγ-stimulated cells without 4-AP, LPS and IFNγ-stimulated cells in 1 and 2 mM 4-AP displayed significant inhibition of NO production (P=0.012 and 0.033) respectively) which correspond to 8% and 7% inhibition of NO production. This indicates that priming with IFNγ allows partial activation of macrophages even during blockage with 4-AP.

TEA decreased the NO production by bone marrow-derived macrophages (Fig. 4-11). Non-stimulated cells showed no nitric oxide production (R_2=0.0007, P=0.826). LPS-stimulated BMDM treated with 2.5 and 10 mM TEA showed significant inhibition of NO production (P=0.0001 and 0.0002 respectively) compared to LPS-stimulated cells without TEA. Compared to LPS and IFNγ-stimulated BMDM without TEA, LPS and IFNγ-stimulated cells in 2.5 and 10 mM TEA displayed significant inhibition of NO production (P=0.0001 for both) which corresponded to 37% and 65% inhibition of NO production.

Quinine decreased the NO production by bone marrow-derived macrophages (Fig. 4-12). Non-stimulated cells produced no nitric oxide. LPS-stimulated BMDM treated with 50, 100, and 250 μM quinine showed significant inhibition of NO production (P=0.016, 0.011, and 0.022 respectively) compared to LPS-stimulated cells without quinine. Compared to LPS and IFNγ-stimulated BMDM without quinine, LPS and IFNγ-stimulated cells in 250 μM quinine displayed significant inhibition of NO production (P=0.0001) while lower concentrations lower than 100 μM had significantly enhanced NO production (P=0.0015, P=0.0001, and P=0.0001 for 10, 25, and 50 μM quinine respectively).

Both 4-AP and infection with *L. major* promastigotes inhibited the NO response by P388D.1 macrophage-like cells (Fig. 4-13 A). There was a higher percent inhibition of NO in cells infected for 3 hours with *L. major* prior to activation with LPS and IFNγ. During this 3-hour pretreatment period, 10 to 25% of these non-stimulated P388D.1 cells will have phagocytosed at least one parasite (Fig. 4.13 B). Increasing parasite numbers did not result in proportional decreases in NO production suggesting that a ratio of 10:1 promastigotes to macrophages was sufficient for maximal inhibition of the NO response (Fig. 4-14). However, soluble LPG from *L. donovani* promastigotes inhibited NO production by P388D.1 cells (Figure 4-15). Non-stimulated cells did not produce NO in the presence of LPG. Cells stimulated with LPS and simultaneously exposed to parasite LPG exhibited depressed NO production at all concentrations of LPG tested. Compared to LPS-stimulated cells treated with medium only, P388D.1 cells exposed to 0.625, 1.25, 2.5, and 5 μM LPG showed significant differences of P=0.0056, P=0.003, P=0.0007, and P=0.001 respectively. Cells stimulated with LPS and IFNγ and exposed to LPG had significantly lower NO production than LPS and IFNγ-stimulated cells not treated with LPG (P=0.0001 for all concentrations of LPG). The inhibitory effect of *L. major* on NO production by P388D.1 cells was not specific to the promastigote stage because amastigotes of *L. major* also inhibited NO production (Fig. 4-16). Non-stimulated cells exposed to amastigotes displayed no nitric oxide production. Compared to LPS-stimulated uninfected controls, LPS-stimulated P388D.1 cells exposed to amastigote-to-macrophage ratios of 10 to 1 and 50 to 1 showed significant inhibition of NO ($P=0.002$ and 0.0001 respectively). Compared to LPS and IFNγ-stimulated uninfected controls, LPS and IFNγ-stimulated P388D.1 cells exposed to amastigote-to-macrophage ratios of 1 to 1 and 50 to 1 showed significant inhibition of NO production ($P=0.0003$ for both). In P388D.1 cells stimulated with IFNγ only, amastigote-to-macrophage ratios higher than 1 to 1 enhanced the NO response ($P=0.0001$ for 5 to 1, 10 to 1, and 50 to 1).

A simultaneous treatment of LPS- or LPS and IFNγ-stimulated cells with 1 mM 4-AP and promastigotes (30:1) caused a decrease in NO production (Fig. 4-17) compared to respective stimulated controls ($P<0.05$). In cells stimulated with 100 and 1000 ng/ml LPS and in IFNγ-treated cells stimulated with 10, 100, and 1000 ng/ml LPS, the combined effect of infection and K^+ channel blockage was significantly greater ($P<0.05$) than the inhibitory effect induced by 4-AP alone or promastigotes alone. Inhibitions of NO production by single or combined treatments with parasite and 4-AP were dependent on the concentrations of IFNγ and LPS. Macrophages stimulated with 1 U/ml IFNγ and 10 ng/ml LPS exhibited a significant reduction in NO production following single or combined treatments with parasite and 4-AP compared to macrophages activated with 1 U/ml IFNγ and 1000 ng/ml LPS.

Interestingly, *L. major* promastigotes did not cause a significant suppression of NO production (Fig. 4-18) by LPS-stimulated bone marrow-derived macrophages ($P=1$) but slightly enhanced the NO production by LPS and IFNγ-stimulated macrophages ($P=0.03$). Compared to the respective stimulated controls,1 mM 4-AP significantly suppressed NO production by LPS- or LPS and IFNγ-stimulated BMDM ($P=0.0002$ and

0.0027, respectively). While combined treatment with 4-AP and *L. major* caused significant inhibition of NO by LPS-stimulated cells (P=0.045), combined treatment followed by LPS and IFNγ-stimulation showed no difference from the respective stimulated control (P=0.892).

The inhibition of NO seen in P388D.1 cells infected with *L. major* promastigotes appeared to be regulated at both the gene and protein levels. There was no change in the expression of iNOS mRNA (Fig. 4-19 A; representative gel) in stimulated cells treated with the K^+ channel blocker 4-AP. However, iNOS expression in infected cells, alone or in combination with K^+ channel blockage, was only slightly higher than in non-stimulated controls (Fig. 4-19 B; mean of 3 gels). The various K^+ channel blockers (4-AP, quinine, and TEA) caused no appreciable decrease in the amount of iNOS enzyme present. *L. major*-infected cells appeared to have produced less iNOS (Fig. 4-20; representative immunoblot). These results suggest that the pathway(s) leading to NO production that are blocked by both the parasite and the K^+ channel inhibitors may not be identical.

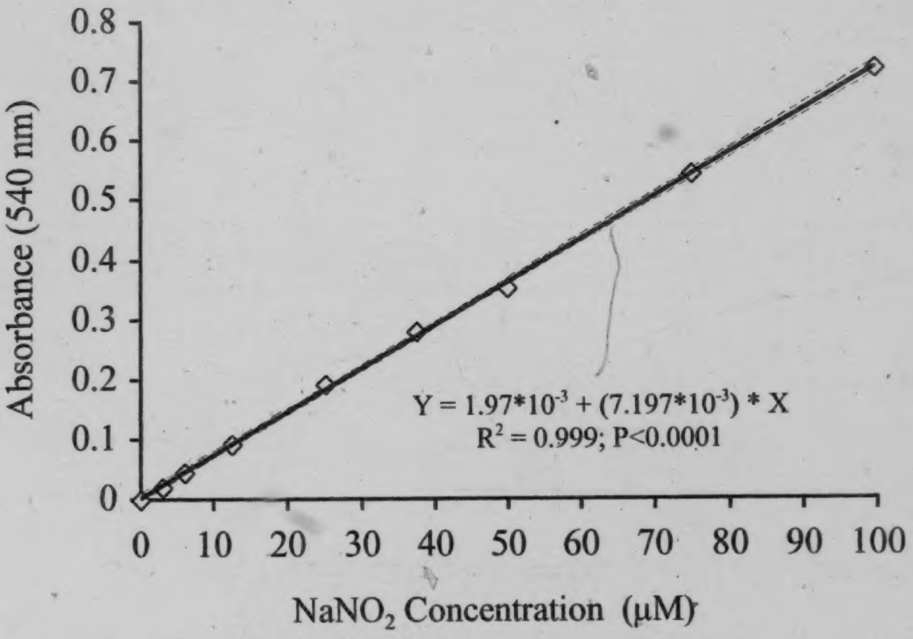

Figure 4-5. Calibration of the NO assay (Griess reaction) using sodium nitrite. The trend line represents the linear regression relationship between the concentration of sodium nitrite and the absorbance at 540 nm following addition of Griess reagents as described in Materials and Methods. The dashed lines indicate 95% confidence limits (upper and lower). The detection limit of this assay is approximately 3 μM.

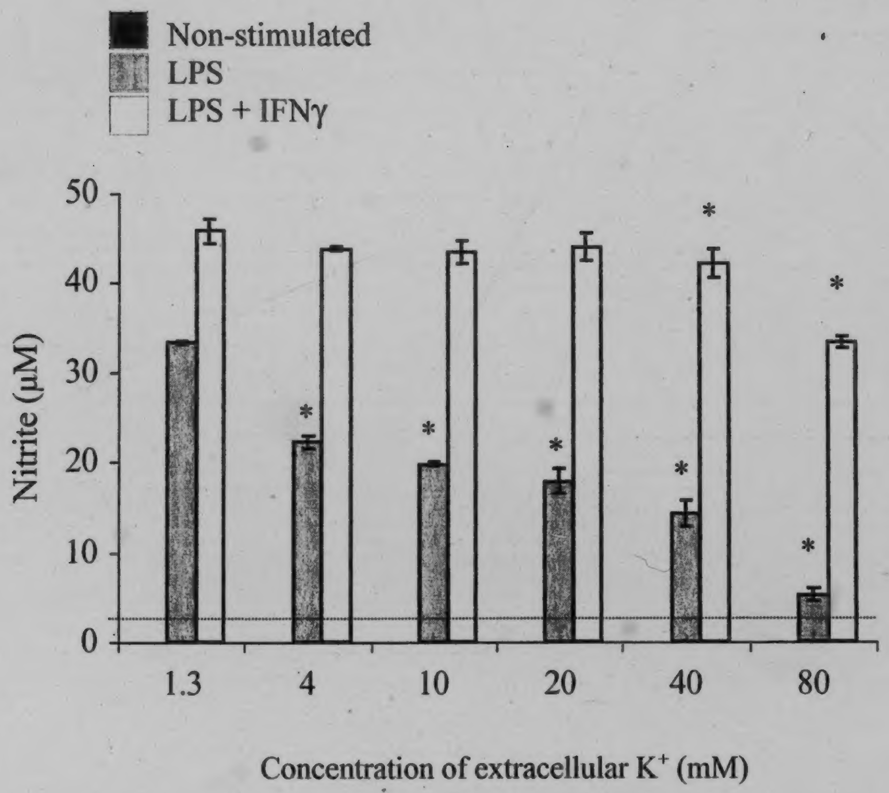

Figure 4-6. Effect of increased extracellular K^+ on nitric oxide (NO) production by P388D.1 macrophage-like cells after 24 hours. Increasing the concentration of K^+ in the medium caused a decrease in NO production by LPS- or LPS and IFNγ-stimulated P388D.1 macrophage-like cells (10 ng/ml LPS; 1 U/ml IFNγ). Values of nitrite (µM) below 3 µM may not be absolute values, as indicated by the dashed line. Data are shown as mean ± s.e.m. (* $P<0.05$ compared to respective non-stimulated, LPS-stimulated, or LPS and IFNγ-stimulated controls in 1.3 mM extracellular K^+). Data shown are a representative of two experiments that were performed.

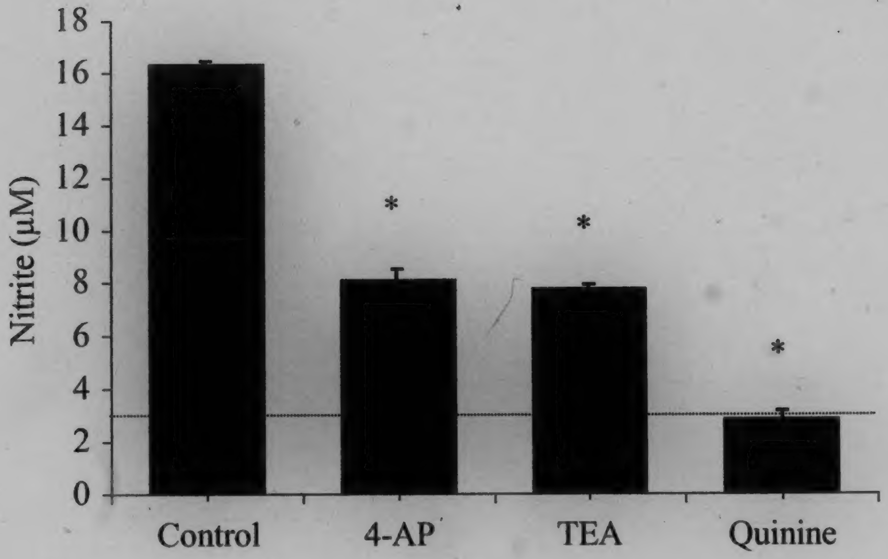

Figure 4-7. Effect of various K^+ channel blockers on nitric oxide (NO) production by P388D.1 macrophage-like cells after 24 hours of stimulation with 10 ng/ml LPS. Values of nitrite (µM) below 3 µM may not be absolute values, as indicated by the dashed line. Data are shown as mean ± s.e.m. (* $P<0.05$ compared to control) Data shown are a representative of two experiments that were performed.

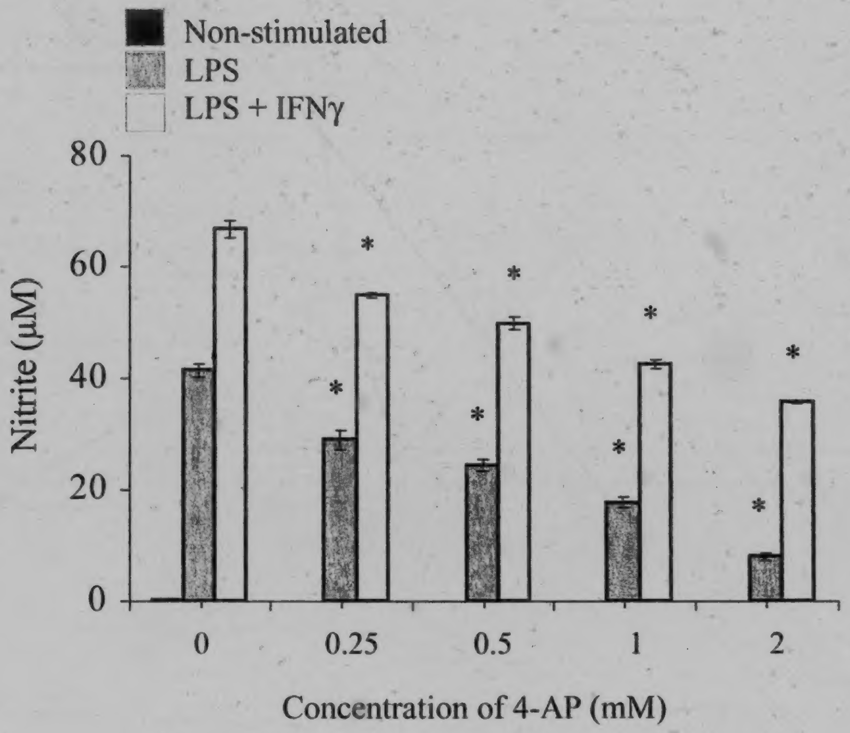

Figure 4-8. Effect of increasing doses of 4-AP on nitric oxide (NO) production by P388D.1 macrophage-like cells after 24 hours. Increasing doses of 4-AP caused inhibition of NO production by LPS- or LPS and IFNγ-stimulated cells (10 ng/ml LPS; 1 U/ml IFNγ). Data are shown as mean ± s.e.m. (* $P<0.05$ compared to respective non-stimulated, LPS-stimulated, or LPS and IFNγ-stimulated controls) Data shown are a representative of two experiments that were performed.

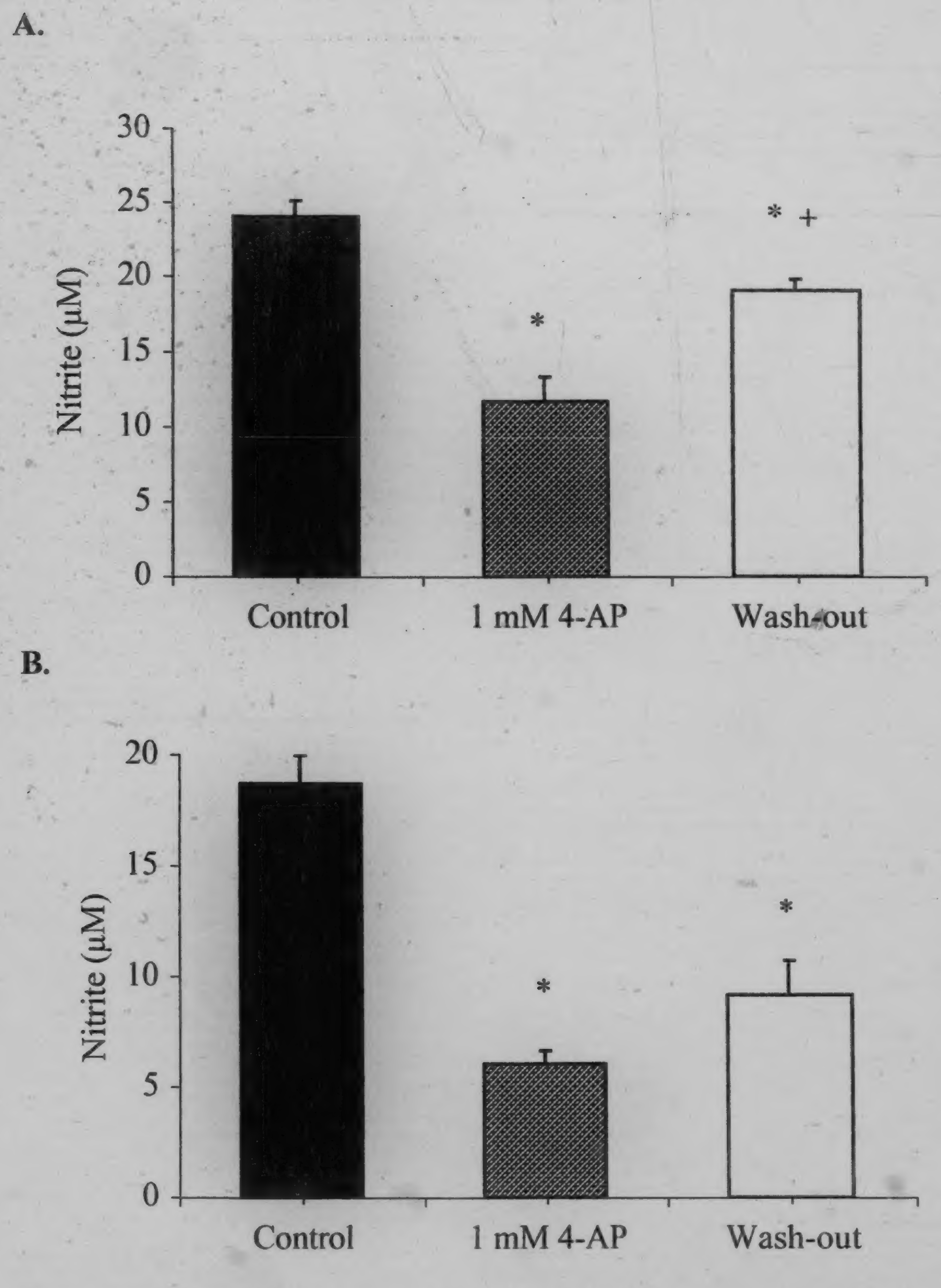

Figure 4-9. Effect of 4-AP washout on nitric oxide (NO) production by P388D.1 macrophage-like cells after 24 hours. Washing out the 4-AP after 3 hours allowed partial recovery of NO production in LPS and IFNγ stimulated P388D.1 cells (A), but not in cells stimulated with LPS only (B) (10 ng/ml LPS; 1 U/ml IFNγ). Data are shown as mean ± s.e.m. (* $P<0.05$ compared to respective LPS- or LPS and IFNγ-stimulated controls; + $P<0.05$ compared to 4-AP-treated cells) Data shown are a representative of two experiments that were performed.

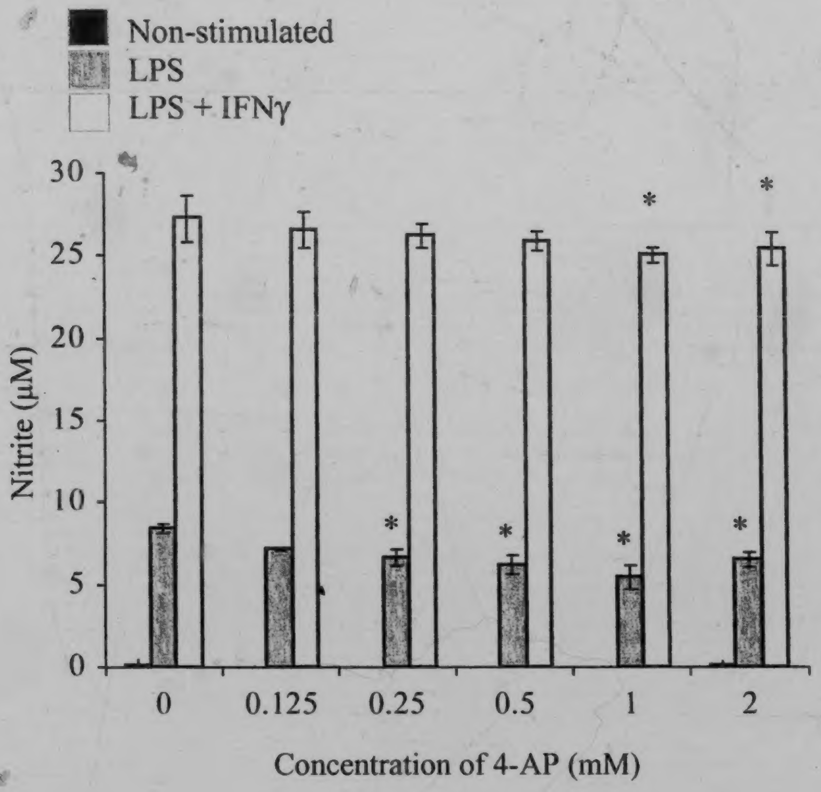

Figure 4-10. Effect of increasing doses of 4-AP on nitric oxide (NO) production by bone marrow-derived macrophages after 24 hours. 4-AP caused some inhibition of NO production by LPS- or LPS and IFNγ-stimulated cells (10 ng/ml LPS; 1 U/ml IFNγ. Data are shown as mean ± s.e.m. (* $P<0.05$ compared to respective non-stimulated, LPS-stimulated, or LPS and IFNγ-stimulated controls) Data shown are a representative of two experiments that were performed.

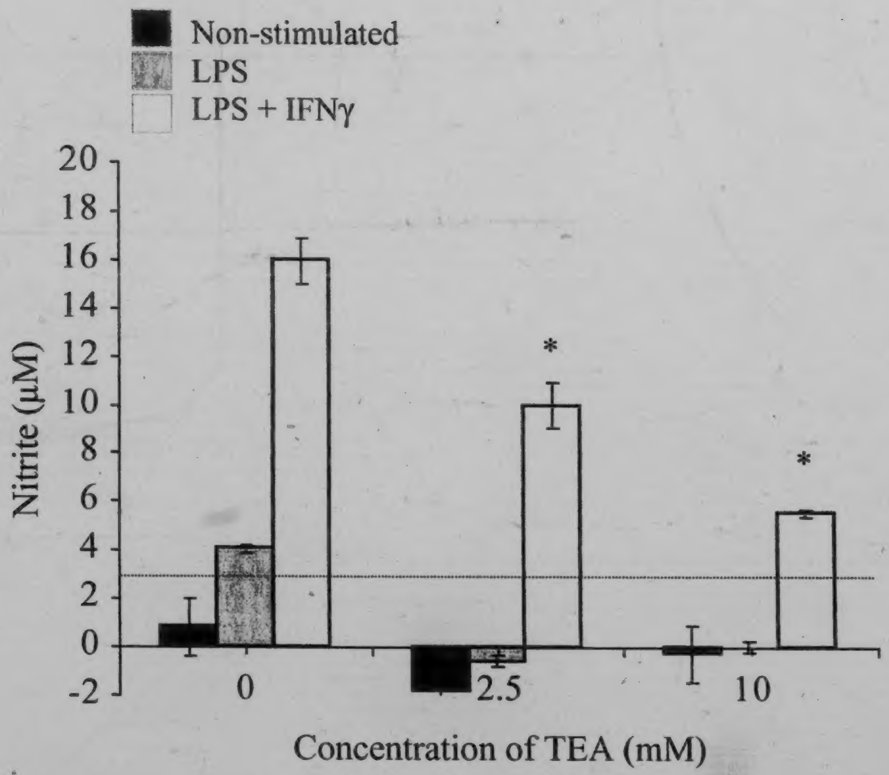

Figure 4-11. Effect of TEA on nitric oxide (NO) production by bone marrow-derived macrophages after 24 hours. TEA inhibited NO production by LPS and IFNγ-stimulated cells (10 ng/ml LPS; 1 U/ml IFNγ). Values of nitrite (μM) below 3 μM may not be absolute, as indicated by the dashed line. Data are shown as mean ± s.e.m. (* $P<0.05$ compared to the LPS and IFNγ-stimulated control in 0 mM TEA) Data shown are a representative of two experiments that were performed.

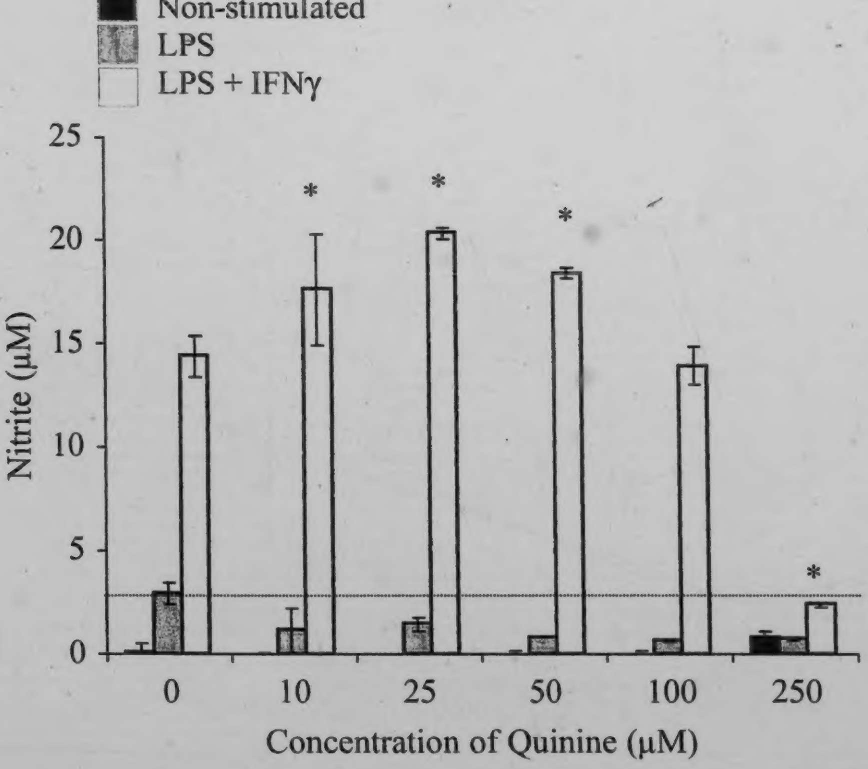

Figure 4-12. Effect of quinine on nitric oxide (NO) production by bone marrow-derived macrophages after 24 hours. Values of nitrite (μM) below 3 μM may not be absolute, as indicated by the dashed line. Data are shown as mean ± s.e.m. (* $P<0.05$ compared to respective non-stimulated, LPS-stimulated (10 ng/ml), or LPS (10 ng/ml) and IFNγ (1 U/ml)-stimulated controls in 0 μM quinine) Data shown are a representative of two experiments that were performed.

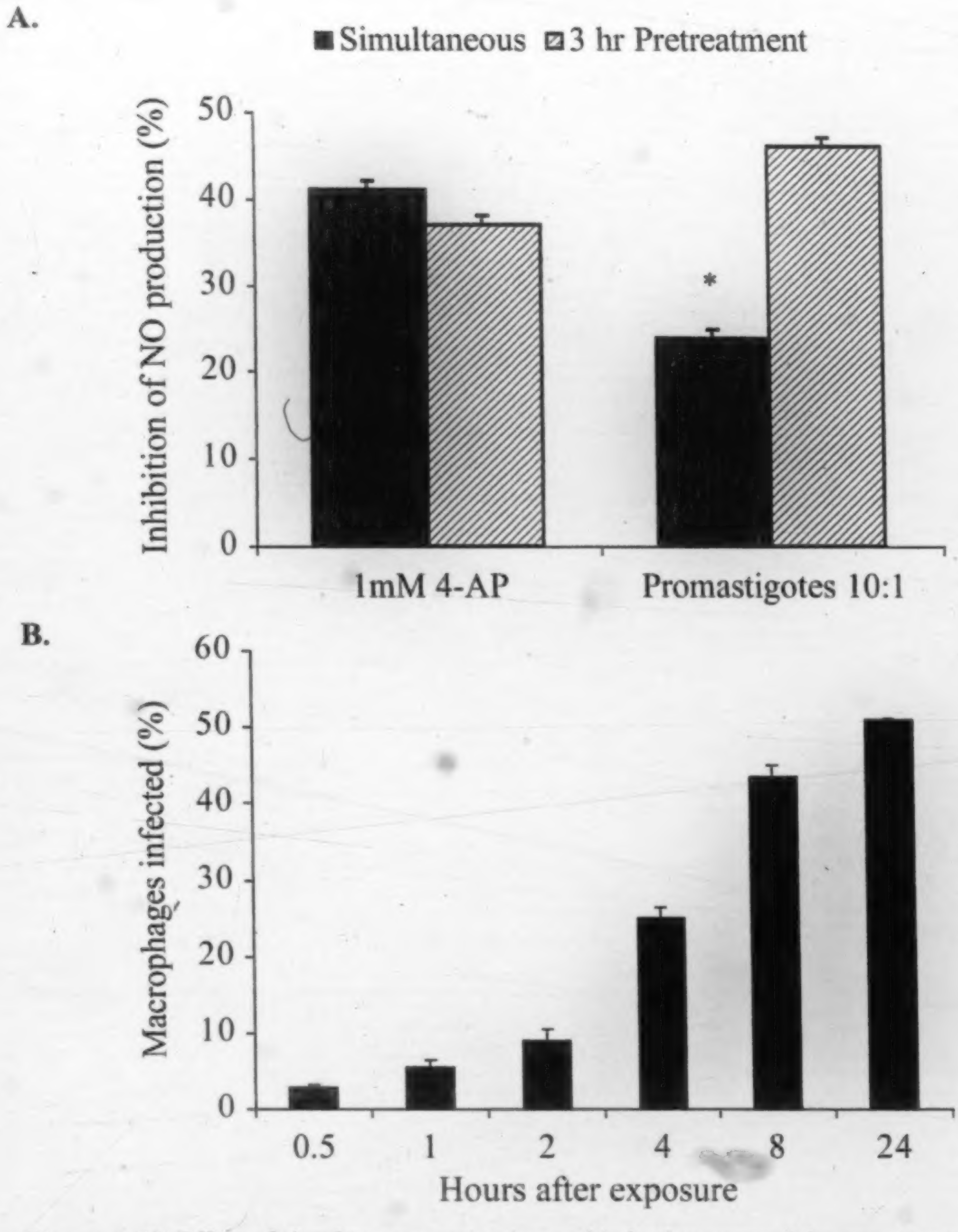

Figure 4-13. Effect of simultaneous activation and infection versus 3-hr. pre-treatment with *Leishmania major* promastigotes or 4-AP on nitric oxide (NO) production by P388D.1 macrophage-like cells after 24 hours. Infection prior to activation with 10 ng/ml LPS caused a greater inhibition of NO production than did simultaneous activation and infection (A). During the pre-treatment, 10 to 25% of cells are infected (B). Data are shown as mean ± s.e.m. (* $P<0.05$ compared to respective 3-hr. pretreatment) Data shown are a representative of two experiments that were performed.

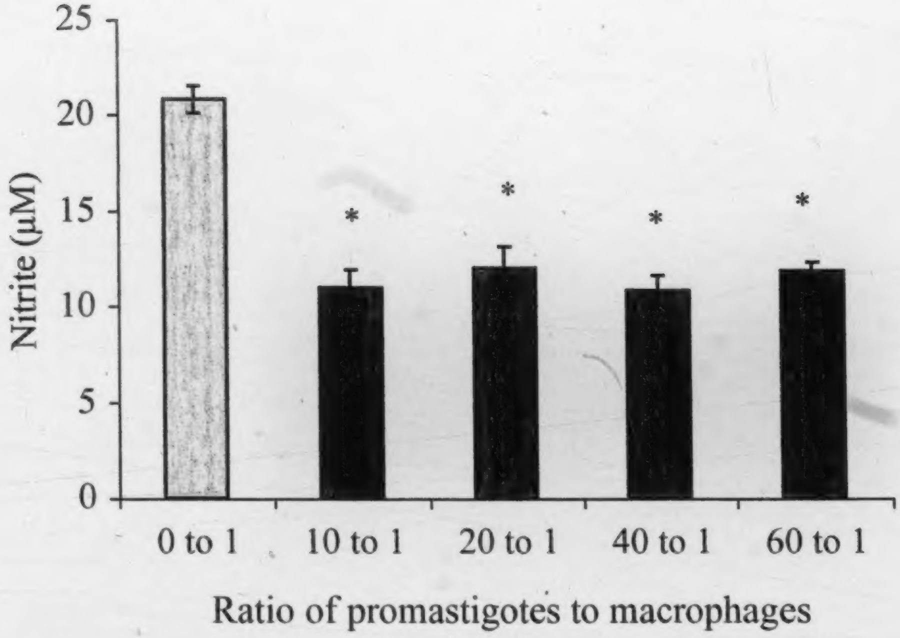

Figure 4-14. Effect of *Leishmania major* promastigote-to-macrophage ratio on nitric oxide (NO) production by P388D.1 macrophage-like cells after 24 hours. Increasing the ratio of promastigotes to macrophages did not further inhibit NO production by cells stimulated with 10 ng/ml LPS. Data are shown as mean ± s.e.m. (* $P<0.05$ compared to non-infected cells) Data shown are a representative of two experiments that were performed.

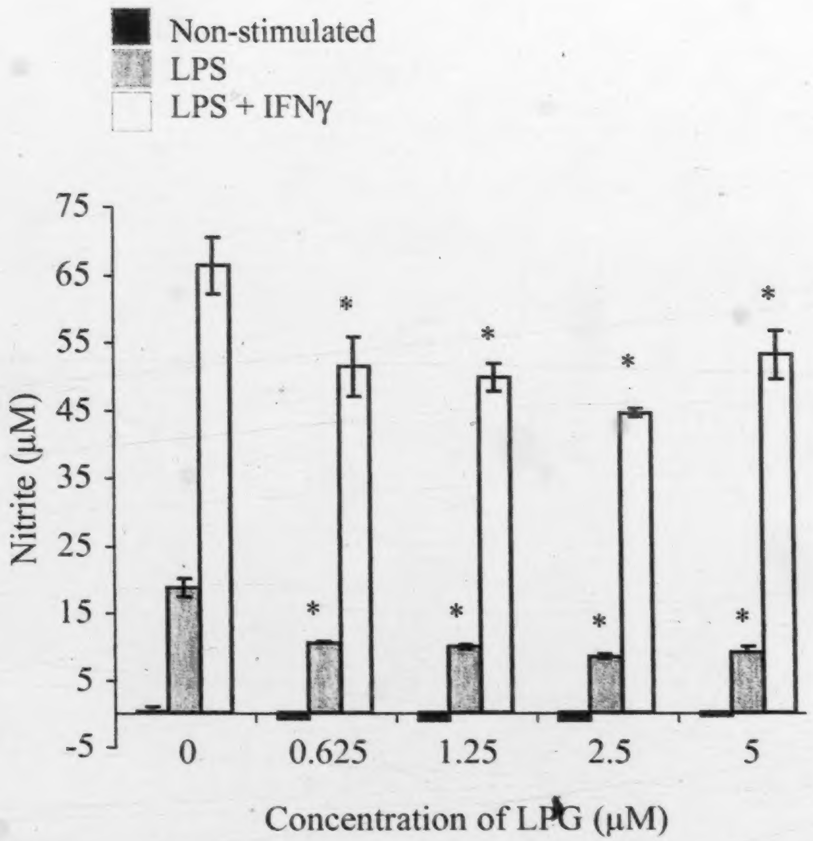

Figure 4-15. Effect of *Leishmania* lipophosphoglycan (LPG) on nitric oxide (NO) production by P388D.1 macrophage-like cells after 24 hours. Data are shown as mean ± s.e.m. (* $P<0.05$ compared to respective non-stimulated, LPS-stimulated (10 ng/ml), or LPS (10 ng/ml) and IFNγ (1 U/ml)-stimulated controls in 0 μM LPG) Data shown are a representative of two experiments that were performed.

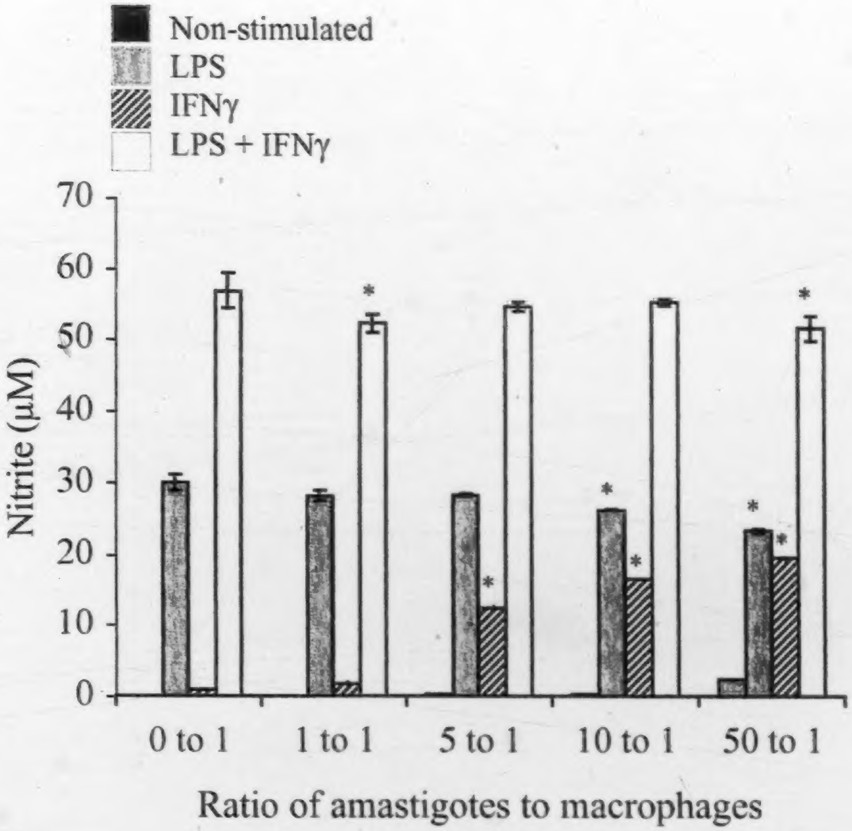

Figure 4-16. Effect of *Leishmania major* amastigote-to-macrophage ratio on nitric oxide (NO) production by P388D.1 macrophage-like cells after 24 hours. While high ratios inhibited NO production by LPS(10 ng/ml)-stimulated or LPS (10 ng/ml) and IFNγ (1 U/ml)-stimulated cells, amastigotes enhanced NO production by IFNγ (1 U/ml)-stimulated cells. Data are shown as mean ± s.e.m. (* $P<0.05$ compared to respective non-stimulated, LPS-stimulated, IFNγ-stimulated, or LPS and IFNγ-stimulated non-infected controls) Data shown are a representative of two experiments that were performed.

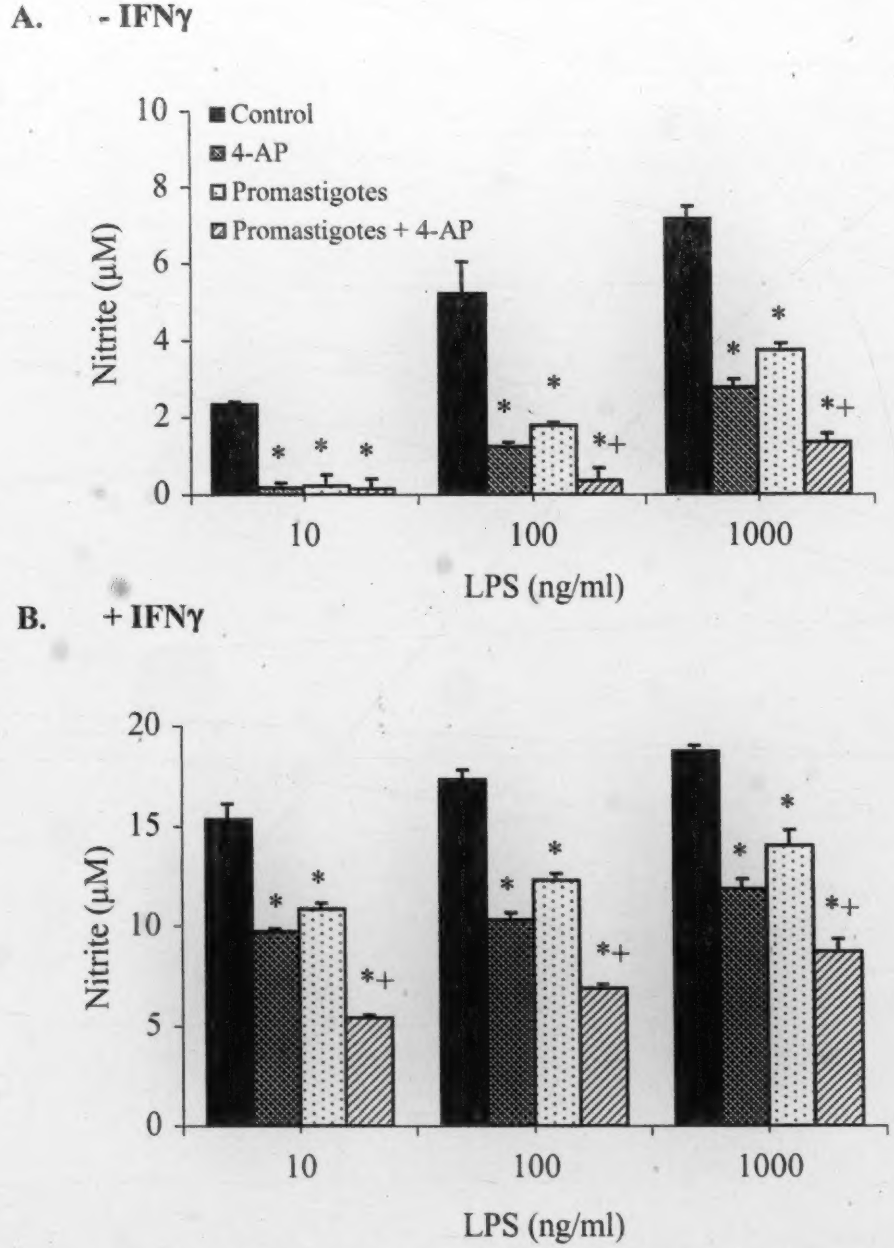

Figure 4-17. Effect of *Leishmania major* promastigotes and 4-AP on NO production by P388D.1 macrophage-like cells. The effect of increasing doses of LPS alone (A) or of LPS and 1 U/ml IFNγ (B) on nitric oxide production by P388D.1 cells treated with K^+ channel blocker 4-AP (1 mM) or *L. major* promastigotes (10:1) was examined. Data are shown as mean ± s.e.m. (* $P<0.05$ compared to respective controls stimulated with 10, 100, or 1000 ng/ml LPS; + $P<0.05$ compared to respective stimulated cells treated with 4-AP or *L. major* promastigotes) Data shown are a representative of two experiments that were performed.

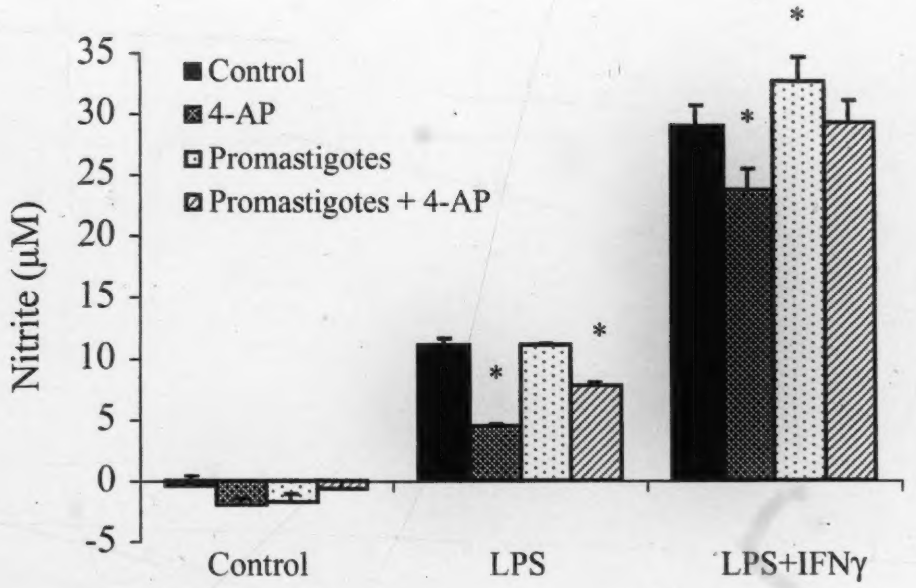

Figure 4-18. Effect of *Leishmania major* promastigotes, alone or in combination with 4-AP (1 mM), on NO production by bone marrow-derived macrophages after 24 hours. Data are shown as mean ± s.e.m. (* $P<0.05$ compared to respective non-stimulated, LPS, or LPS and IFNγ-stimulated controls) Data shown are a representative of two experiments that were performed.

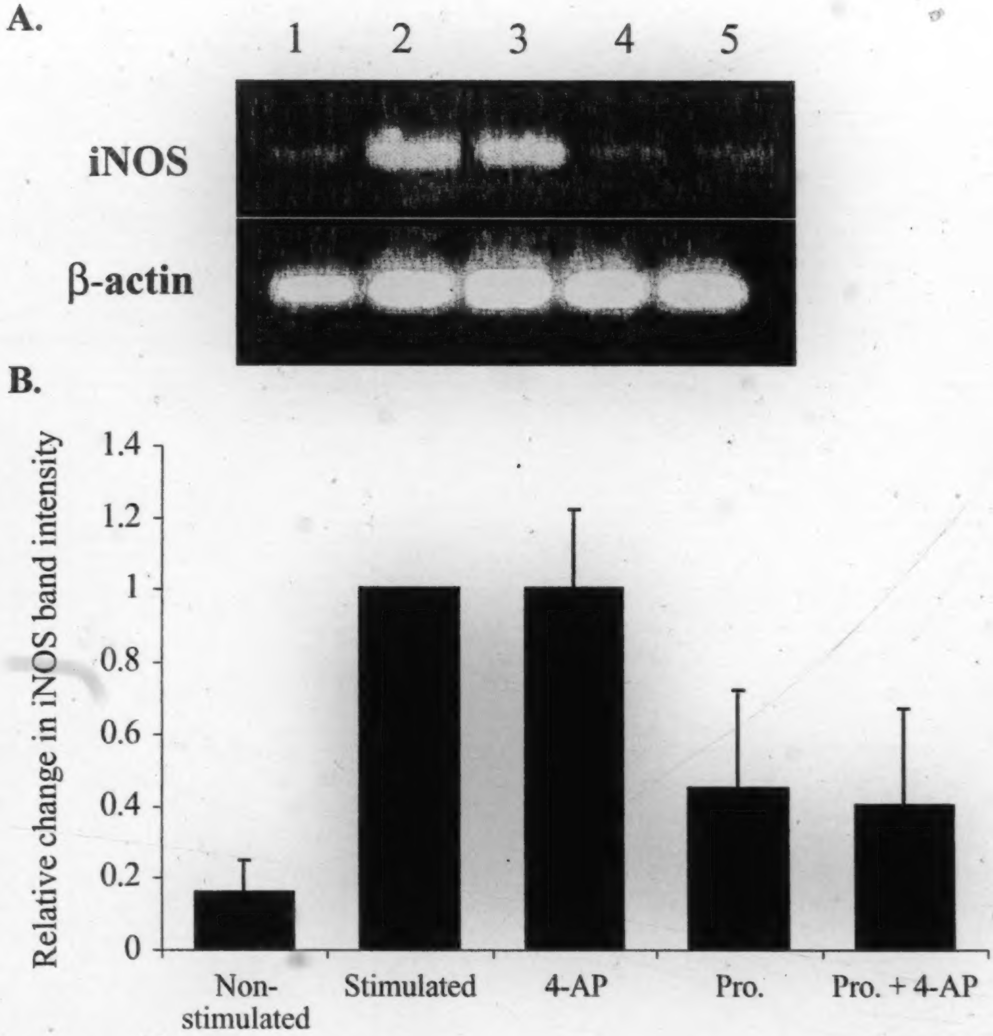

Figure 4-19. Effect of *Leishmania major* or 4-AP on iNOS mRNA expression in P388D.1 macrophage-like cells. At 3 hours post-stimulation, iNOS mRNA expression was lower in stimulated *L. major*-infected cells than in stimulated cells treated with the potassium channel blocker 4-AP, as shown in a representative ethidium bromide-stained gel (A). Lanes represent the following treatments: 1=non-stimulated, 2=stimulated control (LPS+IFNγ), 3= 1 mM 4-AP, 4=10:1 *L. major* promastigotes, 5=1 mM 4-AP and *L. major* promastigotes. Densitometric analysis of iNOS band intensity relative to β-actin band intensity (B). Intensity was normalized to stimulated controls. Data shown are mean ± s.e.m. of three ethidium bromide-stained gels.

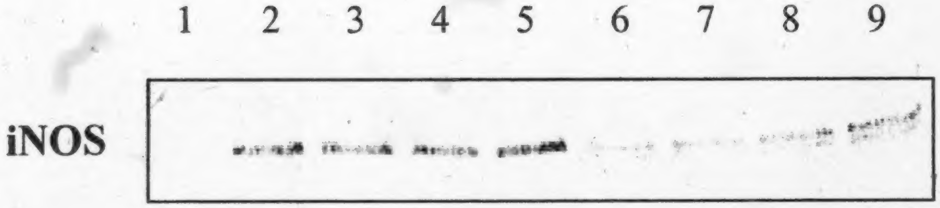

Figure 4-20. Effect of *Leishmania major* or K$^+$ channel blockers on iNOS enzyme availability in P388D.1 macrophage-like cells. At 6 hours post-stimulation, iNOS enzyme availability was lower in stimulated *L. major*-infected cells than in cells treated with potassium channel blockers, as shown in this representative immunoblot (1:1000 anti-mouse iNOS primary antibody). Lanes represent the following treatments: 1=non-stimulated, 2=stimulated control (LPS and IFNγ), 3=1 mM 4-AP, 4=100 μM quinine, 5=10 mM TEA, 6= 10:1 *L. major* promastigotes, 7= *L. major* promastigotes + 4-AP, 8= *L. major* promastigotes + quinine, 9= *L. major* promastigotes + TEA.

4.4 Discussion

It has been demonstrated that alterations in the K^+ channel activity of immune cells can have significant effects on the ability of those cells to mount antimicrobial responses. The data presented here confirm a role for functional K^+ channels in the ability of macrophages to produce cytotoxic molecules, namely reactive nitrogen and oxygen intermediates.

In agreement with our earlier observations (6), the results of this study support the hypothesis that K^+ channel activity is important for NO production by activated P388D.1 macrophages. Treatment with 4-AP, a non-selective potassium channel inhibitor, caused a dose-dependent decrease in NO production by macrophage-like cells and also inhibited the respiratory burst of those cells. In P388D.1 cells, the potassium channel blockers had no effect on iNOS gene expression or protein availability at the concentrations or time points examined.

Similar to the trends seen in P388D.1 cells, 4-AP inhibited the NO production of bone marrow-derived macrophages (BMDM). However, this blocker did not have the same dramatic effect on nitric oxide production by BMDM as it did on P388D.1 cells, as only relatively high concentrations of 4-AP (1 mM and above) suppressed NO production by BMDM stimulated with LPS and IFNγ whereas 0.25 mM 4-AP was enough to significantly suppress NO production by LPS and IFNγ-stimulated P388D.1 cells. Treatments with quinine and TEA also caused significant decreases in nitric oxide production by BMDM (as has been shown for P388D.1 and other macrophage-like cells (6)).

Similar to P388D.1 cells, 4-AP appeared to affect the PMA-induced respiratory burst of bone marrow-derived macrophages. This suggests that the types of K^+ channels which are blocked by 4-AP (notably the inwardly rectifying potassium (KIR) channels) may be involved in the pathway leading to assembly and activation of the NADPH oxidase complex in different cell populations. Furthermore, the results suggest that the K^+ channels blocked by 4-AP and involved in the respiratory burst are probably present in both BMDM and P388D.1 cells. Previous studies have shown that yeast zymosan but not PMA triggered the respiratory burst of bone marrow-derived macrophages, unless the BMDM were cultured with IFNγ or LPS (92). Respiratory burst was observed in PMA-stimulated bone marrow-derived macrophages in these experiments because the BMDM had been exposed to both LPS and IFNγ during activation.

Addition of PMA as a "trigger" to induce the respiratory burst in stimulated macrophages might influence the effect of 4-AP on those cells. For example, PMA could upregulate certain types of K^+ channels involved in macrophage activation. THP-1 monocytes differentiate to macrophages when exposed to PMA during culture, with resulting changes in their K^+ channel repertoire (93). KIR and Ca^{2+}-activated Maxi-K channels were observed exclusively in the macrophage stage of the THP-1 cells (93).

The reason for the difference between the sensitivity of NO production and respiratory burst to potassium channel blockage in BMDM is unknown. P388D.1 cells displayed a generalized suppression of activation in the presence of 4-AP, while the respiratory burst of BMDM appears to be more sensitive to the effects of 4-AP than does the function of NO production. The addition of PMA as a trigger for the respiratory burst response might influence this susceptibility by altering the expression of 4-AP sensitive

K^+ channels in the bone marrow-derived macrophages. More work is needed to fully characterize the differences between BMDM and P388D.1 macrophages.

In a study examining the role of ion channels in the activation of RAW 269 macrophage-like cells or N11 cells (derived from microglia), high concentrations of TEA or 4-AP had no effect on nitric oxide production (23). This clearly shows that macrophages of different origins can respond differently to potassium channel blockage, an observation which has implications for the therapeutic use of K^+ channel blockers as immunosuppressive agents to treat inflammatory diseases (94). The specific types and numbers of ion channels expressed by mononuclear phagocytes depends on the conditions in their immediate environment and may be indicative of a particular state of activation (23). Despite this, the inhibition of NO production and respiratory burst by both P388D.1 cells and BMDM treated with the K^+ channel blockers supports the hypothesis that at least some (unknown) types of K^+ channels are required for full macrophage activation.

Intracellular parasite survival requires the modulation of host immune cell functions. There is increasing evidence that intracellular pathogens actively alter the pathways of cell signaling resulting in macrophage deactivation. Inactivated macrophages become less responsive to immunological stimuli and exhibit reduced antimicrobial activities. Thus, functionally inactivated macrophages provide a suitable environment for the intracellular survival and replication of a range of pathogens. *Leishmania* spp. parasites actively alter the activation and translocation of PKC and disrupt Ca^{2+} regulation of infected macrophages. While there is yet no evidence for direct effects of LPS on Ca^{2+} pumps (95), inhibition of intracellular signaling events mediated through either PKC- or

Ca^{2+}-dependent pathways are believed to be responsible for impaired responsiveness to activating signals such as IFNγ, TNFα, and LPS (see Chapter 2).

L. major promastigotes appeared to suppress the nitric oxide and respiratory burst responses of P388D.1 cells. The suppression of NO production by *L. major* promastigotes and potassium channel blockers was likely due to inhibition through different pathways, as the effects on P388D.1 iNOS mRNA and enzyme were not similar between infected cells and cells exposed to blockers. *L. major* infection alone or in combination with K^+ channel blocker downregulated iNOS mRNA and protein. Compared to stimulated controls, there appeared to be very little expression of iNOS mRNA at 3 hours and a lower amount of iNOS enzyme at 6 hours in *L. major*-infected cells. Despite this there was still some NO production measured in the supernatants of infected, stimulated macrophages at 24 hours. It is quite possible that the infected cells will eventually induce the expression of iNOS mRNA but that the induction of gene and protein simply lags behind that of 4-AP-treated cells. At 24 hours there was a lower accumulation of NO in the supernatants of both blocker-treated cells and infected cells. Thus while there is a suppression of NO in both treatments, the kinetics of the NO induction may differ between infected, stimulated cells and blocker-treated, stimulated cells. It has been demonstrated that K^+ channel inhibitors do not directly affect the function of the iNOS enzyme although they may affect the expression (91), while *Leishmania* spp. parasites directly modulate the signaling pathways leading to expression of iNOS (1, 96). In this study, none of the potassium channel blockers tested resulted in a suppression of iNOS at the gene or protein levels. This indicates that the effect of potassium channel blockers on NO production could be due to effects on other genes or proteins involved in formation of iNOS, or could be due to a rapid turnover of NO as it is formed, the breakdown preventing its accumulation in macrophage supernatants.

The two types of macrophages differed slightly in their immune responses to the parasite. *L. major* infection of bone marrow-derived macrophages (BMDM) resulted in a lower respiratory burst response than was seen in uninfected BMDM, similar to the trend seen in P388D.1 cells. However, promastigotes only inhibited NO production in BMDM treated with the blocker. Amastigotes elicted a respiratory burst much higher than that of promastigotes. This was somewhat unexpected as ingestion of *L. major* amastigotes occurs primarily through the FcR and CR3 receptors, with the CR3 receptor being preferentially utilized because it allows the parasite to enter the cell "silently" by preventing induction of the respiratory burst response (33, 38). The enhanced respiratory burst in LPS- or LPS and IFNγ-stimulated P388D.1 macrophages could be due to the tremendous amount of phagocytic activity occurring in the presence of these amastigotes which, being freshly isolated from infected mice, are presumably opsonized with host antibody and complement. Exposure to PMA, which triggers the respiratory burst, enhances CR3-mediated phagocytosis of *L. major* amastigotes (33). Alternatively, the respiratory burst I observed may have been well past the stage of parasite uptake as the assay was performed at 24 hours, when cells are already infected. Thus, while the uptake itself may be "silent", the infected cells may still be producing ROI which are directed intracellularly, toward the vacuole containing the parasite. That is, the enhanced respiratory burst may be a feature of the infection process as a whole, and little is known about the kinetics of the effector functions in this particular model system. It was found that *L. donovani* amastigotes elicited a weak respiratory burst during their initial phagocytosis by peritoneal macrophages, but that immunologically activated macrophages that acquired leishmanicidal capacity over time could be triggered to release high concentrations of reactive oxygen intermediates such as hydrogen peroxide (97).

Parasite surface molecules, especially LPG which is the major surface molecule of *Leishmania* spp. promastigotes, have been identified as effector molecules responsible for many of the inhibitory effects on macrophage killing responses (44, 87, 98). Glycoinositolphospholipids (GIPLs) are the predominant surface glycolipids in both developmental forms of *L. major* while lipophosphoglycan (LPG) is significantly downregulated in amastigotes. Glycoinositolphospholipids have been shown to inhibit the synthesis of NO in a time- and dose-dependent manner by IFNγ- and LPS-activated J774 macrophage-like cells (49) and LPG has been shown to inhibit NO synthesis by BMDM (44, 45). In this study, the 10:1 ratio of promastigotes to macrophages appeared to be insufficient to inhibit NO production by LPS-stimulated BMDM. However, the inhibitory effect of *L. major* promastigotes on NO production and respiratory burst by IFNγ- and LPS-stimulated P388D.1 cells suggests that the current study's findings of greater inhibition of ROI and RNI by promastigotes than by amastigotes may also be due to a surface molecule such as LPG. This argument is strengthened by the observation that soluble LPG caused an inhibition of NO production by P388D.1 cells.

It has been argued that potassium channels are not involved in the *in vitro* generation of nitric oxide by activated macrophages and microglial cell lines and that it is the alteration of chloride (Cl^-) channels which is more likely to contribute to downregulation of the NO response (23). While the modulation of K^+ channels and Cl^-

channels can both affect a cell's membrane potential, it is K$^+$ channels that play a major role in setting the membrane potential of macrophages. The contribution of each type of channel to the immune responses of macrophages cannot be fully distinguished. However, there is a wealth of data supporting the requirement for K$^+$ channels in the activation of immune cells and the data presented here confirm a role for functional K$^+$ channels in macrophage activation. Thus the effects of potassium channel blockage and *L. major* infection on macrophage membrane physiology were examined.

Chapter 5: Effect of K^+ Channel Blockers on Macrophage Membrane Physiology during *Leishmania major* Infection

5.1 Introduction

Ionic current flow through various types of ion channels has been demonstrated on many occasions to alter immune cell function through modulation of intracellular signaling cascades (99, 100). Indeed, inhibition of potassium currents has been demonstrated to be a potential therapeutic target for treatment of some autoimmune diseases (20, 94). Primary macrophages and macrophage-like model systems have been shown to possess a number of ion channels important for their cytotoxic functions (54-57, 62, 101). As previously mentioned, treatment of P388D.1 macrophage-like cells with the K^+ channel blockers TEA, 4-AP, and quinine significantly reduces production of nitric oxide following activation with LPS and IFNγ, demonstrating a direct link between functional K^+ channels and macrophage ability to mount a cytotoxic response (6).

A major role of K^+ channels in cells is the establishment and maintenance of membrane potential (V_m) (54-56, 101). The main function of K^+ channels within macrophages is believed to be the maintenance of V_m between approximately –30 and –56 mV (54), although this value is variable. Cultured peritoneal macrophages, for instance, have a measured membrane potential between approximately –65 and –95 mV (101). As discussed in Chapter 2, the types, numbers, distribution, and open probabilities of K^+ channels in cells is dependent on various environmental influences.

Alterations in the activity of potassium channels resulting in changes in V_m can have significant effects on proteins and enzymes embedded in the plasma membrane

(102). For instance, K^+ channel activity has been shown to modulate NADPH oxidase activity in human monocyte-derived macrophages (103). Activation of this enzyme, which catalyzes superoxide formation, is dependent on maintenance of membrane V_m directly modulated by the opening of Ca^{2+}-dependent K^+ channels (103). Others have shown that the release of TNFα by LPS-stimulated mouse macrophages is dependent on V_m (74). Modulation of immune cell K^+ channel activity by a least some types of pharmacological inhibitors appears to cause alteration in V_m, which can have deleterious effects on a variety of cellular functions (e.g. NO production, NADPH activity, and TNFα secretion).

Ion channels may be also altered during macrophage infection with intracellular pathogens. Little is known about the effect of parasite invasion on host cell ion channel activity, ion homeostasis and host cell V_m. *L. amazonensis* has been shown to modulate the K^+ channel activity and V_m of J774.1 macrophage-like cells (59), with unknown effects on the immune responses of those macrophages. I hypothesized that the alterations in K^+ channel activity of *L. major*-infected macrophages caused sustained changes in V_m, culminating in the inhibition of effector functions such as the production of RNI and ROI.

The experiments outlined in this Chapter aimed to examine the role of K^+ channels in the physiology of macrophages, particularly in the context of *L. major* infection.

5.2 Determination of Changes in Macrophage Membrane Potential

5.2.1 Experimental design and objectives

5.2.1.1 *Estimating and calibrating macrophage V_m*

The objective of this set of experiments was to calibrate the fluorescence of the bis-oxonol dye and to estimate macrophage plasma membrane potential (V_m) based on predicted values from the literature. P388D.1 cells were washed twice in DMEM by centrifugation at 4°C for 10 minutes, and resuspended in isoosmotic, filter-sterilized KCl solutions (see below). To calibrate fluorescence intensity in relation to V_m, cells were seeded into 6 ml polypropylene tubes containing 1.3, 4, 10, 20, 40, and 80 K^+ (mM) balanced to 144 mM total Na^+/K^+. Each tube also contained 0.8 μM gramicidin, a K^+/Na^+ ionophore, to clamp the relative permeability ratio for K^+ and Na^+ to equal that of gramicidin (1 : 0.05). The values for extracellular potassium concentration ($[K^+]e$) were chosen to give a range from hyperpolarized (low $[K^+]e$) to depolarized (high $[K^+]e$) compared to a normal extracellular $[K^+]e$ of 5.3 mM in DMEM. Solutions were adjusted to the normal osmolarity of DMEM by the addition of 1 M NaCl. KCl solutions (pH 7.4) contained 2% FBS and 1/4 the glucose and amino acids of normal DMEM. After a 15-minute incubation at 37°C and 5% CO_2 in the various solutions, cells were loaded with 5 μM bis-oxonol and incubated for a further 15 minutes at 37°C as described in detail in Materials and Methods. Cells were then washed two times with medium containing the appropriate K^+ concentration and gramicidin and resuspended in the same to a final volume of 250 μl. The relative fluorescence intensity (FL-2) was determined using a flow cytometer, as described in Materials and Methods.

To compensate for variations in the loading efficiencies of bis-oxonol and to allow for comparisons between independent experiments, the fluorescence intensity values were normalized such that cells incubated in the lowest $[K^+]e$ (1.3 mM) had a relative fluorescence equal to 1. Changes in the relative fluorescence units (RFU) of P388D.1 cells in medium containing bis-oxonol were an indication of relative changes in plasma membrane V_m. Predicted values of membrane potential changes (in mV) were calculated using the Goldman-Hodgkin-Katz equation from the known $[K]_o$ and $[Na]_o$ (concentrations of potassium and sodium outside) in the medium, the P_K/P_{Na} ratio of gramicidin (1 : 0.05) and concentrations of potassium and sodium inside the cell estimated at100 mM $[K]_i$ and 8 mM $[Na]_i$. Application of the Goldman-Hodgkin-Katz equation allowed for an estimation of resting membrane potential (V_{rest}). The equation is as follows (51):

$$(1) \qquad V_{rest} = \frac{RT}{F} \log_e \frac{P_K[K]_o + P_{Na}[Na]_o + P_{Cl}[Cl]_o}{P_K[K]_i + P_{Na}[Na]_i + P_{Cl}[Cl]_i}$$

In this equation, R is the gas constant, T is the absolute (Kelvin) temperature, and F is the Faraday constant. It was assumed that Cl^- was close to its equilibrium potential and did not contribute greatly to the resting membrane potential, thus simplifying the equation to:

$$(2) \qquad V_{rest} = \frac{RT}{F} \log_e \frac{1[K]_o + 0.05[Na]_o}{1[K]_i + 0.05[Na]_i}$$

The predicted membrane potential values were used to generate a standard curve for converting fluorescence of bis-oxonol (expressed as relative fluorescence units, RFU) to a predicted membrane potential value (in mV). Small variations in the estimated concentrations of Na^+ and K^+ would produce only slight quantitative, but not qualitative, variations in the estimated values generated for V_m.

5.2.1.2 *Effect of K^+ channel blockers on V_m*

To determine the effects of potassium channel blockers on relative changes of macrophage membrane potential (V_m), cells were seeded into tubes as previously described. Cells were treated with 125 µl of medium (control) or 125 µl of 4-AP (1 mM final). The final volume in all tubes was 500 µl with a final concentration of 2% FBS. After 30 minutes, cells were loaded with 5 µM bis-oxonol as described in Materials and Methods and incubated for a further 15 minutes at 37°C. Cells were then washed once in 3 ml medium (control) or in medium supplemented with potassium channel blockers to remove residual bis-oxonol, resuspended in 250 µl of the same, and the relative fluorescence intensity (FL-2) was determined using a flow cytometer as described in Materials and Methods, and normalized such that fluorescence of cells in DMEM was equal to 1. RFU (relative fluorescence units) were converted to predicted membrane potential values (in mV).

5.2.1.3 *Reversibility of altered V_m by removal of K^+ channel blockers*

To determine whether the potassium channel blockers were directly responsible for alterations of murine macrophage membrane potential, potassium channel blocker wash-out experiments were performed. Cells were seeded and incubated with 1 mM 4-AP for 6 hours. Prior to the addition of 5 µM bis-oxonol, the blockers were removed from the wash-out group by washing the cells twice with 3 ml of medium. After washing, the cells were loaded with 5 µM bis-oxonol as described in Materials and Methods, washed, resuspended in 250 µl of medium with or without blocker as required, and the relative fluorescence intensity (FL-2) was determined using a flow cytometer as described in Materials and Methods, and normalized such that fluorescence of cells in DMEM was equal to 1. RFU (relative fluorescence units) were converted to predicted membrane potential values (in mV).

5.2.1.4 *Effect of L. major infection on V_m*

The objective of this set of experiments was to determine the effects of *L. major* promastigotes on the plasma membrane potential (V_m) of macrophages. Cells were seeded into tubes as previously described. Cells were infected with promastigotes (125 µl) and simultaneously treated with 125 µl of medium (control) or 125 µl of 4-AP (1 mM final). The final volume in all tubes was 500 µl.. After 3, 6, or 24 hours cells were loaded with 5 µM bis-oxonol as described in Materials and Methods, and incubated for a further 15 minutes at 37°C. Cells were then washed once in 3 ml medium with or without blocker as required, to remove residual bis-oxonol and parasites. Cells were resuspended in 250 µl of medium with or without blocker as required. The relative fluorescence intensity (FL-2) was determined using a flow cytometer as described in Materials and Methods, and values were normalized such that fluorescence of control cells was equal to 1. RFU (relative fluorescence units) were converted to predicted membrane potential values (in mV). Gating using flow cytometry was used to ensure that the only the fluorescence of macrophages (R1) was read, eliminating the fluorescent from non-phagocytosed parasites (R2).

5.2.2 Analysis

Data are shown as fluorescence values converted to estimated membrane potential values in mV. Data were analyzed using the Super-ANOVA software for the Power Macintosh. Differences between groups were measured using one and two-factor analysis of variance and a least-squares means test. Probability level of $P<0.05$ was considered significant. All experiments were repeated two or more times.

5.2.3 Results

Increasing the extracellular potassium in the medium depolarized the membrane of P388D.1 cells. Incubation of cells with increasing concentrations of KCl caused a dose-dependent increase in the fluorescence of bis-oxonol loaded cells (Fig. 5-1). Data shown are representative of three experiments that were performed. An equation for conversion of relative fluorescence units (RFU) to predict V_m was generated using the Goldman-Hodgkin-Katz equation as described (Fig. 5-2). In all subsequent figures, RFU has been converted to predicted V_m using this equation.

P388D.1 cells incubated with increasing concentrations of the potassium channel blocker 4-AP (Fig. 5-3) displayed significant depolarization of the plasma membrane after 6 hours ($P=0.0025$, $P=0.0001$, $P=0.0001$, $P=0.0001$ compared to control cells in 0 mM 4-AP). Data shown are a representative of two experiments that were performed.

The depolarization of the P388D.1 plasma membrane with 4-AP (Fig. 5-4) was due to the potassium channel blocker and was significantly different from control cells in

DMEM (P=0.014). The depolarization (by approximately 22 mV) seen in cells treated with 4-AP for 6 hours was fully reversible, because the membrane potential in cells with the blocker washed out was restored to levels not significantly different from controls (P=0.555). The wash-out cells had a membrane potential significantly more negative than 4-AP-treated cells (P=0.007). Data shown are a representative of two experiments that were performed.

Treatment with 4-AP caused a significant depolarization of the plasma membrane of P388D.1 cells at all time points examined (Fig. 5-5) which corresponded to depolarizations of -34, -32, and -34 mV at 3, 6, and 24 hours, respectively (P=0.0001, P=0.0001, and P= 0.0128 compared to respective controls). P388D.1 cells infected with *L. major* promastigotes demonstrated significant changes in V_m after 3 and 6 hours of infection (P=0.015 and P=0.006 compared to respective controls). The decreased fluorescence corresponded to a hyperpolarization of the P388D.1 plasma membrane. After 24 hours, *L. major*-infected cells were significantly depolarized (P=0.0001) compared to control cells (down to -22 mV). Combined treatments with 4-AP and promastigotes also caused a significant depolarization of P388D.1 plasma membrane potential after 6 and 24 hours, which at 6 hours was not significantly different from the membrane potential of cells treated with 4-AP alone (P=0.971). Data shown are a representative of two experiments that were performed.

A calibration curve of bis-oxonol fluorescence (in relative fluorescent units, RFU) versus predicted membrane potential values (mV) was not performed for BMDM. The values were expressed as RFU. Bone marrow-derived macrophages (BMDM) treated with 4-AP (Fig. 5-6) displayed significant depolarization after 24 hours (P=0.0015).

Unlike the response seen in P388D.1 cells, treatment with *L. major* promastigotes alone or in combination with 4-AP did not cause a statistically significant depolarization in BMDM (P=0.254 and 0.218 respectively), although there does appear to be a small depolarization of the membrane of infected cells (RFU > 1). The membrane potential of *L. major* infected cells was not significantly different than cells infected and treated with 4-AP (P=0.903). Data shown are a representative of two experiments that were performed.

Appropriate gating by the flow cytometer was required to eliminate any contribution of bis-oxonol fluorescence that occurred in the presence of unincorporated promastigotes loaded with dye (Fig. 5-7).

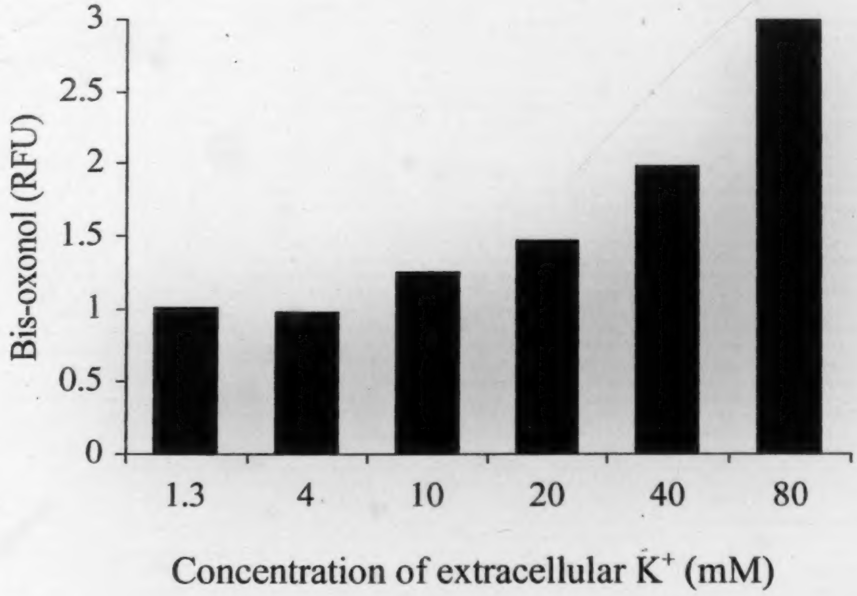

Figure 5-1. Effect of increased extracellular K^+ and gramicidin on membrane potential of P388D.1 macrophage-like cells after 30 minutes. Increasing the extracellular concentration of potassium ($[K^+]_e$) in the presence of 0.8 μM gramicidin caused a depolarization of the plasma membrane of P388D.1 cells, as indicated by increased fluorescence of bis-oxonol. Fluorescence was normalized such that the fluorescence of cells in 1.3 mM K^+ was equal to 1. Data shown are a representative of three experiments that were performed.

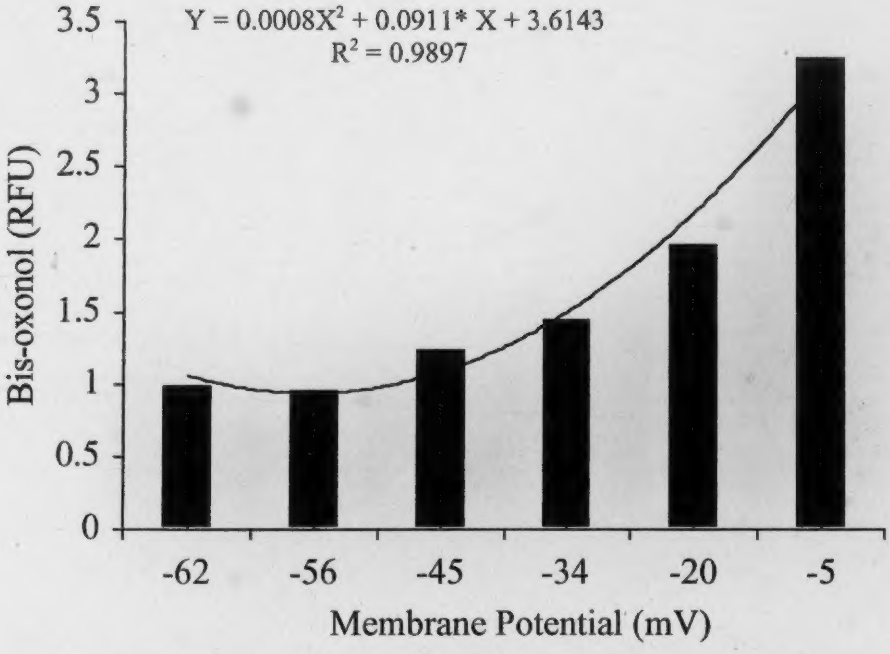

Figure 5-2. Calibration of membrane potential as changes in bis-oxonol fluorescence of P388D.1 macrophage-like cells. Bis-oxonol fluorescence (FL-2) of cells was expressed as relative fluorescence units (RFU) and the membrane potential was based on estimated intracellular concentrations of K^+ and Na^+ of 100 mM and 8 mM, respectively. Fluorescence was calibrated using 0.8 μM gramicidin, a Na^+/ K^+ ionophore. The equation of the trend line is shown.

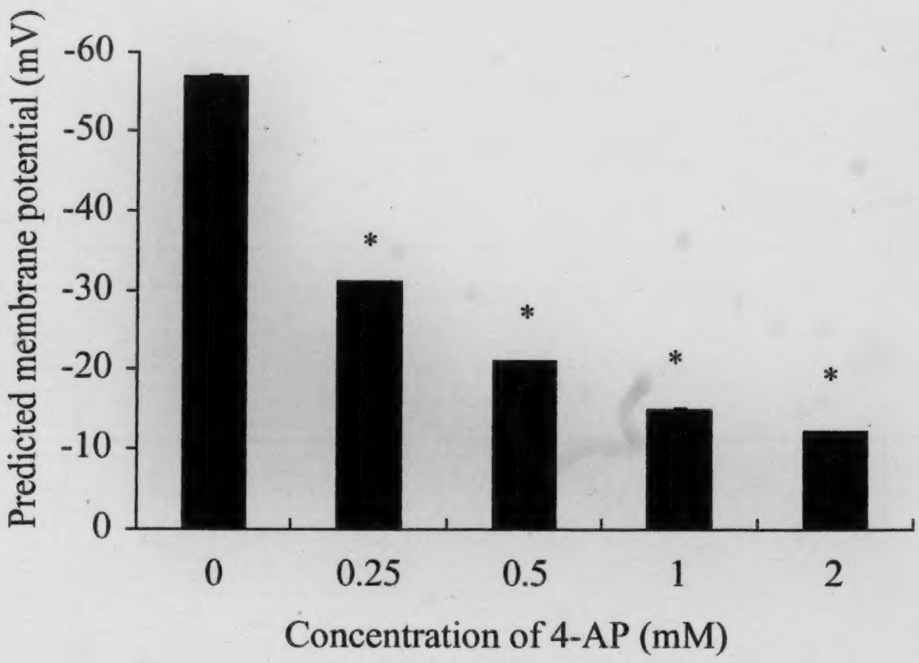

Figure 5-3. Effect of increasing doses of 4-AP on membrane potential of P388D.1 macrophage-like cells. The potassium channel blocker 4-AP caused depolarization of the P388D.1 plasma membrane as measured after 6 hours. Data are shown as mean ± s.e.m. (* $P<0.05$ compared to control) Data shown are a representative of two experiments that were performed.

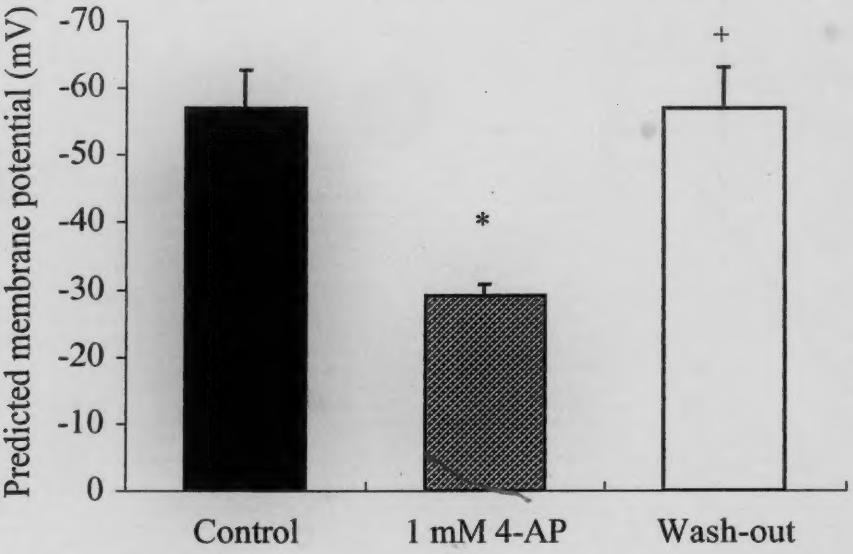

Figure 5-4. Effect of 4-AP on membrane potential of P388D.1 macrophage-like cells. Wash-out experiments show that the 4-AP-induced depolarization of P388D.1 cells was reversible. Data are shown as mean ± s.e.m. (* $P<0.05$ compared to control; + $P<0.05$ compared to 4-AP-treated cells) Data shown are a representative of two experiments that were performed.

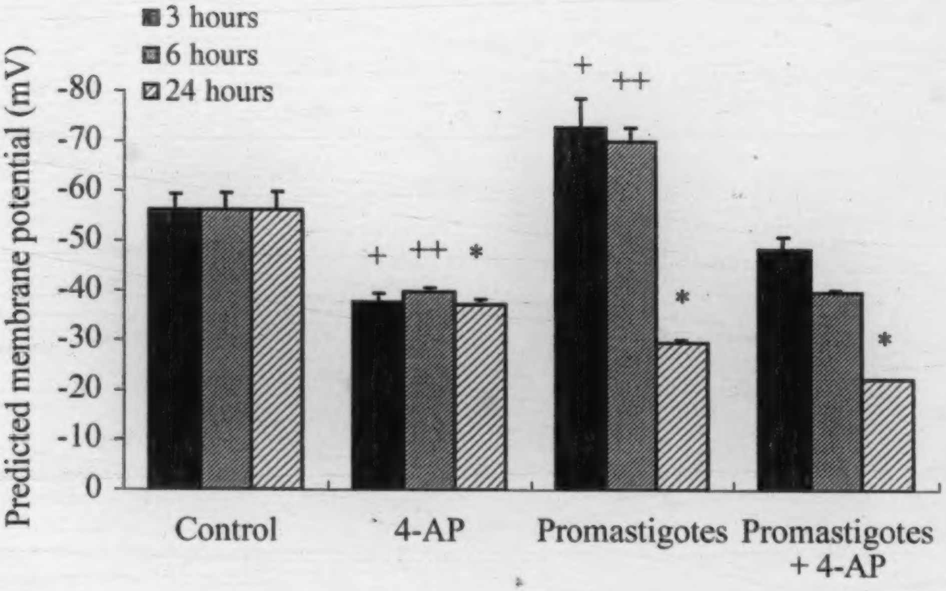

Figure 5-5. Effect of 4-AP and *Leishmania major* promastigotes on membrane potential of P388D.1 macrophage-like cells. Infection with *L. major*, alone or in combination with 4-AP (1 mM), induced a depolarization of P388D.1 plasma membrane after 24 hours. Data are shown as mean ± s.e.m. ($P<0.05$ compared to respective controls at (+) 3 hours, (++) 6 hours, and (*) 24 hours) Data shown are a representative of two experiments that were performed.

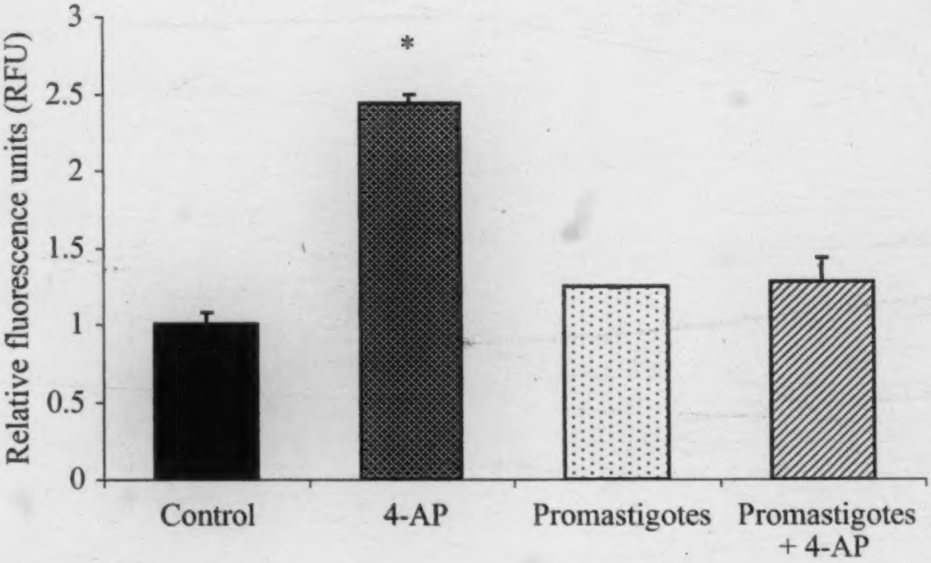

Figure 5-6. Effect of *L. major* promastigotes, alone or in combination with 4-AP (1 mM), on the V_m of bone marrow-derived macrophages (BMDM) after 24 hours. Data are shown as mean ± s.e.m. (* $P<0.05$ compared to control) Data shown are a representative of two experiments that were performed.

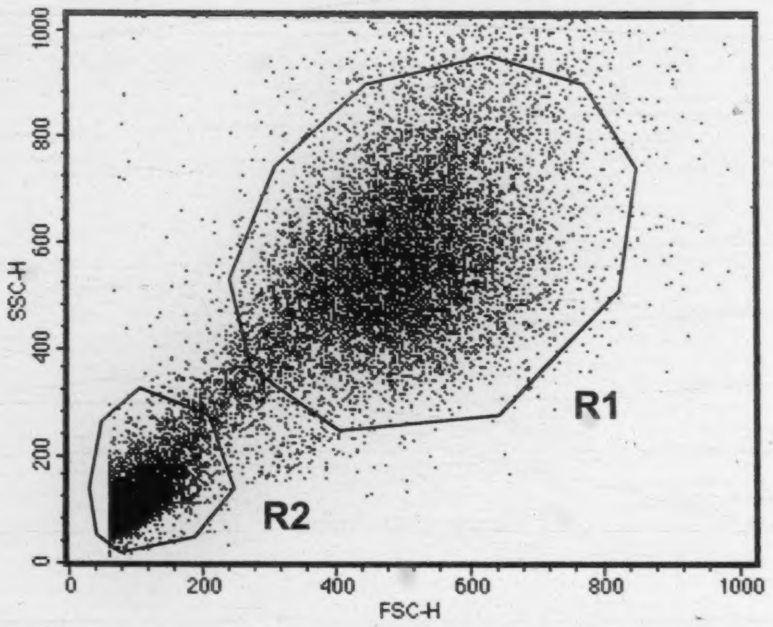

Figure 5-7. Bis-oxonol fluorescence from non-phagocytosed parasites was eliminated by "gating" the two types of cells differently during flow cytometric analysis. Gating was based on their size (FSC-H; forward scatter) and internal complexity (SSC-H; side scatter). The R1 region represents macrophages (P388D.1 cells or bone marrow-derived macrophages) and the R2 region represents *Leishmania major* promastigotes.

5.3 Determination of Changes in K^+ Flux

5.3.1 Experimental design and objectives

The objective of these experiments was to determine the effect of K^+ channel blocker and/or *L. major* promastigotes on unidirectional $^{86}Rb^+$ influx, an indicator of K^+ influx. P388D.1 cells (10 x10^6) were seeded into 25 cm^2 flasks and treated with complete DMEM (control), 1 mM 4-AP, *L. major* promastigotes (10:1), and 1 mM 4-AP and *L. major* promastigotes (10:1). A group of control cells were treated with 3 μm latex beads (10:1; beads-to-macrophage ratio) to determine the effect of *L. major* infection versus phagocytosis alone on the unidirectional influx of $^{86}Rb^+$. The detailed methods for these experiments are described in Materials and Methods.

5.3.2 Analysis

Data were analyzed using the Super-ANOVA software for the Power Macintosh. Differences between groups were measured using one and two-factor analysis of variance and a least-squares means test. Probability level of $P<0.05$ was considered significant. All experiments were repeated two or more times.

5.3.3 Results

Accumulation of $^{86}Rb^+$ in bumetanide and ouabain-blocked P388D.1 macrophage-like cells was steady for 100 minutes but reached a plateau thereafter suggesting that backflux was not a significant problem in this period. Based on these results, a 120-minute $^{86}Rb^+$ influx period was chosen for subsequent experiments (Fig. 5-8).

Treatment with 1 mM 4-AP for 24 hours (Fig. 5-9) caused a significant increase (approximately 2.5-fold) in the unidirectional influx of the K^+ ion tracer $^{86}Rb^+$ (P=0.0001). Similarly, *L. major*-infected P388D.1 cells showed a significant increase in the unidirectional influx of $^{86}Rb^+$ (P=0.0003). No significant differences in rubidium influx were observed among cells treated with 4-AP, *L. major*, or *L. major* and 4-AP. Treating the P388D.1 cells with 4-AP and *L. major* promastigotes increased the unidirectional influx approximately 2.5-fold above controls (P=0.0005). Latex beads (3 μM) did not cause a significant alteration in the unidirectional influx of $^{86}Rb^+$ (control 151 ± 19.6; latex beads 106 ± 19.6 nmol K^+ per 10^6 cells) indicating that physical perturbation of the membrane due to phagocytosis alone was insufficient for inducing the observed increases in potassium influx (P=0.1514).

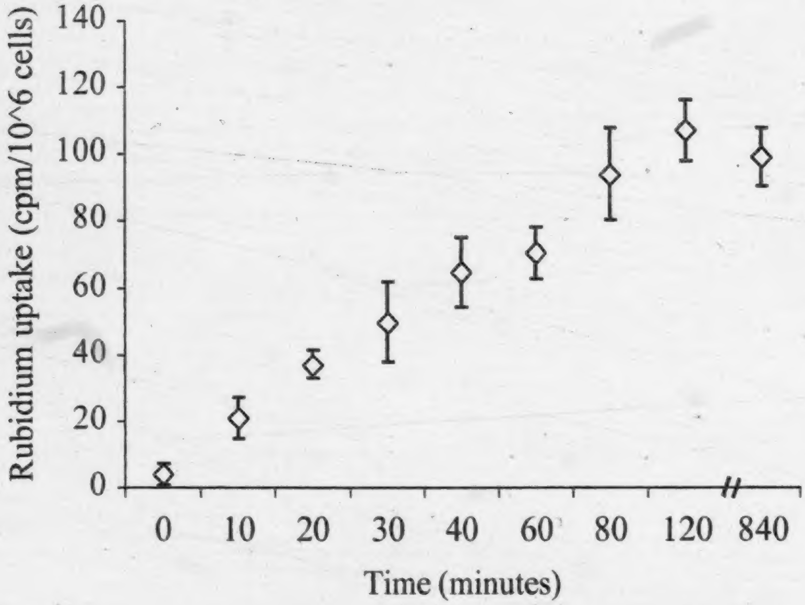

Figure 5-8. Time course of radiolabeled rubidium ($^{86}Rb^+$) uptake into P388D.1 cells. Based on these data, an optimal loading time of 120 minutes was chosen for subsequent experiments. Data are shown as mean ± s.e.m.

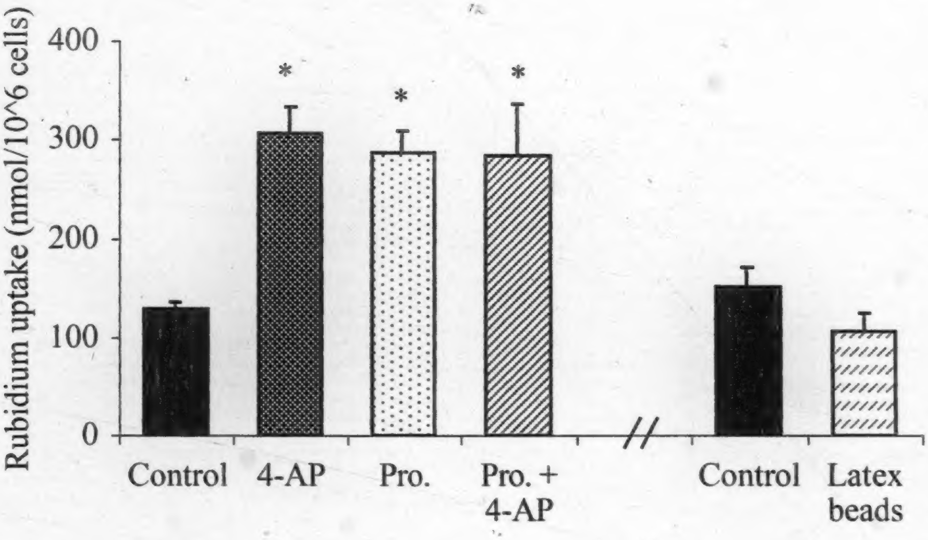

Figure 5-9. Effect of *Leishmania major* promastigotes and K^+ channel blocker 4-AP (1 mM) on the influx radiolabeled rubidium ($^{86}Rb^+$), a tracer for potassium ions, into P388D.1 cells after 24 hours. Data are shown as mean ± s.e.m. (* $P<0.05$ compared to control) Data shown are a representative of two experiments that were performed.

5.4 Discussion

The data presented here demonstrate that the alteration of K^+ channels by potassium channel blockers and *L. major* may modulate the effector functions of murine macrophages.

As discussed in Chapter 2, K^+ channels set the membrane potential (V_m) in macrophages. For the purposes of estimating membrane potential in this study, it was assumed that the contribution of chloride in setting the V_m was negligible. In whole cell patch-clamp examination of THP-1 (cell-line) monocytes, outwardly-rectifying Cl^- currents disappeared after several minutes, and the authors hypothesized that the small initial changes were merely due to equilibration of osmotic balance (93). Other large anion channels were also uncommon in these cells, although a non-selective cation current was present in some (93). Many assumptions were made to calibrate bis-oxonol fluorescence intensity to mV. For example, while the contribution of chloride to the maintenance of V_m may be negligible, the permeability of chloride may change, especially at depolarizing potentials. In addition, estimations of intracellular ion concentrations and of the permeability coefficient for gramicidin were based on literature values for macrophages or macrophage-like cells. True calibration of resting and depolarized V_m necessitates patch-clamping. Thus the values for V_m should be considered estimates.

After 24 hours, the potassium channel blocker 4-AP and *L. major* promastigotes both induced a depolarization of the membrane of P388D.1 cells and an increased influx of K^+ into P388D.1 cells. 4-AP also induced a depolarization of bone marrow-derived macrophages (BMDM) after 24 hours. The mechanism for the depolarization in both cell types, and for the K^+ influx in 4-AP-treated P388D.1 macrophages, is unknown. However, a likely cause for the changes in V_m and for the increase of unidirectional K^+ influx in both cases was an alteration of K^+ channel activity. Blocking K^+ efflux or increasing K^+ influx will both act to depolarize cell membrane potential. The drug 4-AP blocks net K^+ efflux by diffusing into the cell and physically blocking the pore of specific K^+ channels involved in setting the membrane potential. While an increased influx would contribute to a depolarization of the cell membrane potential, the combination of K^+ channel blockage with an increased unidirectional influx might be explained by a secondary cellular response to increase expression of K^+ channels which are sensitive to 4-AP. An increased expression of this K^+ channel would be a futile attempt to counteract the depolarization by 4-AP. The increased expression might create the observed increase in unidirectional influx of $^{86}Rb^+$ in P388D.1 macrophages.

After 24 hours, there was a depolarization of V_m in *L. major*-infected P388D.1 macrophages which corresponded to an increased $^{86}Rb^+$ influx. The mechanism for this is unknown. There may be a secondary cellular response to increase expression of K^+ channels as discussed above. The similarity in the $^{86}Rb^+$ influx responses in cells treated with blockers or the parasite suggests that *L. major* promastigotes may directly or indirectly alter K^+ efflux pathways. Forero *et al.* showed that invasion of murine macrophages by *L. amazonensis* caused a significant hyperpolarization compared with uninfected controls (59). Hyperpolarization was observed for up to 72 hours post-infection and was predominantly a result of elevated intracellular K^+ concentrations which could occur with increased influx through KIR (inwardly-rectifying potassium channels. It was shown that *L. amazonensis* infection produced an upregulation of KIR channels, which play an essential role in establishing and maintaining host cell V_m (59). However, the significance of this observation with regards to macrophage activation and functional responses was not explored.

The data presented here only partially support the observations by Forero *et al.* (59); in P388D.1 cells infected with *L. major* there was a clear depolarization of the macrophage membrane potential at 24 hours, although observations at 3 and 6 hours suggest there is a hyperpolarization of the plasma membrane at those time points (likely a result of phagocytosis). The V_m of infected bone marrow-derived macrophages was not examined at time points earlier than 24 hours. Confocal microscopy of *Toxoplasma gondii*-infected monocytes loaded with bis-oxonol were shown to have a hyperpolarized plasma membrane at 24 hours post-infection while the compartments containing the parasites were depolarized, as indicated by bright fluorescence in the parasitophorous vacuoles (104). The flow cytometric method used in this study to detect bis-oxonol fluorescence could not distinguish between fluorescence from the whole macrophage or from parasite-containing vacuoles within the macrophages. However, the relative ease with which the depolarization could be reversed in the potassium channel blocker wash-out experiments indicates that the fluorescence is mainly localized within the cytoplasm of the cells. The differences between the current study and the studies of other intracellular parasites may be due to the specific macrophage type used, the species of parasite, the order and concentration of activating stimuli to which macrophages were subjected, the technique used to measure membrane potential, or a combination of those factors. Regardless, infection with *L. major* promastigotes appeared to alter the membrane properties of the host cells which, as shown in Chapter 4 of this thesis, may be beneficial for the parasite if it leads to a suppressed cytotoxic response of macrophages.

Many of the mechanisms of macrophage deactivation induced by infections with *Leishmania* spp. appear to be mediated through the actions of parasite molecules on PKC-dependent events. Certain surface molecules of *Leishmania* spp. may be responsible for the macrophage membrane-altering effects. For example, a surface molecule found in *L. amazonensis*, called cytolysin, is a protein that damages the membranes of macrophages by inserting itself into the lipid bilayer and forming non-selective pores (105). In that study, whole-cell patch clamped J774 macrophage-like cells displayed a change from a resting state of inward rectification with a selective permeability for K^+, to a state of increased conductance of inward and outward currents and a shifted reversal potential to less-negative values in the presence of parasite surface molecule (105). The authors state that this cytolysin pore-forming protein is especially relevant to the amastigote stage, as it aids in eventually rupturing the host cell.

Effects on the macrophage membrane were likely mediated by the main candidate surface molecules of *Leishmania* spp. (LPG and GIPLs) which are lipid-soluble and are able to alter intracellular signaling cascades (49). *Leishmania* spp. parasites can alter the plasma membrane of host cells by modulating constitutive transporters to modify ion homeostasis within the host cell or by incorporating LPG or GIPLs from their surface coat (106). LPG appears on the macrophage surface within minutes after phagocytosis (107) indicating that it is rapidly distributed throughout the lipid bilayer of the host cell. Recent studies suggest that LPG can also insert itself in the phagosome membrane resulting in reduced fusogenic properties (98) thereby delaying endocytic trafficking until the parasite is in its replicating form (amastigote).

The ability of pathogens to alter the ion homeostasis of their host cells has been documented by others. For example, *Plasmodium* increases the transport system of the erythrocyte membrane for glucose, phospholipids, purine bases, lactate, nucleotides, anions and cations (108). Changes in plasma membrane function were also induced by cytopathic viruses including HIV-1 (109). These alterations can result in changes in the intracellular content of ions that can contribute to cytolysis and death of the infected cell (110). Increased intracellular concentrations of K^+ and Na^+ occur concomitantly with cytopathic effects induced in a T-cell line acutely infected by HIV (111). Alterations in the basal intracellular concentration of Ca^{2+} ions have been demonstrated by infection of monocytes and cardiac cells with *Leishmania* and *Trypanosama cruzi*, respectively (112-114). These reports show that alteration of host cell ion homeostasis is important for pathogen infection and intracellular survival.

Chapter 6: General Discussion

6.1 Discussion

The work presented in this thesis demonstrates concomitant alterations in production of reactive nitrogen and oxygen intermediates and alterations in membrane potential in P388D.1 macrophage-like cells during *Leishmania major* infection. After 24 hours, there were similar effects of 4-AP and *L. major* on nitric oxide production, respiratory burst, membrane potential, and unidirectional influx of $^{86}Rb^+$ in P388D.1 macrophage-like cells. Alteration of K^+ channels may represent one of the mechanisms employed by *L. major* to inhibit NO production and respiratory burst by activated P388D.1 cells, thereby ensuring their survival in those cells. I found that there was an additive inhibition of NO production during a combined K^+ channel blockage and *L. major* infection. This effect is likely due to the parasite blocking more than just K^+ channel-dependent pathway(s) for nitric oxide production. The results presented in this thesis extend the observations by Forero *et al.* (59) by showing a relationship between alterations of plasma membrane V_m, K^+ fluxes, and inhibition of NO production and respiratory burst, using a different species of *Leishmania*. Potassium channels are involved in the regulation of cytotoxic functions in the murine macrophage-like cell line P388D.1.

Bone marrow-derived macrophages (BMDM) appeared to be similar to P388D.1 cells in their nitric oxide responses to the potassium channel blockers quinine and TEA. The NO inhibition seen during blockage with 4-AP was not as dramatic as in P388D.1

macrophage-like cells. Likewise, *L. major* promastigotes (at a ratio of 10 to 1) had less of an effect on the NO production of stimulated cells, although the respiratory burst of BMDM was inhibited by *L. major* promastigotes. The difference in the immune response to infection with *L. major* between these two types of cells may be related to their unique K^+ channel profiles, since their responses to pharmacological inhibition are slightly different as well.

It has been proposed that potassium channels may actively participate in intracellular signaling cascades by allowing regulation of the intracellular K^+ concentration and alterations in membrane potential (26). Ion channels are at the interface between the extracellular environment and the intracellular signaling processes; in fact some ion channels resemble signaling proteins structurally, as they are integral membrane proteins and have both intracellular and extracellular domains. In the G-protein-gated inwardly rectifying K^+ (GIRK) family of potassium channels found in heart, brain, pancreas, and other tissues, residues in the protein subunits of the channels may be covalently modified by G-proteins indicating that potassium channels might be directly involved in signal transduction (76, 115, 116).

A variety of stimuli including cytokines and endotoxins (LPS) regulate the secretion of reactive oxygen and nitrogen intermediates by macrophages. The direct intercalation and lateral diffusion of LPS in the plasma membranes of monocytes and macrophages was proposed to initiate signaling and induce activation by exerting steric stress on a "putative signaling protein" (77). It was proposed that an ion channel might be acting as a signal-transducing protein also by way of stress on the membrane (117). In a subsequent study a Ca^{2+}- and voltage-dependent K^+ channel (a MaxiK channel) was identified as the putative signaling protein (78). A recent paper proposing a new model for LPS recognition suggested an immediate link between K^+ channels and the LPS activation cluster (LACK) consisting of CD14, LPS in conjunction with LBP, TLR4, and accessory proteins such as MD-2 (25). The LPS signaling pathway is of utmost importance in activating macrophages for a killing response. This was the first report directly implicating the interaction of a K^+ channel with such a fundamental, well-studied activation pathway. It had previously been suggested that LPS interaction with a signal-transducing ion channel could lead to "mismatches" in intracellular ion concentrations, provoking the activation of the signaling cascade (118). In addition, membrane depolarization with medium containing 140 mM K^+ caused translocation of protein kinase C (PKC) to the subnuclear region of PU5-1.8 macrophage-like cells (119) indicating that PKC activation downstream of the signal transduction is dependent on membrane potential and membrane stability.

Signaling proteins are often modulated by addition of phosphate groups to serine, threonine, or tyrosine residues, creating binding sites for downstream signaling molecules. There is evidence to suggest that protein phosphorylation at tyrosine residues modulates K^+ channels (120), supporting the theory of K^+ channel involvement in intracellular signaling. Voltage-dependent K^+ channels are substrates of Src- and PYK2-tyrosine kinases (TK) and are stimulated by increased PKC levels, and inwardly rectifying K^+ channels (KIR) which sustain the membrane potential are also directly modulated by tyrosine kinases (120). In rat basophilic leukocytes, inhibitors of protein tyrosine phosphatase (PTP) block currents through recombinant KIR channels (120).

It is possible that there are tyrosine-kinase mediated interactions between cytokine receptors and KIR channels. Tyrosine kinase-linked pathways regulate macrophage functions such as phagocytosis and production of antimicrobial molecules during *Leishmania* spp. infection (121). As such, the pathogenesis of leishmaniasis may be attributed to the activation of tyrosine phosphatases leading to inhibition of MAP kinases and downregulation of c-fos gene expression (122). Presumably, this would lead to a failed iNOS induction, as MAP kinases activate transcription factors such as NFκB (21), which play a major role in macrophage activation. Tyrosine phosphorylation is a short-lived local event that occurs early in *Leishmania* spp. infection (121). PTP inhibitors can cause alterations in the balance between tyrosine kinase and phosphatase, resulting in restriction of leishmaniasis (123).

A number of different types of potassium channels could be involved in the activation of macrophages under the conditions described in this thesis. Much of what is known about macrophage potassium channel profiles has been acquired from electrophysiological studies of microglia (brain macrophages), which with respect to their kinetic and pharmacological properties generally exhibit the same features as other macrophage populations (124). Inwardly rectifying potassium channels (KIR) are used to control a cell's resting membrane voltage (50). KIR channels are open at rest and may be downregulated in activated microglia, accompanied by an upregulation of delayed rectifier channels (124). Delayed rectifier channels in brain macrophages are much more sensitive to 4-AP (in the 1 to 5 mM range) than to TEA (124), which is a generally observed response in the P388D.1 cells. It is possible that the suppression of activation that was seen in P388D.1 macrophage-like cells is partially due to the blockage of delayed-rectifier channels. The role of various K^+ channels in membrane physiology differs from cell type to cell type. In microglia, delayed outward rectifying channels might be involved in repolarizing the membrane after depolarization; a hyperpolarized membrane is thought to be required for functions such as phagocytosis and cytokine secretion (124). A negative membrane potential is required to maintain calcium influx and regulate gene expression in immune cells (124). Altering this state will undoubtedly affect macrophage activation. As demonstrated here, depolarization of the membrane potential has negative consequences for ROI and RNI production by macrophages.

Interestingly, macrophage stretch sensitive K^+ channels are activated upon adherence, are pharmacologically inhibited by 4-AP and barium chloride but not TEA, and respond to IL-2 and IL–6 but not TGF-β (70). It is likely that these stretch sensitive channels are activated during the steric stress associated with assembly of the LACK in the membrane following LPS stimulation. Although the features of these K^+ channels are similar to the pharmacological profile of K^+ channel blockage in P388D.1 cells (4-AP >> TEA (6)), it is unlikely that these stretch sensitive K^+ channels are the main channels involved in the LPS-induced expression of genes such as iNOS, since blockage with 4-AP did not appear to affect iNOS mRNA at 3 hours in the cell line macrophages, despite the inhibition of NO after 24 hours.

Maintenance of cell membrane potential close to a specific value helps potassium channels establish conditions that allow intracellular signaling events to occur (26). As mentioned, potassium channels might be directly involved in gene upregulation following macrophage activation (e.g. increased expression of iNOS) (26). Alternatively, modulation of potassium channels might alter ion homeostasis sufficiently to allow for changes in intracellular conditions, leading to upregulated gene expression (26). For this reason, ion channels are a legitimate target for parasites entering host cells. I hypothesized that ion channels, particularly potassium channels, are targeted by *L. major* during the initial stages of infection since the distribution of K^+ channels throughout the plasma membrane of the macrophage means that any alteration in the channels has the potential to result in immediate effects on macrophage physiology and antimicrobial responses. It has been demonstrated that *Leishmania* spp. parasites shed part of their surface coat (for example, LPG) upon binding to and entering a host cell (98, 107). In this manner, immunomodulatory parasite molecules could immediately spread throughout the lipid bilayer of the host cell and begin disabling the cell's immune responses at the very early stages of infection. I have shown that LPG causes an inhibition of NO production by P388D.1 cells. In addition, the depolarization seen in infected P388D.1 cells at 24 hours does not correspond to a great respiratory burst. This indicates that the depolarization is not due to the respiratory burst *per se* but could be due to the some feature of the *L. major* parasite, likely its surface chemistry.

Although P388D.1 macrophage-like cells and bone marrow-derived macrophages possess common features, it is important to note that because the cells differ in origin, they will presumably differ slightly in their physiology and immune responses as well. P388D.1 cells and bone marrow-derived macrophages (BMDM) are both characterized as macrophages due to their functional responses (phagocytosis, production of nitric oxide, production of cytokines) and due to the presence of certain surface molecules including CR3 and FcR. They also display non-specific esterase activity, characteristic of macrophages. However, there are important differences between the two cell types as well. P388D.1 cells are derived from the DBA/2 strain of mice, are formed through a methylcholanthrene-induced tumour and are of the mature macrophage differentiation state (79). Bone marrow macrophages are primary cells, differentiated and enriched for by selection with the cytokine M-CSF. These BMDM cells are more inflammatory than P388D.1 cells. While there are no detailed descriptions in the literature of K^+ currents in P388D.1 cells, it is known that bone marrow-derived macrophages grown in the presence of M-CSF express mainly an inward rectifying K^+ current when at rest (58). A patch-clamp analysis comparing human monocyte-derived macrophages and the cell line U-937 revealed that only the human macrophages displayed calcium-activated K^+ channels, and that although there were voltage-gated potassium (KV) channels present in both cell types their kinetics differed significantly (125). Thus, there are limitations to the comparisons that can be made between primary cells and tumour cell-derived macrophage-like cells.

The fact that the BMDM nitric oxide response was weakly inhibited by the K^+ channel blocker 4-AP while the response of the P388D.1 cells was much more dramatic correlates with the fact that BMDM are relatively low responders to LPS stimulation. They produce small quantities of NO unless IFNγ is added as a priming signal, while P388D.1 cells have a significant nitric oxide response with LPS stimulation that is enhanced upon addition of IFNγ. Interestingly, both cell types responded to quinine in a similar manner. Quinine may be a better overall non-selective blocker that “overrides” the activation responses independently of LPS and IFNγ. Alternatively, the blockers used in this study may affect slightly different pathways of activation. For example, the pathway of activation blocked by 4-AP might somehow involve the pathway induced by

LPS stimulation alone, while quinine might not, such that the bone marrow-derived macrophages which have a limited response to LPS alone are also poor responders to 4-AP as an activation-inhibiting factor. Potassium channels may be involved in the priming stage of macrophage activation, because treatment with IFNγ alone is sufficient to prime macrophages for antimicrobial activity (6). In addition, the observation that the recovery of NO production after K^+ channel blocker wash-out is enhanced if macrophages are stimulated with LPS and IFNγ, rather than LPS alone, supports the hypothesis that potassium channels may be involved in the priming stage of activation.

The results described in this thesis may be particular to the species of *Leishmania* examined. Members of this genus differ in their pathologic outcomes in various tissues. For example, in experiments examining inoculation of various species of *Leishmania* into dorsal air pouches in mice, *L. major* promastigotes were better than *L. donovani* promastigotes at inducing proinflammatory cytokine secretion and chemokine gene expression in pouch exudates (48). *L. major* infection also elicited increased chemokine receptor gene expression, indicating that *L. major* is a strong inducer of the early inflammatory response, compared with *L. donovani*. These events may restrict this parasite to the inoculation site, favoring the development of cutaneous lesions clinically associated with *L. major* (48).

Presumably, alteration of K^+ homeostasis in the whole cell will also modulate K^+ flux into the phagocytic vacuole; this might have different effects on different pathogens. In a recent study where *Salmonella enterica* was observed living in the high potassium environment of the *Salmonella*-containing vacuole (SCV) of macrophages, the authors concluded that high levels of potassium might be one of several important signals for this intracellular pathogen (126) as it allows the use of gluconate and related sugars as a carbon source within macrophages. On the other hand, in neutrophils a surge of K^+ ions into the vacuole accompanies an influx of high concentrations of ROI. This is followed by activation of cationic granule proteins, including elastase and cathepsin G, which are responsible for the destruction of *Staphylococcus aureus* bacteria (127). When exposed to pneumococcal cell wall components from the Gram-positive bacterium *Streptococcus pneumoniae*, microglia exhibited outwardly rectifying K^+ currents with concomitant suppression of inwardly rectifying currents (128). This was accompanied by production of many proinflammatory cytokines including TNFα, IL-6 and -12, and macrophage inflammatory proteins. The authors state that this effect is distinct from the mechanisms induced by LPS from Gram-negative bacteria (128). It is possible, therefore, that different pathogen products signal through pathways in the macrophage in which some signaling components are shared and some are unique.

6.2 Future Directions

The relationship between *Leishmania* parasites and their host cells is a well-studied one. However, the interactions between the two are complex and much is still unknown about macrophage activation during infection.

The role of macrophage K^+ channels in LPS and IFNγ signaling under normal growth conditions and under conditions of potassium channel blockage must be examined at the molecular level to fully understand the signaling events of those pathways. Candidate intracellular signaling molecules to focus on include inositol triphosphate, diacylglycerol, NFκB, and the protein kinase C (PKC) enzymes. The involvement of potassium channels in macrophage activation should be explored more fully by examining the effects of more specific K^+ channel blockers. This could be accompanied by a study of the effects of blockers on other macrophage types (other macrophage cell lines, inflammatory and resident peritoneal macrophages, etc.) from mice and from other species. Ideally, electrophysiological analysis (patch-clamping) should be done on macrophages under normal activating conditions and under conditions of potassium channel blockage to validate the bis-oxonol assay as an indicator of membrane potential.

To examine the effects of these K^+ channel inhibitors on infection, it would be interesting to see the influence of other *Leishmania* species or *Leishmania* gene knock-out parasites (e.g. LPG-deficient mutants) or other intracellular pathogens on the process of macrophage inactivation through intracellular signaling events. A molecular analysis of K^+ channel types present in various types of macrophages could be undertaken. It would be interesting to determine whether there is preferential upregulation of K^+ channel types following interactions with LPS, IFNγ, parasite molecules, or other stimulatory factors. Macrophages should be treated with various potassium channel blockers and the ability to resist infection with *L. major* and to kill parasites after infection should be analyzed, to determine whether the blocker's ability to suppress ROI and RNI production enhances parasite persistence within macrophages.

Further investigation and identification of the role(s) of K^+ channels in macrophage activation during infection with *L. major* would provide useful information on the mechanisms responsible for downregulation of activation and promotion of parasite survival. Because nitric oxide and the respiratory burst are important effector functions in the resolution of leishmaniasis, investigations into the pathway(s) leading to production of these cytotoxic molecules may aid in the development of immunomodulatory therapies to treat infections with such intracellular pathogens.

Literature Cited

1. Nandan D., Lo R., Reiner N.E. (1999) Activation of phosphotyrosine phosphatase activity attenuates mitogen-activated protein kinase signaling and inhibits c-fos and nitric oxide synthase expression in macrophages infected with *Leishmania donovani*. Infection and Immunity. **67**(8): 4055-63.

2. Reiner N.E. (1994) Altered cell signaling and mononuclear phagocyte deactivation during intracellular infection. Immunology Today. **15**(8): 374-81.

3. Descoteaux A., Prive C. (2000) *Leishmania donovani* promastigotes evade the activation of mitogen-activated protein kinases p38, c-Jun N-terminal kinase, and extracellular signal-related kinase-1/2 during infection in naïve macrophages. European Journal of Immunology. **30**: 2235-44.

4. Feng G.J., Goodridge H.S., Harnett M.M., et al. (1999) Extracellular signal-related kinase (ERK) and p38 mitogen-activated protein (MAP) kinases differentially regulate the lipopolysaccharide-mediated induction of inducible nitric oxide synthase and IL-12 in macrophages: *Leishmania* phosphoglycans subvert macrophage Il-12 production by targeting ERK MAP kinase. Journal of Immunology. **163**: 6403-12.

5. Ray M., Gam A.A., Boykins R.A., et al. (2000) Inhibition of interferon-gamma signaling by *Leishmania donovani*. Journal of Infectious Diseases. **181**: 1121-8.

6. Lowry M.A., Goldberg J.I., Belosevic M. (1998) Induction of nitric oxide (NO) synthesis in murine macrophages requires potassium channel activity. Clinical and Experimental Immunology . **111**(3): 597-603.

7. Amer A.O., Swanson M.S. (2002) A phagosome of one's own: a microbial guide to life in the macrophage. Current Opinion in Microbiology. **5**(1): 56-61.

8. Levitz S.M., Nong S.-H., Seetoo K.F., et al. (1999) *Cryptococcus neoformans* resides in an acidic phagolysosome of human macrophages. Infection and Immunity. **67**(2): 885-90.

9. Stafford J.L., Neumann N.F., Belosevic M. (2002) Macrophage-mediated innate host defense against protozoan parasites. Critical Reviews in Microbiology. **28**(3): 187-248.

10. Goldsby R.A., Kindt T.J., Osborne B.A. (2000). Kuby Immunology. Fourth ed. W.H. Freeman and Company: New York.

11. Barreda D.R., Hanington P.C., Belosevic M. (2003) Regulation of myeloid development and function by colony stimulating factors. Developmental and Comparative Immunology. (In press).

12. Neumann N.F. Regulation of antimicrobial mechanisms of macrophages of goldfish (*Carassius auratus*) [Ph.D.]. Edmonton: University of Alberta; 1999.

13. Naito M. (1993) Macrophage heterogeneity in development and differentiation. Archives of Histology and Cytology. **56**(4): 331-51.

14. Aderem A. (2002) How to eat something bigger than your head. Cell. **110**: 5-8.

15. Gagnon E., Duclos S., Rondeau C., et al. (2002) Endoplasmic reticulum-mediated phagocytosis is a mechanism of entry into macrophages. Cell. **110**: 119-31.

16. Garin J., Diez R., Kieffer S., et al. (2001) The phagosome proteome: insight into phagosome functions. Journal of Cell Biology. **152**: 165-80.

17. Oppenheim J.J., Leonard E.J. In: Human Monocytes (1989). Zembala M, Asherson GL, editors. Academic Press, Ltd.: San Diego, CA. p. 1-7.

18. Vazquez-Torres A., Fang F.C. (2001) Oxygen-dependent anti-*Salmonella* activity of macrophages. Trends in Microbiology. **9**(1): 29-33.

19. Marletta M.A., P.S. Y., Iyengar R., et al. (1988) Macrophage oxidation of L-arginine to nitrite and nitrate: nitric oxide is an intermediate. Biochemistry. **27**(24): 8706-11.

20. Stuehr D.J., Marletta M.A. (1987) Induction of nitrite/nitrate synthesis in murine macrophages by BCG infection, lymphokines, or interferon-gamma. Journal of Immunology. **139**(2): 518-25.

21. Chan E.D., Riches D.W. (2001) IFNg and LPS induction of iNOS is modulated by ERK, JNK/SAPK, and p38(mapk) in a mouse macrophage cell line. American Journal of Physiology (Cellular Physiology). **280**(3): C441-50.

22. Nathan C. (2003) Oxygen and the inflammatory cell. Nature. **422**: 675-6.

23. Brown H., Kozlowski R., Perry H. (1998) The importance of ion channels for macrophage and microglial activation *in vitro*. Glia. **22**(1): 94-7.

24. Assreuy J., Cunha F.Q., Epperlein M., et al. (1994) Production of nitric oxide and superoxide by activated macrophages and killing of *Leishmania major*. European Journal of Immunology. **24**(3): 672-6.

25. Triantafilou M., Triantafilou K. (2002) Lipopolysaccharide recognition: CD14, TLRs and the LPS-activation cluster. Trends in Immunology. **23**(6): 301-4.

26. Lowry M.A. Role of Ion Channels in Macrophage Activation [M.Sc.]. Edmonton: University of Alberta; 1998.

27. Kane M.M., Mosser D.M. (2000) *Leishmania* parasites and their ploys to disrupt macrophage activation. Current Opinion In Hematology. **7**: 26-31.

28. Nandan D., Reiner N.E. (1995) Attenuation of gamma interferon-induced tyrosine phosphorylation in mononuclear phagocytes infected with *Leishmania donovani*: selective inhibition of signaling through Janus kinases and Stat1. Infection and Immunity. **63**(11): 4495-500.

29. World Health Organization. (2003) Disease information: leishmaniasis. Retrieved May 3, 2003 from: http://www.who.int/tdr/diseases/leish/diseaseinfo.htm

30. el-Hassan A.M., Zijlstra E.E. (2001) Leishmaniasis in Sudan. Cutaneous leishmaniasis. Transactions of the Royal Society of Tropical Medicine and Hygiene. **95**(1): S1-17.

31. Zijlstra E.E., el-Hassan A.M. (2001) Leishmaniasis in Sudan. Post kala-azar dermal leishmaniasis. Transactions of the Royal Society of Tropical Medicine and Hygiene. **95 Suppl 1**: S59-76.

32. Cunningham A.C. (2002) Parasitic adaptive mechanisms in infection by *Leishmania*. Experimental and Molecular Pathology. **72**: 132-41.

33. Guy R.A. Mechanisms of Entry of *Leishmania major* into Macrophages [Ph.D.]. Edmonton: University of Alberta; 1995.

34. World Health Organization. (2003). Fact Sheet #116: The Leishmaniases and *Leishmania*/HIV Co-infections. Retrieved May 3, 2003 from: http://www.who.int/inf-fs/en/fact116.html

35. Sacks D.L., Kamhawi S. (2001) Molecular aspects of parasite-vector and vector-host interactions in leishmaniasis. Annual Reviews in Microbiology. **55**(1): 453-83.

36. Sacks D.L. (2001) *Leishmania*-sand fly interactions controlling species-specific vector competence. Cellular Microbiology. **3**(4): 189-96.

37. Guilpin V.O., Swardson-Olver C., Nosbisch L., et al. (2002) Maxadilan, the vasodilator/immunomodulator from *Lutzomyia longipalpis* sand fly saliva, stimulates haematopoiesis in mice. Parasite Immunology. **24**(8): 437-46.

38. Guy R.A., Belosevic M. (1993) Comparison of receptors required for entry of *Leishmania major* amastigotes into macrophages. Infection and Immunity. **61**(4): 1553-8.

39. Krishnan L., Guilbert L.J., Wegmann T.G., et al. (1996) T helper 1 response against *Leishmania major* in pregnant C57BL/6 mice increases implantation failure and fetal resorptions. Correlation with increased IFNg and TNF and reduced IL-10 production by placental cells. Journal of Immunology. **156**(2): 653-62.

40. Chiang S.-C., Ali V., Huang A.-L., et al. (2001) Molecular, cellular, and functional characterizations of a novel ICAM-like molecule of the immunoglobulin superfamily from *Leishmania mexicana amazonensis*. Molecular and Biochemical Parasitology. **112**: 263-75.

41. Ropert C., Gazzinelli R.T. (2000) Signaling of immune system cells by glycosylphosphatidylinositol (GPI) anchor and related structures derived from parasitic protozoa. Current Opinion in Microbiology. **3**: 395-403.

42. Gruenheid S., Finlay B.B. (2003) Microbial pathogenesis and cytoskeletal function. Nature. **422**: 775-81.

43. Porte F., Liautard J.-P., Kohler S. (1999) Early acidification of phagosomes containing *Brucella suis* is essential for intracellular survival in murine macrophages. Infection and Immunity. **67**(8): 4041-7.

44. Descoteaux A., Turco S.J., Sacks D.L., et al. (1991) *Leishmania donovani* lipophosphoglycan selectively inhibits signal transduction in macrophages. Journal of Immunology. **146**(8): 2747-53.

45. Descoteaux A., Matlashewski G., Turco S.J. (1992) Inhibition of macrophage protein kinase C-mediated protein phosphorylation by *Leishmania donovani* lipophosphoglycan. Journal of Immunology. **149**(9): 3008-15.

46. Liew F.Y., Wei X.-Q., Proudfoot L. (1997) Cytokines and nitric oxide as effector molecules against parasitic infections. Philosophical Transactions of the Royal Society of London (Biological Sciences). **352**(1359): 1311-5.

47. Matlashewski G., Moore K.J. (1994) Intracellular infection by *Leishmania donovani* inhibits macrophage apoptosis. Journal of Immunology. **152**(6): 2930-7.

48. Matte C., Olivier M. (2002) *Leishmania*-induced cellular recruitment during the early inflammatory response: modulation of proinflammatory mediators. The Journal of Infectious Diseases. **185**: 673-81.

49. Proudfoot L., O'Donnell C.A., Liew F.Y. (1995) Glycoinositolphospholipids of *Leishmania major* inhibit nitric oxide synthesis and reduce leishmanicidal activity in murine macrophages. European Journal of Immunology. **25**(3): 745-50.

50. Hille B. (2001). Ion Channels of Excitable Membranes. Sinauer Associates, Inc.: Sunderland, MA.

51. Randall D., Burggren W., French K. (1997). Animal Physiology: Mechanisms and Adaptations. Fourth ed. W.H. Freeman and Company: New York.

52. Giorgetti A., Carloni P. (2003) Molecular modeling of ion channels: structural predictions. Current Opinion in Chemical Biology. **7**(1): 150-6.

53. Qiu M.R., Campbell T.J., Breit S.N. (2002) A potassium ion channel is involved in cytokine production by activated human macrophages. Clinical and Experimental Immunology . **130**(1): 67-74.

54. Gallin E.K. (1991) Ion channels in leukocytes. Physiol Rev. **71**(3): 775-811.

55. Gallin E.K., McKinney L.C. (1988) Patch-clamp studies in human macrophages: single-channel and whole-cell characterization of two K^+ conductances. Journal of Membrane Biology. **103**(1): 55-66.

56. Gallin E.K., Sheehy P.A. (1985) Differential expression of inward and outward potassium currents in the macrophage-like cell line J774.1. Journal of Physiology. **369**: 475-99.

57. Randriamampita C., Trautmann A. (1987) Ionic channels in murine macrophages. Journal of Cell Biology. **105**(2): 761-9.

58. Eder C., Fischer H.G. (1997) Effects of colony-stimulating factors on voltage-gated K^+ currents of bone marrow-derived macrophages. Naunyn Schmiedebergs Arch Pharmacol. **355**(2): 198-202.

59. Forero M.E., Marin M., Corrales A., et al. (1999) *Leishmania amazonensis* infection induces changes in the electrophysiological properties of macrophage-like cells. Journal of Membrane Biology. **170**(2): 173-80.

60. Doyle D.A., Cabral J.M., Pfuetzner R.A., et al. (1998) The structure of the potassium channel: molecular basis of K^+ conduction and selectivity. Science. **280**(5360): 69-77.

61. MacKinnon R., Cohen S.L., Kuo A., et al. (1998) Structural conservation in prokaryotic and eukaryotic potassium channels. Science. **280**: 106-9.

62. Hille B. (1978) Ionic channels in excitable membranes. Current problems and biophysical approaches. Biophysical Journal. **22**(2): 283-94.

63. Ruta V., Jiang Y., Lee A., et al. (2003) Functional analysis of an archaebacterial voltage-dependent K^+ channel. Nature. **422**: 180-5.

64. Jiang Y., Ruta V., Chen J., et al. (2003) The principle of gating charge movement in a voltage-dependent K^+ channel. Nature. **423**: 42-8.

65. Nishida M., MacKinnon R. (2002) Structural basis of inward rectification: cytoplasmic pore of the G-protein-gated inward rectifier GIRK1 at 1.8 A resolution. Cell. **111**(7): 957-65.

66. Guidoni L., Carloni P. (2002) Tetraethylammonium binding to the outer mouth of the KcsA potassium channel: implications for ion permeation. J Recept Signal Transduct Res. **22**(1-4): 315-31.

67. Munoz-Caro C., Nino A. (2002) The nature of the receptor site for the reversible K^+ channel blocking by aminopyridines. Biophys Chem. **96**(1): 1-14.

68. Stafford J.L., Galvez F., Goss G.G., et al. (2002) Induction of nitric oxide and respiratory burst response in activated goldfish macrophages requires potassium channel activity. Developmental and Comparative Immunology. **26**(5): 445-59.

69. Krause K.H., Demaurex N., Jaconi M., et al. (1993) Ion channels and receptor-mediated Ca^{2+} influx in neutrophil granulocytes. Blood Cells. **19**: 165-75.

70. Martin M.A., Nauseef W.M., Clark R.A. (1988) Depolarization blunts the oxidative burst of human neutrophils: parallel effects of monoclonal antibodies, depolarizing buffers, and glycolytic inhibitors. Journal of Immunology. **140**: 3928-35.

71. Eleno N., Botanna L., Espinosa J. (1990) K^+-channel blocking drugs induce histamine release and $^{45}Ca^+$ uptake in isolated mast cells. International Archives of Allergy and Applied Immunology. **92**: 162-7.

72. Janiszewski J., Huizinga J.D., Blennerhassett M.G. (1992) Mast cell ionic channels: significance for stimulus-secretion coupling. Canadian Journal of Physiology and Pharmacology. **70**: 1-7.

73. Schlicter L., Sidell N., Hagiwara S. (1986) Potassium channels mediate killing in human natural killer cells. Proceedings of the National Academy of Science, United States of America. **83**: 451-5.

74. Haslberger A., Romanin C., Koerber R. (1992) Membrane potential modulates release of tumor necrosis factor in lipopolysaccharide-stimulated mouse macrophages. Molecular Biology of the Cell. **3**: 451-60.

75. Maruyama N., Kakuta Y., Yamauchi K., et al. (1994) Quinine inhibits production of tumor necrosis factor-alpha from human alveolar macrophages. Am J Respir Cell Mol Biol. **10**(5): 514-20.

76. McKinney L.C., Gallin E.K. (1992) G-protein activators induce a potassium conductance in murine macrophages. Journal of Membrane Biology. **130**(3): 265-76.

77. Schromm A.B., Brandenburg K., Loppnow H., et al. (2000) Biological activities of lipopolysaccharides are determined by the shape of their lipid A portion. European Journal of Biochemistry. **267**: 2008-13.

78. Blunck R., Scheel O., Muller M., et al. (2001) New insights into endotoxin-induced activation of macrophages: involvement of a K^+ channel in transmembrane signaling. Journal of Immunology. **166**(2): 1009-15.

79. Koren H.S., Handwergen B.S., Wunderlich J.R. (1975) Identification of macrophage-like characteristics in a cultured murine tumor line. Journal of Immunology. **114**: 894-7.

80. Belosevic M., Davis C.E., Meltzer M.S., et al. (1988) Regulation of activated macrophage antimicrobial activities. Identification of lymphokines that cooperate with IFN-gamma for induction of resistance to infection. Journal of Immunology. **141**(3): 890-6.

81. Belosevic M., Finbloom D.S., Van Der Meide P.H., et al. (1989) Administration of monoclonal anti-IFN-gamma antibodies in vivo abrogates natural resistance of C3H/HeN mice to infection with *Leishmania major*. Journal of Immunology. **143**(1): 266-74.

82. Earle W.R., et al. (1943) Production of malignancy in vitro. IV. The mouse fibroblast cultures and changes seen in the living cells. Journal of the National Cancer Institute. **4**: 165-212.

83. Sacks D.L., Hieny S., Sher A. (1985) Identification of cell surface carbohydrate and antigenic changes between noninfective and infective developmental stages of *Leishmania major* promastigotes. Journal of Immunology. **135**(1): 564-9.

84. Dall'Asta V., Gatti R., Orlandini G., et al. (1997) Membrane potential changes visualized in complete growth media through confocal laser scanning microscopy of bis-oxonol-loaded cells. Exp. Cell. Res. **231**(2): 260-8.

85. Epps D.E., Wolfe M.L., Groppi V. (1994) Characterization of the steady-state and dynamic fluorescence properties of the potential-sensitive dye bis-(1,3-dibutylbarbituric

acid)trimethine oxonol (DiBac4(3)) in model systems and cells. Chem Phys Lipids. **69**(2): 137-50.

86. Kumar P., Pai K., Pandey H.P., et al. (2002) NADH-oxidase, NADPH-oxidase and myeloperoxidase activity of visceral leishmaniasis patients. Journal of Medical Microbiology. **51**(10): 832-6.

87. Chawla M., Vishwakarma R.A. (2003) Alkylacylglycerolipid domain of GPI molecules of *Leishmania* is responsible for inhibition of PKC-mediated c-fos expression. J. Lipid Res. **44**(3): 594-600.

88. DeCoursey T.E., Morgan D., Cherny V.V. (2002) The voltage dependence of NADPH oxidase reveals why phagocytes need proton channels. Nature. **422**: 531-4.

89. Liew F.Y., Millott S., Parkinson C., et al. (1990) Macrophage killing of *Leishmania* parasite in vivo is mediated by nitric oxide from L-arginine. Journal of Immunology. **144**(12): 4794-7.

90. Murray H.W., Nathan C.F. (1999) Macrophage microbicidal mechanisms in vivo: reactive nitrogen versus oxygen intermediates in the killing of intracellular visceral *Leishmania donovani.* Journal of Experimental Medicine. **189**(4): 741-6.

91. Wu C.C., Thiemermann C., Vane J.R. (1995) Glibenclamide-induced inhibition of the expression of inducible nitric oxide synthase in cultured macrophages and in the anaesthetized rat. British Journal of Pharmacology. **114**: 1273-81.

92. Phillips W.A., Hamilton J.A. (1989) Phorbol ester-stimulated superoxide production by murine bone marrow-derived macrophages requires preexposure to cytokines. Journal of Immunology. **142**: 2445-9.

93. Kim S.Y., Silver M.R., DeCoursey T.E. (1996) Ion channels in THP-1 monocytes. Journal of Membrane Biology. **152**: 117-30.

94. Beeton C., Barbaria J., Giraud P., et al. (2001) Selective blocking of voltage-gated K^+ channels improves experimental autoimmune encephalomyelitis and inhibits T cell activation. Journal of Immunology. **166**(2): 936-44.

95. Hoffmann A., Kann O., Ohlemeyer C., et al. (2003) Elevation of basal intracellular calcium as a central element in the activation of brain macrophages (microglia): suppression of receptor-evoked calcium signaling and control of release function. Journal of Neuroscience. **23**(11): 4410-9.

96. Proudfoot L., Nikolaev A.V., Feng G.J., et al. (1996) Regulation of the expression of nitric oxide synthase and leishmanicidal activity by glycoconjugates of *Leishmania* lipophosphoglycan in murine macrophages. Proceedings of the National Academy of Science. **93**(20): 10984-9.

97. Haidaris C.G., Bonventre P.F. (1982) A role for oxygen-dependent mechanisms in killing of *Leishmania donovani* tissue forms by activated macrophages. Journal of Immunology. **129**(2): 850-5.

98. Miao L., Stafford A., Nir S., et al. (1995) Potent inhibition of viral fusion by the lipophosphoglycan of *Leishmania donovani*. Biochemistry. **34**(4): 4676-83.

99. Calahan M.D., Wulff H., Chandy K.G. (2001) Molecular properties and physiological roles of ion channels in the immune system. Journal of Clinical Immunology. **21**(4): 235-52.

100. Colden-Stanfield M. (2002) Clustering of very late antigen-4 integrins modulates K^+ currents to alter Ca^{2+}-mediated monocyte function. American Journal of Physiology (Cellular Physiology). **283**(3): C990-C1000.

101. Gallin E.K., Livengood D.R. (1981) Inward rectification in mouse macrophages: evidence for a negative resistance region. Am J Physiol. **241**(1): C9-17.

102. Chandy K.G., Gutman G.A., Grissmer S. (1993) Physiological role, molecular structure, and evolutionary relationships of voltage-gated potassium channels in T-lymphocytes. Sem Neurosci. **5**: 123-34.

103. Schmid-Antomarchi H., Schmid-Alliana A., Romey G., et al. (1997) Extracellular ATP and UTP control the generation of reactive oxygen intermediates in human macrophages through the opening of a charybdotoxin-sensitive Ca^{2+}-dependent K^+ channel. Journal of Immunology. **159**: 6209-15.

104. Bouchot A., Millot J.M., Charpentier S., et al. (2001) Membrane potential changes after infection of monocytes by *Toxoplasma gondii.* International Journal for Parasitology. **31**(10): 1114-20.

105. Noronha F.S.M., Cruz J.S., Beirao P.S.L., et al. (2000) Macrophage damage by *Leishmania amazonensis* cytolysin: evidence of pore formation on cell membrane. Infection and Immunity. **68**(8): 4578-84.

106. Gero A.M., Upston J.M. (1992) Altered membrane permeability: A new approach to malaria chemotherapy. Parasitology Today. **8**: 283-6.

107. Tolson D.L., Turco S.J., Pearson T.W. (1990) Expression of a repeating phosphorylated disaccharide lipophosphoglycan epitope on the surface of macrophages infected with *Leishmania donovani*. Infection and Immunity. **58**(11): 3500-7.

108. Cranmer S.L., Conant A.R., Gutteridge W.E., et al. (1995) Characterization of the enhanced transport of L- and D-lactate into human red blood cells infected with *Plasmodium falciparum* suggests the presence of a novel saturable lactate proton cotransporter. Journal of Biological Chemistry. **270**: 15045-52.

109. Visentin S., Renzi M., Levi G. (2001) Altered outward-rectifying K^+ current reveals microglial activation induced by HIV-1 Tat protein. Glia. **33**(3): 181-90.

110. Makutonina A., Voss T.G., Plymale D.R., et al. (1996) Human immunodeficiency virus infection of T-lymphoblastoid cells reduces intracellular pH. Journal Of Virology. **70**(10): 7049-55.

111. Voss T.G., Fermin C.D., Levy J.A., et al. (1996) Alteration of intracellular potassium and sodium concentrations correlates with induction of cytopathic effects by human immunodeficiency virus. Journal of Virology. **70**(8): 5447-54.

112. Andrews N.W. (1995) Lysosome recruitment during host cell invasion by *Trypanosoma cruzi*. Trends in Cell Biology. **5**(133-137).

113. Eilam Y., El-On J., Spira D.T. (1985) *Leishmania major*: excreted factor, calcium ions, and the survival of amastigotes. Experimental Parasitology. **59**: 161-8.

114. Olivier M. (1996) Modulation of host cell intracellular Ca^{2+}. Parasitology Today. **12**: 145-50.

115. Jelacic T.M., Kennedy M.E., Wickman K., et al. (2000) Functional and biochemical evidence for G-protein-gated inwardly rectifying K^+ (GIRK) channels composed of GIRK2 and GIRK3. Journal of Biological Chemistry. **275**(46): 36211-6.

116. Wickman K., Clapham D.E. (1995) Ion channel regulation by G proteins. Physiological Reviews. **75**(4): 865-85.

117. Seydel U., Scheel O., Muller M., et al. (2001) A K^+ channel is involved in LPS signaling. Journal of Endotoxin Research. **7**(3): 243-7.

118. Seydel U. (1998) Molecular Basis of Endotoxin Toxicity. Ann NY Acad Sci. **851**(1): 406-7.

119. Kong S.K., Choy Y.M., Fung K.P., et al. (1991) Membrane depolarization induces protein kinase C translocation and voltage operated calcium channel opening in PU5-1.8 cells. Protein kinase C as a negative feedback modulator for calcium signaling. Second Messengers Phosphoproteins. **13**(2-3): 117-30.

120. Wischmeyer E., Doring F., Karschin A. (1998) Acute suppression of inwardly rectifying Kir2.1 channels by direct tyrosine kinase phosphorylation. Journal of Biological Chemistry. **273**(51): 34063-8.

121. Martiny A., Vannier-Santos M.A., Borges V.M., et al. (1996) *Leishmania*-induced tyrosine phosphorylation in the host macrophage and its implication to infection. European Journal of Cell Biology. **71**(2): 206-15.

122. Nandan D., Knutson K.L., Lo R., et al. (2000) Exploitation of host cell signaling machinery: activation of macrophage phosphotyrosine phosphatases as a novel mechanism of molecular microbial pathogenesis. Journal of Leukocyte Biology. **67**(4): 464-70.

123. Olivier M., Romero-Gallo B.J., Matte C., et al. (1998) Modulation of interferon-gamma-induced macrophage activation by phosphotyrosine phosphatases inhibition. Effect on murine leishmaniasis progression. Journal of Biological Chemistry. **273**(22): 13944-9.

124. Eder C. (1998) Ion channels in microglia (brain macrophages). American Journal of Physiology (Cellular Physiology). **275**(2): C327-42.

125. Guy R.A., Belosevic M. (1995) Response of scid mice to establishment of *Leishmania major* infection. Clinical and Experimental Immunology . **100**(3): 440-5.

126. McCann F.V., Keller T.M., Guyre P.M. (1987) Ion channels in human macrophages compared with the U-937 cell line. Journal of Membrane Biology. **96**(1): 57-64.

127. Eriksson S., Lucchini S., Thompson A., et al. (2003) Unraveling the biology of macrophage infection by gene expression profiling of intracellular *Salmonella enterica*. Molecular Microbiology. **47**(1): 103-18.

128. Reeves E.P., Lu H., Jacobs H.L., et al. (2002) Killing activity of neutrophils is mediated through activation of proteases by K^+ flux. Nature. **416**(6878): 291-7.

129. Prinz M., Kann O., Draheim H.J., et al. (1999) Microglial activation by components of gram-positive and -negative bacteria: distinct and common routes to the induction of ion channels and cytokines. Journal of Neuropathology and Experimental Neurology. **58**(10): 1078-89.

Appendix 1

1-1. Cunningham's medium for growth of *Leishmania major* promastigotes

Group 1	
Ingredient	**#g per 1 L**
NaH_2PO_4	0.53
$MgCl_2\ 6H_2O$	3.04
$MgSO_4\ 7H_2O$	3.7
KCl anhydrous	2.98
For 1 L, dissolve Group 1 ingredients in 100 ml Milli-Q H_2O	
Group 2	
Ingredient	**#g per 1 L**
$CaCl_2\ 2H_2O$	0.15
For 1 L, dissolve Group 2 ingredients in 50 ml Milli-Q H_2O	
Group 3	
Ingredient	**#g per 1 L**
Glucose	0.7
β-D-Fructose	0.4
Sucrose	0.4
For 1 L, dissolve Group 3 ingredients in 100 ml Milli-Q H_2O	
Group 4	
Ingredient	**#g per 1 L**
L-Malic acid	0.67
α-Ketoglutaric acid	0.37
Fumaric acid	0.55
Succinic acid	0.06
For 1 L, dissolve Group 4 ingredients in 100 ml Milli-Q H_2O	

Group 5	
Ingredient	**#g per 1 L**
β-alanine	2
DL-alanine	1.09
L-arginine	0.44
L-asparagine	0.24
L-aspartic acid*	0.11
L-cysteine HCl	0.08
L-cysteine	0.03
L-glutamic acid	0.25
Glycine	0.12
L-Histidine	0.16
DL-isoleucine*	0.09
L-leucine	0.09
L-lysine	0.15
DL-methionine	0.2
L-phenylalanine	0.2
L-proline	6.9
DL-serine	0.2
L-taurine	0.27
DL-threonine	0.1
L-tryptophan	0.1
L-tyrosine	0.2
DL-valine	0.21
L-glutamine	1.64
phenol red	0.015
For 1 L, dissolve all of the Group 5 ingredients in a small volume of water. Add 2 ml of vitamin mix. Bring to 650 ml with Milli-Q water.	

***Dissolve in 5 ml Milli-Q water before adding to rest of ingredients.**

Stir the individual solutions and then pool them together. Adjust the pH to 7.4 with 10-20 ml of 2N NaOH. Adjust the final volume to 1 L. Filter sterilize through a 0.22 μm filter. Store at -20°C.

To make 100 ml of complete Cunninham's medium, combine 40 ml of Cunningham's, 40 ml of DMEM containing gentamicin, and 20 ml of heat-inactivated fetal bovine serum (FBS).

1-2. DEPC water

Add 1 ml of diethlypyrocarbonate (DEPC) to 1000 ml of Milli-Q water. Shake vigorously. Incubate at 37° C overnight. Autoclave the solution 2 to 3 times.

1-3. TE buffer

Ingredient	Final concentration
0.121 g Tris HCl	10 mM
1 ml 0.1 M EDTA	1 mM

Bring to a total of 100 ml with Milli-Q water. Filter sterilize through a 0.22 μm filter.

1-4. 20X TAE buffer

Combine 96.88 g of Tris base, 45.92 ml of 0.5 M EDTA, and 40 ml of glacial acetic acid. Bring to a total of 1000 ml with Milli-Q water. Adjust pH to 7.7. Working concentration of 1X should be filter sterilized through a 0.22 μm filter.

1-5. Lysis buffer for isolation of protein

Ingredient	Final concentration
Triton X-100	1% (v/v)
PMSF	10 mM

Dissolve in PBS.

1-6. Separating and stacking gels for SDS-PAGE

Volumes for two 10% mini-gels

Separating gel	
Ingredient	**Volume**
Milli-Q water	11.275 ml
Separating buffer: 1.5 M Tris/SDS pH 8.8	5.6 ml
40 % acrylamide	5.625 ml
De-gas and add:	
10% APS*	75 μl
TEMED	15 μl

*10% APS: 0.1 g ammonium persulfate per 1 ml Milli-Q water.

Volumes for two 10% mini-gels

Stacking gel	
Ingredient	**Volume**
Milli-Q water	4.84 ml
Stacking buffer: 0.5 M Tris/SDS pH 6.8	1.9 ml
40 % acrylamide	0.731 ml
De-gas and add:	
10% APS*	37.5 µl
TEMED	7.5 µl

*10% APS: 0.1 g per 1 ml Milli-Q water.

1-7. Separating buffer

Add 91 g of Tris base per 500 ml of Milli-Q water (1.5 M). Adjust pH to 8.8 with HCl. Filter. Add 2 g of SDS. Store at 4°C.

1-8. Stacking buffer

Add 6.05 g of Tris base per 100 ml of Milli-Q water (0.5 M). Adjust pH to 6.8 with HCl. Filter. Add 0.4 g of SDS. Store at 4°C.

1-9. 5X running buffer

Combine 15 g of Tris base, 72 g of glycine, and 5 g of SDS and bring to 1000 ml with Milli-Q water. The pH should be between 8.3 and 8.6.

1-10. Blot buffer (Transfer buffer)

Combine 6.06 g of Tris base, 28.8 g of glycine, and 400 ml of methanol and bring to 2000 ml with Milli-Q water. The pH should be between 8.1 and 8.4.

1-11. Ovalbumin blocking buffer

Ingredient	Final concentration
Ovalbumin (chicken egg albumin)	3% (w/v)
Triton-X 100	0.1% (v/v)
Sodium azide	0.1% (v/v)

Dissolve in 1X TBS with stirring 1 to 2 days at 4°C. Clarify by centrifugation.

1-12. Tris-buffered saline (TBS)

Combine 16.4 g of NaCl and 2.42 g of Tris base. Bring to a total of 2000 ml with Milli-Q water.

1-13. Tween-Tris-buffered saline (TTBS)

Add 0.5 ml of Tween-20 to 1000 ml of TBS.

1-14. Bovine serum albumin blocking buffer (BSA)

Add 0.5 g of BSA to 100 ml of TTBS.

1-15. Coomassie blue gel-staining solution

For 500 ml of staining solution, combine 0.5 g of Coomassie blue, 200 ml of methanol, 50 ml of glacial acetic acid, and 250 ml of Milli-Q water.

1-16. Coomassie gel-destaining solution

Combine 40 ml of methanol, 10 ml of glacial acetic acid, and 50 ml of Milli-Q water.

Curriculum vitae

Kristine D. Scott

Department of Biological Sciences
CW-405 Biological Sciences Building
University of Alberta
Edmonton, AB T6G 2E9

EDUCATION

Sept. 2000-June 2003

Department of Biological Sciences, University of Alberta
M. Sc. Candidate, Cell Biology/Physiology Research Interest Group

Thesis topic: A role for K^+ channels in macrophage inactivation during infection with the intracellular parasite *Leishmania major*

May 2000

Department of Biology, Memorial University of Newfoundland (MUN)
B. Sc. (Honours), General Biology
Graduated with First Class Honours

Thesis topic: Effect of Toxaphene on liver of yellowtail flounder (*Pleuronectes ferrugineus* Storer)

RESEARCH EXPERIENCE

September 2000-June 2003
Dept. of Biological Sciences, University of Alberta
Graduate Student Researcher

May-August 2000
Faculty of Medicine, Memorial University of Newfoundland
Student Researcher/Summer Fellowship
Project title: Rescue of axotomized neurons using the neurotrophin brain-derived neurotrophic factor (BDNF) and the free radical inhibitor L-NAME

June-August 1999
Department of Biology, Memorial University of Newfoundland
Cytology Assistant

June 1999-March 2000
Ocean Sciences Centre/Department of Biology, Memorial University of Newfoundland
Student Research Assistant

TEACHING EXPERIENCE

September 2002-April 2003
Department of Biological Sciences, University of Alberta
Teaching assistant for Biology 107 (Introductory Cell Biology)

HONOURS AND AWARDS

Graduate

Sept. 2002-April 2003	Graduate Teaching Assistantship
Sept. 2002-April 2003	Faculty of Science Graduate T.A. Scholarship
May 2002	Canadian Society of Zoologists Parasitology Section Poster Prize, Annual Meeting in Lethbridge, AB
April 2002	Department of Alberta Learning Graduate Studies Scholarship
Sept. 2000-Sept. 2002	Natural Sciences and Engineering Research Council of Canada (NSERC) Post-Graduate Scholarship (PGS A)
Sept. 2000-Sept. 2002	Walter H. Johns Graduate Fellowship
Sept. 2000	Faculty of Science Graduate Scholarship

Undergraduate

May-August 2000	Undergraduate Research Fellowship, Faculty of Medicine, MUN
1999-2000	Faculty of Science Dean's List, MUN
1996-1997	Dr. Maurice Saval Scholarship, Faculty of Science, MUN
1995-1996	Faculty of Science Dean's List, MUN
1995	MUN Faculty Association Scholarship

REFEREED PUBLICATIONS

Scott, K.D., J.L. Stafford, F. Galvez, M. Belosevic, and G.G. Goss. (In press.) Plasma membrane depolarization reduces nitric oxide (NO) production in P388D.1 macrophage-like cells during *Leishmania major* infection. *Cellular Immunology.*

Scott, K., G.E. Fåhræus-Van Ree, and C.C. Parrish. (2002). Sex Differences in Hepatic Lipids of Toxaphene-Exposed Juvenile Yellowtail Flounder (*Pleuronectes ferrugineus* Storer). *Ecotoxicology and Environmental Safety.* 51,168-176. Environmental Research, Section B.

OTHER CONTRIBUTIONS

Scott, K., J.L. Stafford, F. Galvez, M. Belosevic, and G. Goss. (2003). "Alterations In Macrophage K^+ Channel Activity: Evidence For A Suppression Of Key Effector Functions During *Leishmania major* Infection". Poster presentation. Annual meeting of the Canadian Society for Immunology. Lake Louise, AB, Canada. March 28-30, 2003.

Scott, K., J.L. Stafford, G. Goss, and M. Belosevic. (2002). "Alterations In Macrophage K^+ Channel Activity". Oral presentation. ICOPA (International Congress of Parasitology) X. Vancouver, BC, Canada. August 8-11, 2002.

Scott, K.D., J.L. Stafford, F. Galvez, M. Belosevic, and G. Goss. (2002). "*Leishmania major* Suppresses the Macrophage Nitric Oxide Response through K^+ Channel Modulation." Oral presentation. Annual meeting of the Canadian Society of Zoologists (CSZ). Lethbridge, AB, Canada. May 7-11, 2002.

Scott, K., J.L. Stafford, F. Galvez, G. Goss, and M. Belosevic. (2001). "Murine Macrophages Infected with *Leishmania major* Exhibit Reduced Nitric Oxide Production Associated with Alterations in K^+ Channel Activity". Poster presentation. Joint meeting of International Cytokine Society (ICS) and Society for Leukocyte Biology (SLB*)*. Maui, HI, USA. November 8-11, 2001.

SOCIETIES AND MEMBERSHIPS

2003	Student member, *Canadian Society for Immunology*
2002-2003	Student member, *Canadian Society of Zoologists*
2001-2003	Student member, *Society for Leukocyte Biology*

VOLUNTEER AND MENTORING EXPERIENCE

Feb. 2003	**WISEST** (Women in Scholarship, Engineering, Science, and Technology) -CHOICES Conference for Grade 6 girls -Instructed 4 sessions of "Banana DNA Extraction" laboratory exercise
Sept. 2002	**Department of Biological Sciences Mentorship Program**
Feb. 2002	**WISEST** -CHOICES Conference -Instructed 4 sessions of a "Physiology of the Heart: Electrocardiography" laboratory exercise